AD_____

Award Number: DAMD17-01-1-0765

TITLE: Common Mechanisms of Neuronal Cell Death After Exposure
to Diverse Environmental Insults: Implications for
Treatment

PRINCIPAL INVESTIGATOR: Brian R. Pike, Ph.D.
Gerry Shaw, Ph.D.

CONTRACTING ORGANIZATION: University of Florida
Gainesville, Florida 32611-5500

REPORT DATE: October 2002

TYPE OF REPORT: Annual

PREPARED FOR: U.S. Army Medical Research and Materiel Command
Fort Detrick, Maryland 21702-5012

DISTRIBUTION STATEMENT: Approved for Public Release;
Distribution Unlimited

20030801 028

REPORT DOCUMENTATION PAGE

Form Approved
OMB No. 074-0188

Public reporting burden for this collection of information is estimated to average 1 hour per response, including the time for reviewing instructions, searching existing data sources, gathering and maintaining the data needed, and completing and reviewing this collection of information. Send comments regarding this burden estimate or any other aspect of this collection of information, including suggestions for reducing this burden to Washington Headquarters Services, Directorate for Information Operations and Reports, 1215 Jefferson Davis Highway, Suite 1204, Arlington, VA 22202-4302, and to the Office of Management and Budget, Paperwork Reduction Project (0704-0188), Washington, DC 20503

1. AGENCY USE ONLY (Leave blank)	2. REPORT DATE October 2002	3. REPORT TYPE AND DATES COVERED Annual (27 Sep 01 –26 Sep 02)

4. TITLE AND SUBTITLE
Common Mechanisms of Neuronal Cell Death After Exposure to Diverse Environmental Insults: Implications for Treatment

5. FUNDING NUMBERS
DAMD17-01-1-0765

6. AUTHOR(S):
Brian R. Pike, Ph.D.
Gerry Shaw, Ph.D.

7. PERFORMING ORGANIZATION NAME(S) AND ADDRESS(ES)

University of Florida
Gainesville, Florida 32611-5500

E-Mail: pike@ufbi.ufl.edu

8. PERFORMING ORGANIZATION REPORT NUMBER

9. SPONSORING / MONITORING AGENCY NAME(S) AND ADDRESS(ES)

U.S. Army Medical Research and Materiel Command
Fort Detrick, Maryland 21702-5012

10. SPONSORING / MONITORING AGENCY REPORT NUMBER

11. SUPPLEMENTARY NOTES
report contains color

12a. DISTRIBUTION / AVAILABILITY STATEMENT
Approved for Public Release; Distribution Unlimited

12b. DISTRIBUTION CODE

13. Abstract *(Maximum 200 Words)* *(abstract should contain no proprietary or confidential information)*
Neuronal cell death after exposure to neurotoxins or after central nervous system (CNS) injury is the major cause of devastating neurological pathologies associated with military combat-related morbidity and mortality. An understanding of the cellular and molecular mechanisms contributing to neuronal cell death is critical to development of appropriate treatment strategies. Although the environmental causes of CNS injury are diverse (e.g., penetrating injuries, concussive injuries, neurotoxin exposure, etc.), we hypothesize that regardless of the injury mechanisms, a relatively small subset of cellular and molecular events is responsible for the vast majority of cell death. The research results contained in this annual report summarize the findings of the first year of supported research on this grant. We have made great progress in implementing the proposed studies and have generated a wealth of data that supports both our broad and specific hypotheses. Importantly, our research indicates that the calcium activated family of cysteine proteases - the calpains - are rapidly activated in response to a variety of cellular insults while the cysteine protease caspase-3 is only activated in response to more specific cellular signals. This results suggest that inhibition of both calpain and caspase may provide greater neuroprotection than either inhibitor given alone.

14. SUBJECT TERMS
brain trauma, cell death, neurotoxins, preteases, calpains, caspases

15. NUMBER OF PAGES
76

16. PRICE CODE

17. SECURITY CLASSIFICATION OF REPORT Unclassified	18. SECURITY CLASSIFICATION OF THIS PAGE Unclassified	19. SECURITY CLASSIFICATION OF ABSTRACT Unclassified	20. LIMITATION OF ABSTRACT Unlimited

NSN 7540-01-280-5500

Standard Form 298 (Rev. 2-89)
Prescribed by ANSI Std. Z39-18
298-102

Table of Contents

I. INTRODUCTION

Traumatic brain injury (TBI) is a significant health care issue in the United States affecting more than 2 million persons annually, with approximately 500,000 hospital admissions. In addition, TBI caused by concussive injury or by penetrating objects such as bullets or shrapnel is a major cause of death and disability observed in military combat casualty care. Although there has been much progress in understanding the pathological mechanisms associated with TBI, knowledge of the complex and varied biochemical, cellular, and molecular cascades affecting the traumatized brain are poorly understood. However, recent advances by our laboratory and others have demonstrated prominent roles for two families of cysteine proteases, calpains and caspases, as executioners of cell death after TBI. Importantly, we have recently found that calpains and/or caspase-3 may be independently or concurrently activated after TBI in different brain regions and at different times after sustained head injury. However, the mechanisms that regulate differential activation of these death-effecting enzymes in various brain regions are unknown. Importantly, recent development of various models of cell death using cell cultures has allowed investigators to systematically study individual components of mechanical and biochemical insults associated with TBI. For example, TBI in humans and other mammals results in both necrotic and apoptotic cell death caused by different biochemical events. Cell culture models (*in vitro* models) allow for study of necrosis or apoptosis in isolation or concurrently depending on the model employed. Thus, **the major goal of the scientific work proposed for year one of the current grant was to demonstrate that various CNS-related insults produce differential activation of calpain and caspase-3 proteases depending upon the pathological signal and/or neuronal cell type. In addition, the proposed work is designed to demonstrate that distinct cell death modalities are better defined by such biochemical markers than by the current standard approaches of phenotypic descriptions of apoptosis and necrosis.** Importantly, the work generated during the first year of funding on the current grant has demonstrated that calpains and caspase-3 proteases can be individually or concurrently activated depending on the mode and/or magnitude of the initiating stimulus. In addition, this work demonstrates the use of calpain or caspase-3 generated protein fragments as specific markers for identification of apoptotic or necrotic cell death independent of classically defined morphological definitions. It is thought that results of this research will advance an understanding of the varied pathological responses to cellular insult, and will provide a sound foundation for eventual use of therapeutic interventions in numerous disorders of the central nervous system.

II. BODY

Statements of Work (SOW) for Year 1:

SOW 1a: *To examine calpain and caspase-3 activation in primary mixed and neuronally enhanced septo-hippocampal cultures following CNS-related insults (mechanical stretch injury, glucose-oxygen deprivation, glutamate toxicity) or neurotoxic production of apoptotic (by staurosporine) or necrotic (by maitotoxin) cell death phenotypes.*

SOW 1b: *To examine relationships between archetypal apoptotic and necrotic cell death phenotypes and calpain and caspase-3 activation after CNS-related injury or after neurotoxin exposure.*

PROGRESS TOWARDS MEETING SOWs

Progress Towards Meeting SOW 1a:

An important issue in neurobiology is the understanding of cellular and molecular mechanisms involved in neuronal cell death after CNS insults such as ischemia, seizure, and traumatic brain and spinal cord injury. As recently as 1993 it was generally accepted that neuronal death after acute neurological insult was necrotic in nature and that apoptotic cell death was reserved for organism development. Currently, both necrotic and apoptotic components of neuronal death have been documented in various neurodegenerative disorders and neurological insults, including traumatic brain injury.

However, the overly simplistic binary classification scheme of "necrotic" and "apoptotic" cell death tends to break down in complex cell death systems that are characterized by both necrotic and apoptotic cell death (e.g., TBI, SCI, ischemia). In fact, it is now recognized that the broad spectrum of classically defined morphological characteristics of apoptosis rarely occurs after CNS injury such as TBI or ischemia. What's more,

Exposure to Maitotoxin (MTX) or Staurosporine (Stau)

Figure 1

after ischemia and TBI, both necrotic and apoptotic morphological characteristics have been observed within the same cell, suggesting a more complex pathway(s) to cell death than previously recognized. This discrepancy in cell death classification has lead some researchers to argue that classical apoptosis does not occur during neurodegeneration or acute CNS injury, while others argue that classical apoptosis does occur, but that it is masked by features of non-apoptotic cell death. Our laboratory favors the latter hypothesis and our results obtained during this first year funding period provide further support for this hypothesis.
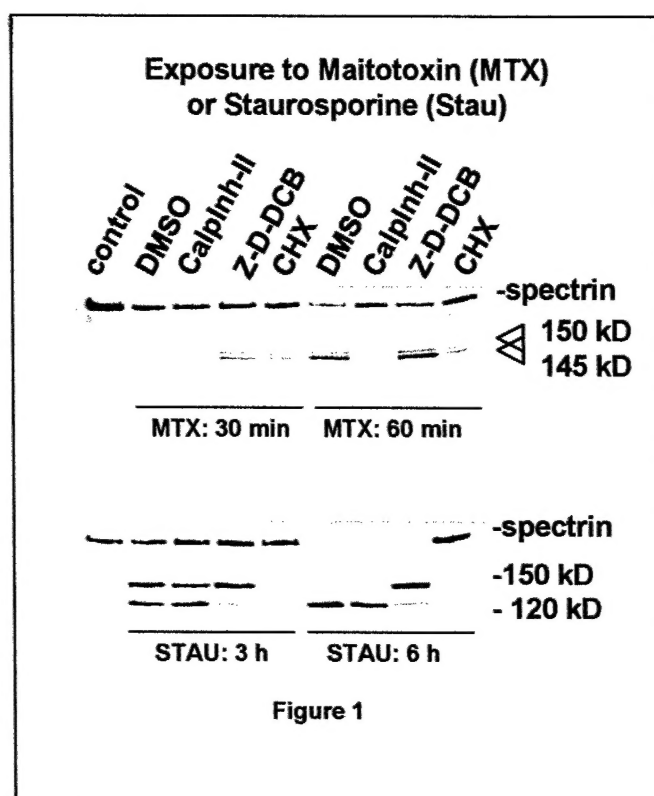
Western blot analysis of calpain and caspase-3 activation during necrosis or apoptosis

Our first aim was designed to demonstrate that cell culture models of apoptosis and necrosis result in differential activation of the cysteine proteases calpain or caspase-3 and that differential activation of these proteases can be used as biochemical markers of apoptotic or necrotic cell death. **Figure 1** illustrates representative western blots of protein extracted from cells induced to die by necrosis (Maitotoxin exposure) or by apoptosis (staurosporine exposure). These data indicate that the cytoskeletal protein α-spectrin (280 kDa) is cleaved by calpain to a 145 kDa fragment during maitotoxin-induced necrosis and to a 120 kDa fragment by caspase-3 during staurosporine-induced apoptosis. Note that the calpain-generated 145 kDa fragment can be inhibited by calpain inhibitor-II but not by a caspase inhibitor (Z-D-DCB). Conversely, the caspase-
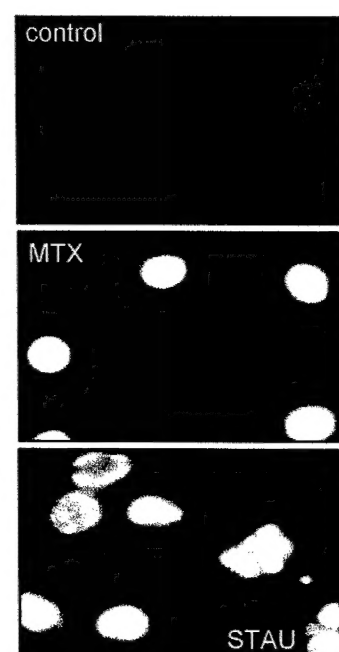

Figure 2

3-generated 120 kDa fragment is inhibited by Z-D-DCB but not by calpain inhibitor-II.

Evaluation of nuclear morphological alterations during necrosis or apoptosis

Calpain or caspase-3 activation in models of maitotoxin or staurosporine were also associated with necrotic or apoptotic nuclear profiles. **Figure 2** illustrates the classic cell death profiles of septo-hippocampal cell nuclei stained with Hoechst 33258. Note the normal, diffuse pattern of chromatin staining of control nuclei stained with Hoechst 33258. In contrast, maitotoxin-induced necrosis resulted in hyperchromatic nuclear staining with the necrotic nuclei maintaining the normal shape, whereas staurosporine-induced apoptosis resulted in nuclei undergoing various stages of nuclear disassembly, including chromatin condensation, margination, and apoptotic body formation.

Western blot analysis of calpain and caspase-3 activation after mechanical stretch injury to septo-hippocampal cell cultures

A major biomechanical force encountered by the brain during concussive head injury is that of rapid deformation and tensile strain, or stretch injury. Several *in vitro* systems have been designed to model this sort of mechanical injury by culturing cells onto deformable substrates that are then exposed to an applied load.
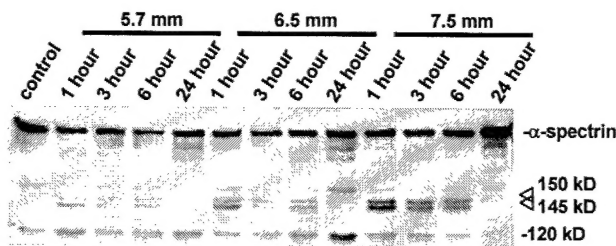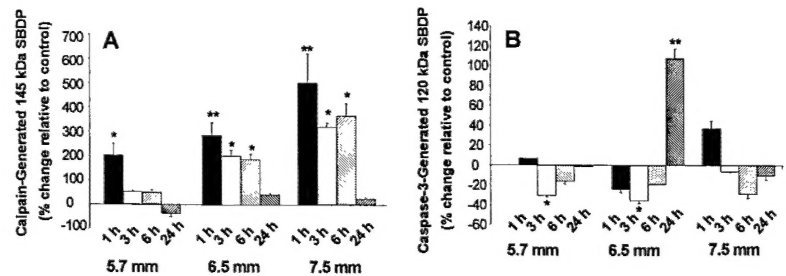

Figure 3

Figure 4

Ellis and coworkers (1995) have developed and characterized a model of stretch injury and have reported a number of stretch-induced cellular alterations including mitochondrial swelling, increased plasma membrane permeability (Ellis et al., 1995), influx of extracellular Ca^{2+} (Rzigalinski et al., 1996), phospholipase C activation, arachidonic acid release (Lamb et al., 1997), and membrane depolarization (Tavalin et al., 1997). However, the effects of stretch-injury on numerous other biochemical and morphological variables related to *in vivo* brain injury, including calpain and caspase-3 activation, have not been previously investigated.

Figure 3 is a Western Blot illustrating calpain and caspase-3 cleavage of α-spectrin to signature 145 kDa and 120 kDa fragments, respectively, after mild (5.7 mm), moderate (6.5 mm) and severe (7.5 mm) stretch injury. These results indicated distinctive temporal processing of α-spectrin by calpain or caspase-3 that included rapid but brief calpain activation (1-6 hours after each injury level) followed by delayed caspase-3 activation (24 hours after 6.5 mm injury). Note that the levels of calpain-generated 145 kDa product, measured by densitometry (**Figure 4**) was related to injury magnitude and that increases in the caspase-3 generated 120 kDa fragment were only observed 24 h after 6.5 mm injury.

Evaluation of nuclear morphological alterations after stretch injury

Mechanical stretch injury resulted in heterogeneous subpopulations of cell nuclei that were characteristic of apoptosis or necrosis during the acute period (1-6 hours) after injury (**Figure 5**). By twenty-four hours after injury, nuclear alterations were exclusively apoptotic-like. Interestingly, this pattern of cell death has also been reported after *in vivo* traumatic brain injury. For instance, Conti et al. (1998) observed large increases in TUNEL-positive non-apoptotic cells neighboring a smaller number of TUNEL-positive apoptotic cells in cortex 24 hours after lateral fluid percussion brain injury. Similarly, our laboratory has also reported heterogeneous populations of TUNEL-positive necrotic-like and TUNEL-positive apoptotic-like cells in cortical regions 24 hours after

Figure 5

lateral cortical impact traumatic brain injury (Newcomb et al., 1999). Thus, after stretch injury, apoptosis may be mediated initially by a caspase-3 independent pathway (absence of nuclear fragmentation and apoptotic bodies) and later by a caspase-3 dependent pathway (presence of nuclear fragmentation and apoptotic bodies). It is tempting to speculate that calpain may be involved as an effector of apoptosis during the early period after stretch injury as our laboratory has shown that calpain contributes to apoptotic cell death (Pike et al., 1998) and calpain, but not caspases, has recently been shown to promote apoptotic-like events during platelet activation (Wolf et al., 1999). Future work will address these hypotheses after stretch injury in CNS cells.
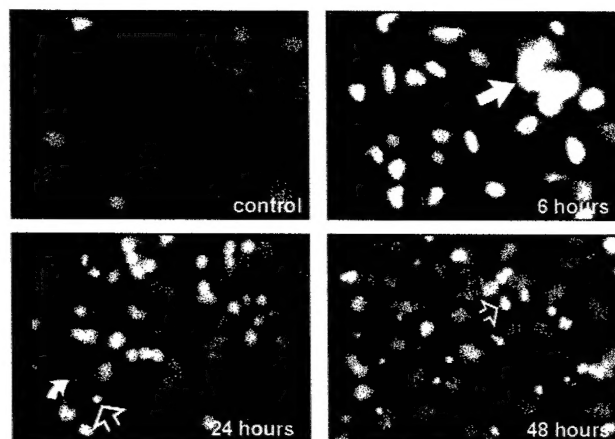
Progress Towards Meeting SOW 1b:

Apoptotic and necrotic cell death have historically been characterized based on distinguishing morphological characteristics, such as nuclear alterations as in Figures 2 and 5 above. These binary classification schemes are typically used in model systems characterized by homogenous populations of either necrotic or apoptotic cell death (e.g., maitotoxin, staurosporine, development) where the mode of cell death is obvious. However, in complex systems such as ischemia or TBI, cell death is typically characterized by heterogeneous cell death profiles that are not readily identifiable as classically necrotic or apoptotic. In addition, ischemia is a major pathological component of TBI. Thus, the purpose of Aim II was to examine calpain and caspase-3 activation in relation to morphological alterations following exposure to a variety of cellular insults.

Biochemical markers of cell death

Using antibodies against the calpain-generated 150 kDa fragment and the caspase-3-generated 120 kDa fragment to α-spectrin, we used double labeling immunocytochemistry to examine calpain and caspase-3 activation patterns during various modes of cell death and compared these staining patterns to nuclear morphology using Hoechst 33228 staining in the same cells (**Figure 6**). Note that maitotoxin-induced
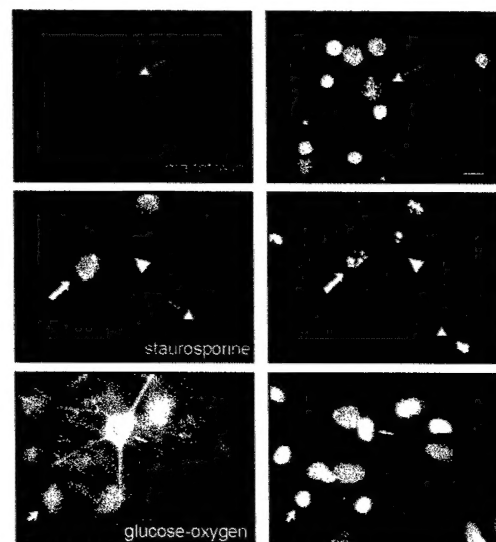
Figure 6

7

necrotic cell death resulted in calpain (red fluorescence) but not caspase-3 activation. Additionally, maitotoxin caused nuclear morphological alterations that were classically necrotic (diffusely stained, hyperchromatic nuclei). In contrast, staurosporine-induced apoptosis resulted in both calpain and caspase-3 activation (red and yellow fluorescence) and nuclear morphological alterations that were classically apoptotic (condensed, fragmented nuclear chromatin). Interestingly, cell cultures exposed to glucose-oxygen deprivation (a model of the ischemic component of TBI) resulted in both calpain and caspase-3 activation similar to staurosporine; however, nuclear morphological alterations were ambiguous and could not by readily classified as necrotic or apoptotic. These results clearly indicate that although caspase-3 (an apoptotic effector) was activated in this model, morphological alterations could not be used in this system to determine the mode of cell death. Thus, our results indicate that biochemical assays of cell death may prove more useful in complex neuropathological models of CNS injury such as ischemia, spinal cord injury, and traumatic brain injury.

III. KEY RESEARCH ACCOMPLISHMENTS

- Characterized differential patterns of calpain and caspase-3 activation after chemical and mechanical insults to primary septo-hippocampal cell cultures.
- Characterized morphological profiles of cells undergoing classic apoptotic or classic necrotic cell death and provided morphological comparisons to dying cells after a variety of neurochemical or mechanical cell death.
- Demonstrated that classic cell death profiles of apoptosis and necrosis are highly correlated with specific activation patterns of calpain and/or caspase-3 protease activation.
- Demonstrated that calpain activation is a common event of cell death regardless of injury mechanisms while caspase-3 has a more limited role that is dependent upon the mode of cellular injury.
- Demonstrated that cellular insults that produce heterogeneous cell death profiles (i.e., mixed apoptotic and necrotic) are better characterized by specific biochemical events (e.g., calpain or caspase-3 activation) than through traditional morphological characterization.

IV. REPORTABLE OUTCOMES

There are several reportable outcomes that are supported or based on experience supported by this award and are listed as follows:

i. Abstracts

Pike, B.R., Ringger, N.C., McKinsey, D.M., Tolentino, P.J., DeFord, S.M., Brabham, J.G., and Hayes, R.L. (2002). Effects of injury severity on regional and temporal mRNA expression levels of calpains and caspases after traumatic brain injury in rats. Journal of Neurotrauma, (in press).

Johnson, E.A., **Pike**, B.R., Tolentino, P., Hayes, R.L., and Pineda, J. (2002). Up-regulation of the cell cycle/inhibitor of apoptosis protein survivin in astrocytes and neurons after TBI in rats. Journal of Neurotrauma, (in press).

Larner, S.F., **Pike**, B.R., and Hayes, R.L. (2002). Effects of injury severity on regional and temporal caspase-12 mRNA expression levels after traumatic brain injury in rats. Journal of Neurotrauma, (in press).

DeFord, S.M., Slemmer, J.E., Weber, J.T., De Zeeuw, C.I., **Pike**, B.R., and RL Hayes. (2002). In vivo and in vitro evidence of cytoskeletal synaptic protein alterations following repeated mild TBI. <u>Journal of Neurotrauma</u>, (in press).

Ringger, N.C., Shepard, T.M., Johnson, E.A., West, M., Hayes, R.L., **Pike**, B.R. (2001). Comparison of calpain and caspase-3 activation during necrosis, apoptosis and endoplasmic reticulum stress. <u>Society for Neuroscience Abstracts</u>, 27(1):566.

Shepard, T.M., **Pike**, B.R., Hayes, R.L., and Wirth, E.D. (2001). Calcium-mediated calpain activation and cell death in the hippocampal slice. <u>Society for Neuroscience Abstracts</u>, 27(1):566.

Johnson, E.A., Wang, K.K.W., **Pike**, B.R., and Hayes, R.L. (2001). Evidence of calpain activation in brain macrophages after traumatic brain injury in rats. <u>Society for Neuroscience Abstracts</u>, 27(1):564.

Beer, R., Franz, G., Krajewski S., **Pike**, B.R., Hayes, R.L., Reed, J.C., Schmutzhard, E., Poewe, W., and Kampfl, A. (2001). Temporal and spatial profile of caspase-8 expression and proteolysis after experimental traumatic brain injury. <u>Society for Neuroscience Abstracts</u>, 27(1):566.

Shepherd, T.M., **Pike**, B.R., Thelwall, P.E., Hayes, R.L., and Wirth, E.D. (2001). Diffusion-weighted magnetic resonance imaging of cell death in rat hippocampal slices. <u>Journal of Neurotrauma</u>, 18(10):1167.

DeFord, S.M., **Pike**, B.R., and Hayes, R.L. (2001). Temporal profile of α-spectrin breakdown products following repeated vs. single mild head injury in mice. <u>Journal of Neurotrauma</u>, 18(10):1165.

Johnson, E.A., Wang, K.K.W., **Pike**, B.R., and Hayes, R.L. (2001). Evidence of calpain activation in brain macrophages after traumatic brain injury. <u>Journal of Neurotrauma</u>, 18(10):1132.

Ringger, N.C., Shepard, T.M., Johnson, E.A., Larner, S.F., West, M.F., Hayes, R.L., and **Pike**, B.R. (2001). Comparison of calpain and caspase-3 activation during necrosis, apoptosis and endoplasmic reticulum stress. <u>Journal of Neurotrauma</u>, 18(10):1163.

Franz, G., Beer, R., Krajewski S., Reed, J.C., **Pike**, B.R., Hayes, R.L., Wang, K.K., and Kampfl, A. (2001). Temporal and spatial profile of caspase-8 expression and proteolysis after experimental traumatic brain injury. <u>Journal of Neurotrauma</u>, 18(10):1164.

ii. Manuscripts

Franz, G., Beer, R., Intemann, D., Krajewski, S., Reed, J.C., Engelhardt, K., **Pike**, B.R., Hayes, R.L., Wang, K.K., Schmutzhard, E., and Kampfl A. (2002). Temporal and spatial profile of Bid cleavage after experimental traumatic brain injury. <u>Journal of Cerebral Blood Flow and Metabolism</u>, 22(8):951-958.

Pike, B.R., Flint, J., Dutta, S., Johnson, E., Wang, K.K.W., and Hayes, R.L. (2001). Accumulation of calpain-cleaved non-erythroid αII-spectrin in cerebrospinal fluid after traumatic brain injury in rats. <u>Journal of Neurochemistry</u>, 78(6):1297-1306.

Newcomb-Fernandez, J.K., Zhao, X., **Pike**, B.R., Wang, K.K.W., Kampfl, A., Beer, R., DeFord, S.M., and Hayes, R.L. (2001). Concurrent assessment of calpain and caspase-3 activation after oxygen-glucose deprivation in primary septo-hippocampal cultures. <u>Journal of Cerebral Blood Flow and Metabolism</u>, 21(11):1281-1294.

Beer, R., Franz, G., Krajewski, S., **Pike**, B.R., Hayes, R.L., Reed, J.C., Wang, K.K., Klimmer, C., Schmutzhard, E., Poewe, W., Kampfl, A. (2001). Temporal and spatial profile of caspase 8 expression and proteolysis after experimental traumatic brain injury. <u>Journal of Neurochemistry</u>, 78(4):862-873.

Zhao, X., Bausano, B., **Pike**, B.R., Newcomb-Fernandez, J.K., Wang, K.K.W., Shohami, E., Ringger, N.C., DeFord, S.M., Anderson, D.K., Hayes, R.L. (2001). TNF-α stimulates caspase-3 activation and apoptotic cell death in primary septo-hippocampal cultures. <u>Journal of Neuroscience Research</u>, 64(2):121-131.

iii. Oral Presentations

Calpain-Cleaved αII-Spectrin Breakdown Products as Prototypical Biomarkers of Traumatic Brain Injury. Invited presentation at the Veteran's Administration Medical Center, Gainesville, Florida, September 20th, 2002.

Development of Biochemical Markers of Traumatic Brain Injury. Invited presentation at the National Institute of General Medical Sciences, Bethesda, Maryland, July 29th, 2002.

Accumulation of αII-Spectrin and Calpain-Cleaved αII-Spectrin Breakdown Products in CSF After Traumatic Brain Injury in Rats. Invited presentation at the 33rd Annual Meeting of the American Society for Neurochemistry, Palm Beach, Florida, June 24th, 2002.

Biomarkers in Traumatic Brain Injury. Invited presentation at the First Annual Retreat of the Center for Traumatic Brain Injury Studies, University of Florida, Gainesville, Florida, February 23, 2002.

New Insights into the Role of Calpain Activation After Traumatic Brain Injury. Invited presentation at the 25th annual meeting of the Williamsburg Traumatic Brain Injury International Conference, Williamsburg, Virginia, June 9, 2001.

iv. Employment

Based in part to the research supported by this grant, I have been offered and I have accepted a position as a Scientific Review Administrator (SRA) in the Office of Scientific Review (OSR) at the National Institute of General Medical Sciences (NIGMS) of the National Institutes of Health (NIH). My appointment to this position is effective on November 4th, 2002.

V. CONCLUSIONS

The results of this research lend support to our broad hypothesis that regardless of the injury mechanism, a relatively small subset of cellular and molecular events are responsible for the majority of cell death. Based on these findings, it is hoped that further elucidation of the common cell death mechanisms will lead to the development of portable, practical, and potent genetic therapies and pharmacotherapies for the treatment of a broad range of CNS injuries. For example, our research has demonstrated that calpains are destructive proteases that are activated rapidly to a variety of cellular insults to primary cell cultures including mechanical deformation and in response to exogenous chemical challenge from compounds such as staurosporine and maitotoxin and in response to increased levels of glutamate or TNF-α. Importantly, our research has also demonstrated that calpains are important effectors of cell death and are rapidly activated in rodent models of traumatic brain injury. In addition, our research has also indicated that calpains play a role in cell death in both necrosis and apoptosis. The ubiquitous cellular distribution of calpains and the rather promiscuous role of calpains in executing cell death regardless of injury modality strongly indicates the rapid prophylactic use of calpain inhibitors for emergency treatment of head injury victims. In contrast, although the caspase-3 cysteine protease has garnered much more scientific attention than calpain, our research indicates that the role of caspase-3 as an effector of cell death is more tightly regulated to specific cellular signals and is not a broad cell death protease. In addition, our research also indicates that although calpains can be independently activated and lead to cell death, caspase-3 is almost always activated with calpains. In addition, the role of caspase-3 as an effector of cell death in the CNS appears to be limited to apoptosis. However, because brain trauma results in heterogeneous populations of necrotic and apoptotic cell death, our research indicates that the most neuroprotective strategy will likely be a cocktail of calpain, caspase, and other protease inhibitors.

So What?

The importance of the results obtained by our research are twofold. First, research conducted during the funding period have provided new insights into the cellular events responsible for activating calpains and/or caspase-3. We have also shown, that in contrast to classically described dichotomies of necrotic and apoptotic cell death phenotypes, cell death phenotypes can vary greatly depending on the nature of the death inducing stimulus. The nature of the cell death phenotype is primarily dependent on the relative activation profiles of calpain and caspase-3 proteases. Thus, our research has shown that biochemical indices provide better determinants of cellular fate than do morphological ones. Second, our research indicates that calpains and caspases are major common effectors of cell death that are activated in response to a wide range of cellular insults. This finding strongly indicates the prophylactic use of calpain and caspase protease inhibitors as neuroprotective strategy for CNS injury. However, because current calpain and caspase inhibitors do not readily cross the blood brain barrier and have potentially harmful side effects, their use is not currently warranted for human use. Nonetheless, it is anticipated that development of safer and more effective calpain and caspase inhibitors will dramatically improve patient outcome in numerous CNS injuries and diseases.

V. REFERENCES

Conti, A.C., Raguhpathi, R., Trojanowski, J.Q., and McIntosh, T.K. (1998). Experimental brain injury induces regionally distinct apoptosis during the acute and delayed post-traumatic period. J Neurosci. 18(15), 5663-5672.

Ellis, E.F., McKinney, J.S., Willoughby, K.A., Liang, S., and Povlishock, J.T. (1995). A new model for rapid stretch-induced injury of cells in culture: characterization of the model using astrocytes. J. Neurotrauma. 12, 325-339.

Lamb, R.G., Harper, C.C., McKinney, J.S., Rzigalinski, B.A., and Ellis, E.F. (1997). Alterations in phosphatidylcholine metabolism of stretch-injured cultured rat astrocytes. J. Neurochem. **68,** 1904-1910.

Newcomb, J.K., Zhao, X., Pike, B.R., and Hayes, R.L. (1999). Temporal profile of apoptotic-like changes in neurons and astrocytes following controlled cortical impact injury in the rat. Exp. Neurol. 158, 76-88.

Pike, B.R., Zhao, X., Newcomb, J.K., Wang, K.K.W., Posmantur, R.M., and Hayes, R.L. (1998). Temporal relationships between de novo protein synthesis, calpain and caspase 3-like protease activation, and DNA fragmentation during apoptosis in septo-hippocampal cultures. J. Neurosci. Res. **52,** 505-520.

Rzigalinski, B.A., Liang, S., McKinney, J.S., and Ellis, E.F. (1996). The effect of calcium on astrocyte injury. FASEB J. **10,** A280-A281.

Tavalin, S.J., Ellis, E.F., and Satin, L.S. (1997). Inhibition of the electrogenic Na pump underlies delayed depolarization of cortical neurons after mechanical injury or glutamate. J. Neurophysiol. 77, 632-638.

Wolf, B.B., Goldstein, J.C., Stennicke, H.R., Beere, H., Amarante-Medes, G.P., Salvesen, G.S., and Green, D.R. (1999). Calpain functions in a caspase-independent manner to promote apoptosis-like events during platelet activation. Blood. **94(5),** 1683-1692.

List of Personnel Receiving Pay on DAMD17-01-1-0765

Name	Role on Project
Brian R. Pike, Ph.D.	PI
Gerry P. Shaw, Ph.D.	Co-PI
Jeremy Flint	Technician
Petra Cook	Technician
Cui Yang	Post-doc
Miguel Torres	Student Worker

BIBLIOGRAPHY

Brian R. Pike, Ph.D.

Book Chapters

Pike, B.R. (2001). Mechanical injury to cell and tissue cultures. In J. Marwah, E. Dixon, and N. Banik (eds.), Traumatic CNS Injury, pp. 203-230. Prominent Press, Scottsdale, AZ.

Pike, B.R. (2001). *In vitro* models of traumatic brain injury. In L.P. Miller and R.L. Hayes (eds.), Head Trauma: Basic, Preclinical and Clinical Aspects, pp. 37-64. John Wiley & Sons, Inc. New York.

Hayes, R.L., Newcomb, J.K., Pike, B.R., and DeFord, S.M. (2001). Contributions of calpains and caspases to cell death following traumatic brain injury. In L.P. Miller and R.L. Hayes (eds.), Head Trauma: Basic, Preclinical and Clinical Aspects, 219-237. John Wiley & Sons, Inc. New York.

Newcomb, J.K., Pike, B.R., Zhao, X., and Hayes, R.L. (2000). Concurrent assessment of calpain and caspase-3 activity by means of western blots of protease-specific spectrin breakdown products. In J.S. Elce (ed.), Methods in Molecular Biology, vol. 144, pp. 219-223: Calpain Methods and Protocols. Humana Press Inc., Totowa, NJ.

Zhao, X., Newcomb, J.K., Pike, B.R., and Hayes, R.L. (2000). Casein zymogram assessment of μ-calpain and m-calpain activity after traumatic brain injury in the rat in vivo. In J.S. Elce (ed.), Methods in Molecular Biology, vol. 144, pp. 117-120: Calpain Methods and Protocols. Humana Press Inc., Totowa, NJ.

Manuscripts In Review

Beer, R., Franz, G., Tauber, H., Reindl, M., Lassmann, H., Pike, B.R., Hayes, R.L., Krajewski, S., Reed, J.C., Schmutzhard, E., Poewe, W., and Kampfl, A. (2002). Oligodendrocyte reaction and changes in myelin protein expression after experimental traumatic brain injury. (in review).

Angileri, F.F., Flint, J., Germanò, A., de Divitiis, O., Hayes, R.L., and Pike, B.R. (2002). Post-injury induced hypothermia or administration of calpain inhibitor 2 attenuates hippocampal, but not cortical, calpain-mediated proteolysis after experimental traumatic brain injury in rats. (in review).

Germanò, A., Arcadi, F., Costa, C., DeFord, S.M., Pike, B.R., Hayes, R.L., Bramanti, P., d'Avella, D., Anderson, D.K., and Tomasello, F. (2002). Protective effects of the NMDA receptor antagonist FBM on behavioral and BBB changes after experimental subarachnoid hemorrhage. (in review).

Refereed Original Articles in Journals

Franz, G., Beer, R., Intemann, D., Krajewski, S., Reed, J.C., Engelhardt, K., Pike, B.R., Hayes, R.L., Wang, K.K., Schmutzhard, E., and Kampfl A. (2002). Temporal and spatial profile of Bid cleavage after experimental traumatic brain injury. Journal of Cerebral Blood Flow and Metabolism, 22(8):951-958.

Germanò, A., Costa, C., DeFord, S.M., Angileri, F.F., Arcadi, F., Pike, B.R., Bramanti, P., Bausano, B., Zhao, X., Day, A.L., Anderson, D.K., and Hayes, R.L. (2002). Systemic administration of a calpain inhibitor reduces behavioral deficits and blood-brain barrier permeability changes after experimental subarachnoid hemmorrhage in the rat. Journal of Neurotrauma, 19(7):887-896.

Tolentino, P.J., DeFord, S.M., Notterpeck, L., Glenn, C.C., Pike, B.R., Wang, K.K.W., and Hayes, R.L. (2002). Upregulation of tissue-type transglutaminase after traumatic brain injury. Journal of Neurochemistry, 80(4):579-588.

Pike, B.R., Flint, J., Dutta, S., Johnson, E., Wang, K.K.W., and Hayes, R.L. (2001). Accumulation of calpain-cleaved non-erythroid αII-spectrin in cerebrospinal fluid after traumatic brain injury in rats. Journal of Neurochemistry, 78(6):1297-1306.

Newcomb-Fernandez, J.K., Zhao, X., **Pike**, B.R., Wang, K.K.W., Kampfl, A., Beer, R., DeFord, S.M., and Hayes, R.L. (2001). Concurrent assessment of calpain and caspase-3 activation after oxygen-glucose deprivation in primary septo-hippocampal cultures. Journal of Cerebral Blood Flow and Metabolism, 21(11):1281-1294.

Beer, R., Franz, G., Krajewski, S., **Pike**, B.R., Hayes, R.L., Reed, J.C., Wang, K.K., Klimmer, C., Schmutzhard, E., Poewe, W., Kampfl, A. (2001). Temporal and spatial profile of caspase 8 expression and proteolysis after experimental traumatic brain injury. Journal of Neurochemistry, 78(4):862-873.

Zhao, X., Bausano, B., **Pike**, B.R., Newcomb-Fernandez, J.K., Wang, K.K.W., Shohami, E., Ringger, N.C., DeFord, S.M., Anderson, D.K., Hayes, R.L. (2001). TNF-α stimulates caspase-3 activation and apoptotic cell death in primary septo-hippocampal cultures. Journal of Neuroscience Research, 64(2):121-131.

Beer, R., Franz, G., Srinivasan, A., Hayes, R.L., **Pike**, B.R., Zhao, X., Schmutzhard, E., Poewe, W., and Kampfl, A. (2000). Temporal profile and cell subtype distribution of activated caspase-3 following experimental traumatic brain injury. Journal of Neurochemistry, 75(3):1264-1273.

Pike, B.R., Zhao, X., Newcomb, J.K., Glenn, C.C., Anderson, D.K., and Hayes, R.L. (2000). Stretch injury causes calpain and caspase-3 activation and necrotic and apoptotic cell death in septo-hippocampal cell cultures. Journal of Neurotrauma, 17(4):283-298.

Zhao, X., Newcomb, J.K., **Pike**, B.R., Wang, K.K.W., d'Avella, D., and Hayes. R.L. (2000). Novel characteristics of glutamate-induced cell death in primary septo-hippocampal cultures: relationship to Calpain and caspase-3 protease activation. Journal of Cerebral Blood Flow and Metabolism, 20(3):550-562.

Zhao, X., **Pike**, B.R., Newcomb, J.K., Wang, K.K.W., Posmantur, R.M., and Hayes, R.L. (1999). Maitotoxin induces calpain but not caspase-3 activation and necrotic cell death in primary septo-hippocampal cultures. Neurochemical Research, 24(3): 371-382.

Newcomb, J.K., Zhao, X., **Pike**, B.R., and Hayes, R.L. (1999). Temporal profile of apoptotic-like changes in neurons and astrocytes following controlled cortical impact injury in the rat. Experimental Neurology, 158:76-88.

Newcomb, J.K., **Pike**, B.R., Zhao, X., Banik, N., and Hayes, R.L. (1999). Altered calpastatin protein levels following traumatic brain injury in rat. Journal of Neurotrauma, 16(1): 1-11.

Pike BR, Zhao X, Newcomb JK, Posmantur RM, Wang KKW, and Hayes RL. (1998). Regional calpain and caspase-3 proteolysis of α-spectrin after traumatic brain injury. NeuroReport, 9(11): 2437-2442.

Pike BR, Zhao X, Newcomb JK, Wang KKW, Posmantur RM, and Hayes RL (1998). Temporal relationships between *de novo* protein synthesis, calpain and caspase 3-like protease activation, and DNA fragmentation during apoptosis in septo-hippocampal cultures. Journal of Neuroscience Research, 52: 505-520.

Qiu YH, Zhao X, Hayes RL, Perez-Polo JR, **Pike** BR, Huang L, Clifton GL, and Yang K. (1998). Activation of phosphatidylinositol 3-kinase by brain-derived neurotrophic factor gene transfection in septo-hippocampal cultures. Journal of Neuroscience Research, 52:192-200.

Zhao X, Newcomb JK, Posmantur RM, Wang KKW, **Pike** BR, and Hayes RL. (1998). pH dependency of mu-calpain and m-calpain activity assayed by casein zymography following traumatic brain injury in the rat. Neuroscience Letters, 247(1):53-57.

Dixon CE, Markgraf CG, Angileri F, **Pike** BR, Wolfson B, Newcomb JK, Bismar MM, Blanco AJ, Clifton GL, and Hayes RL. (1998). Protective effects of moderate hypothermia on behavioral deficits but not necrotic cavitation following cortical impact injury in the rat. Journal of Neurotrauma, 15(2), 95-103.

Zhao X, Posmantur R, Kampfl A, Liu SJ, Wang KKW, Newcomb JK, **Pike** BR, Clifton GL, and Hayes RL. (1998). Subcellular localization and duration of μ-calpain activity following traumatic brain injury in the rat: A casein zymography study. Journal of Cerebral Blood Flow and Metabolism, 18, 161-167.

Pike BR, Hamm RJ, Temple MD, Buck DL, and Lyeth BG. (1997). Effect of tetrahydroaminoacridine, a cholinesterase inhibitor, on cognitive performance following experimental brain injury. Journal of Neurotrauma, 14(12), 897-905.

2

Pike BR, and Hamm RJ. (1997). Chronic administration of a partial muscarinic M1 receptor agonist attenuates decreases in forebrain choline acetyltransferase immunoreactivity following experimental brain trauma. Experimental Neurology, 147, 55-65.

Newcomb JK, Kampfl A, Posmantur RM, Zhao X, Pike BR, Liu SJ, Clifton GL, and Hayes RL. (1997). Immunohistochemical study of calpain-mediated breakdown products to α-spectrin following controlled cortical impact injury in the rat. Journal of Neurotrauma, 14(6), 369-383.

Pike BR, and Hamm RJ. (1997). Activating the Post-traumatic Cholinergic System for the Treatment of Cognitive Impairment Following Traumatic Brain Injury. Pharmacology, Biochemistry, & Behavior, 57(4), 785-791.

Wiley JL, Compton AD, Pike BR, Temple MD, McElderry JW, and Hamm RJ. (1996). Reduced sensorimotor reactivity following traumatic brain injury in rats. Brain Research, 716, 47-52.

Hamm RJ, Temple MD, Pike BR, O'Dell DM, Buck DL, and Lyeth BG. (1996). Working memory deficits following traumatic brain injury in the rat. Journal of Neurotrauma, 13, 317-323.

Hamm RJ, Temple MD, Pike BR, and Ellis EF. (1996). The effect of post-injury administration of polyethylene glycol-conjugated superoxide dismutase (Pegorgotein, Dismutec®) or lidocaine on behavioral function following fluid percussion brain injury in rats. Journal of Neurotrauma, 13, 325-332.

Hamm RJ, Temple MD, O'Dell DM, Pike BR, and Lyeth BG. (1996). Exposure to environmental complexity promotes recovery of cognitive function after traumatic brain injury. Journal of Neurotrauma, 13, 41-47.

Hamm RJ, Pike BR, Temple MD, O'Dell DM, and Lyeth, BG. (1995). The effect of postinjury kindled seizures on cognitive performance of traumatically brain-injured rats. Experimental Neurology, 136, 143-148.

Pike BR, and Hamm RJ. (1995). Post-injury administration of BIBN 99, a selective muscarinic M_2 receptor antagonist, improves cognitive performance following traumatic brain injury in rats. Brain Research, 686, 37-43.

Hamm RJ, Pike BR, O'Dell DM, Phillips LL, and Lyeth BG (1995). Impaired gustatory neophobia following traumatic brain injury in rats. Journal of Neurotrauma, 12 (3), 307-314.

Hamm RJ, Pike BR, O'Dell DM, and Lyeth BG. (1994). Traumatic brain injury enhances the amnesic effect of a glutamatergic antagonist. Journal of Neurosurgery, 81, 267-271.

Hamm RJ, Pike BR, O'Dell DM, Lyeth BG, and Jenkins LW. (1994). The rotarod test: An evaluation of its effectiveness in assessing motor deficits following traumatic brain injury. Journal of Neurotrauma, 11(2), 187-196.

Hamm RJ, O'Dell DM, Pike BR, and Lyeth BG. (1993). Cognitive impairment following traumatic brain injury: The effect of pre- and post-injury administration of scopolamine and MK-801. Cognitive Brain Research, 1, 223-226.

Hamm RJ, Lyeth BG, Jenkins LW, O'Dell DM, and Pike BR. (1993). Selective cognitive impairment following traumatic brain injury in rats. Behavioural Brain Research, 59, 169-173.

Published Abstracts

Pike, B.R., Ringger, N.C., McKinsey, D.M., Tolentino, P.J., DeFord, S.M., Brabham, J.G., and Hayes, R.L. (2002). Effects of injury severity on regional and temporal mRNA expression levels of calpains and caspases after traumatic brain injury in rats. Journal of Neurotrauma, (in press).

Flint, J., Pike, B.R., Hayes, R.L., Moffett; J.R., Dave, J.R., Lu, X.-C.M., and Tortella, F.C. (2002). Accumulation of calpain and caspase-3 cleaved αII-spectrin breakdown products in CSF after middle cerebral artery occlusion in rats. Journal of Neurotrauma, (in press).

d'Avella, D., Aguennouz, M., Angileri, F.F., de Divitiis, O., Germanò, A., Toscano, A., Tomasello, F., Vita, G., **Pike**, B.R., Wang, K.K.W., and Hayes, R.L. (2002). Accumulation of calpain and caspase-3 cleaved αII-spectrin breakdown products in CSF of patients with severe traumatic brain injury. Journal of Neurotrauma, (in press).

Gabrielli, A., **Pike**, B.R., Hayes, R.L., Layon, A.J., Idris, A.H. (2002). Gas chromatography and mass spectrometry assessment of F_2-isoprostane levels in CSF after traumatic brain injury in rats. Journal of Neurotrauma, (in press).

Ringger, N.C., Silver, X., O'Steen, B., Brabham, J.G., Deford, S.M., **Pike**, B.R., Pineda, J., and Hayes, R.L. (2002). CSF accumulation of calpain-specific αII-spectrin breakdown products are associated with injury magnitude and lesion volume after traumatic brain injury in rats. Journal of Neurotrauma, (in press).

Johnson, E.A., **Pike**, B.R., Tolentino, P., Hayes, R.L., and Pineda, J. (2002). Up-regulation of the cell cycle/inhibitor of apoptosis protein survivin in astrocytes and neurons after TBI in rats. Journal of Neurotrauma, (in press).

Larner, S.F., **Pike**, B.R., and Hayes, R.L. (2002). Effects of injury severity on regional and temporal caspase-12 mRNA expression levels after traumatic brain injury in rats. Journal of Neurotrauma, (in press).

DeFord, S.M., Slemmer, J.E., Weber, J.T., De Zeeuw, C.I., **Pike**, B.R., and RL Hayes. (2002). In vivo and in vitro evidence of cytoskeletal synaptic protein alterations following repeated mild TBI. Journal of Neurotrauma, (in press).

Waghray, A., DeFord, S.M., Tolentino, P.J., **Pike**, B.R., Glenn, C.C., Notterpek, L., Wang, K.K.W., and Hayes, R.L. (2002). Tissue-type transglutaminase expression after traumatic brain injury. Journal of Neurotrauma, (in press).

Tolentino, P.J., Waghray, A., **Pike**, B.R., Glenn, C.C., Notterpek, L., Wang, K.K.W., and Hayes, R.L. (2002). Tissue-type transglutaminase expression following middle cerebral artery occlusion. Journal of Neurotrauma, (in press).

Tortella, F.C., Moffett, J.R., Dave, J.R., Lu, X.-C.M., Flint, J., Hayes. R.L., and **Pike**, B.R. (2002). Calpain and caspase-3 cleaved αII-spectrin breakdown products (SBDPs) in CSF after middle cerebral artery occlusion in rats. Society for Neuroscience Abstracts, (in press).

Pike, B.R., Flint, J., Dutta, S., Wang, D.S., Wang, K.K.W., and Hayes, R.L. (2002). Accumulation of spectrin and calpain-cleaved spectrin breakdown products in CSF after traumatic brain injury in rats. Journal of Neurochemistry, 18(Suppl. 1):73.

Wang, D.S., Tolentino, P.J., Fan, T., **Pike**, B.R., Wang, K.K.W., Day, A.L., and Hayes R.L. (2002). Induction of tissue transglutaminase in response to ischemic brain injury. Journal of Neurochemistry, 18(Suppl. 1):109.

Pike, B.R., Flint, J., Dutta, S., Glenn, C.C., Wang, K.K.W., and Hayes, R.L. (2001). Accumulation of calpain-cleaved αII-spectrin breakdown products in CSF after traumatic brain injury in rats. Society for Neuroscience Abstracts, 27(1):564.

Ringger, N.C., Shepard, T.M., Johnson, E.A., West, M., Hayes, R.L., **Pike**, B.R. (2001). Comparison of calpain and caspase-3 activation during necrosis, apoptosis and endoplasmic reticulum stress. Society for Neuroscience Abstracts, 27(1):566.

Shepard, T.M., **Pike**, B.R., Hayes, R.L., and Wirth, E.D. (2001). Calcium-mediated calpain activation and cell death in the hippocampal slice. Society for Neuroscience Abstracts, 27(1):566.

Johnson, E.A., Wang, K.K.W., **Pike**, B.R., and Hayes, R.L. (2001). Evidence of calpain activation in brain macrophages after traumatic brain injury in rats. Society for Neuroscience Abstracts, 27(1):564.

Beer, R., Franz, G., Krajewski S., **Pike**, B.R., Hayes, R.L., Reed, J.C., Schmutzhard, E., Poewe, W., and Kampfl, A. (2001). Temporal and spatial profile of caspase-8 expression and proteolysis after experimental traumatic brain injury. Society for Neuroscience Abstracts, 27(1):566.

Tolentino, P.J., DeFord, S.M., Notterpeck, L., Glenn, C.C., **Pike**, B.R., Wang, K.K.W., and Hayes, R.L. (2001). Upregulation of tissue-type transglutaminase after traumatic brain injury. Society for Neuroscience Abstracts, 27(1):569.

Shepherd, T.M., **Pike**, B.R., Thelwall, P.E., Hayes, R.L., and Wirth, E.D. (2001). Diffusion-weighted magnetic resonance imaging of cell death in rat hippocampal slices. Journal of Neurotrauma, 18(10):1167.

Flint, J., Dutta S., Wang, K.K.W., DeFord, S.M., Hayes, R.L., and **Pike**, B.R. (2001). Accumulation of αII-spectrin and calpain-cleaved αII-spectrin breakdown products in CSF after traumatic brain injury in rats. Journal of Neurotrauma, 18(10):1184.

DeFord, S.M., **Pike**, B.R., and Hayes, R.L. (2001). Temporal profile of alpha-spectrin breakdown products following repeated vs. single mild head injury in mice. Journal of Neurotrauma, 18(10):1165.

Tolentino, P.J., DeFord, S.M., Notterpeck, L., Glenn, C.C., **Pike**, B.R., Wang, K.K.W., and Hayes, R.L. (2001). Upregulation of tissue-type transglutaminase after traumatic brain injury. Journal of Neurotrauma, 18(10):1141.

Johnson, E.A., Wang, K.K.W., **Pike**, B.R., and Hayes, R.L. (2001). Evidence of calpain activation in brain macrophages after traumatic brain injury. Journal of Neurotrauma, 18(10):1132.

Ringger, N.C., Shepard, T.M., Johnson, E.A., Larner, S.F., West, M.F., Hayes, R.L., and **Pike**, B.R. (2001). Comparison of calpain and caspase-3 activation during necrosis, apoptosis and endoplasmic reticulum stress. Journal of Neurotrauma, 18(10):1163.

Beer, R., Franz, G., Tauber, H., Reindl, M., Lassmann, H., **Pike**, B.R., and Hayes, R.L. (2001). Oligodendrocyte reaction and changes in myelin protein expression after experimental TBI. Journal of Neurotrauma, 18(10):1163.

Franz, G., Beer, R., Krajewski S., Reed, J.C., **Pike**, B.R., Hayes, R.L., Wang, K.K., and Kampfl, A. (2001). Temporal and spatial profile of caspase-8 expression and proteolysis after experimental traumatic brain injury. Journal of Neurotrauma, 18(10):1164.

Pike, B.R., Johnson, E., Flint, J., Glenn, C.C., and Hayes, R.L. (2000). Prolonged calpain activation in regions of tissue atrophy after traumatic brain injury. Restorative Neurology and Neuroscience, 16(3,4):166.

Hayes, R.L., Newcomb, J.K., **Pike**, B.R., Zhao, X., Wang, K.K.W., and Anderson, D.K. (2000). Concurrent calpain and caspase-3 activation following oxygen-glucose deprivation. Restorative Neurology and Neuroscience, 16(3,4):163.

Beer, R., Franz, G., Hayes, R.L., **Pike**, B.R., Srinivasan, A., and Kampfl, A. (2000). Temporal profile and cell subtype distribution of activated caspase-3 following experimental TBI. Restorative Neurology and Neuroscience, 16(3,4):164.

Glenn, C.C., McKinsey, D.M., Earnhardt, J.N., **Pike**, B.R., Nick, H.S., Hayes, R.L., and Anderson, D.K. (2000). Differential gene expression analysis after spinal cord injury by subtraction/suppression hybridization. Journal of Neurotrauma, 17(10):946.

Hayes, R.L., Newcomb, J.K., **Pike**, B.R., Zhao, X., Wang, K.K.W., and Anderson, D.K. (2000). Oxygen-glucose deprivation produces concurrent calpain and caspase-3 activation. Journal of Neurotrauma. 17(10), 949.

Beer, R., Franz, G., Hayes, R.L., **Pike**, B.R., Srinivasan, A., and Kampfl, A. (2000). Temporal profile and cell subtype distribution of activated caspase-3 following experimental traumatic brain injury. Society for Neuroscience Abstracts, 26(2), 2300.

Pike, B.R., Anderson, D.K., and Hayes, R.L. (2000). Mechanisms of cell death following traumatic brain injury: biochemical insights into expression of cell death phenotypes. Journal of Neurochemistry, 74(suppl.), S40A.

Pike, B.R., Zhao, X., Newcomb, J.K., and Hayes, R.L. (1999). Comparison of caspase-3 and calpain substrate cleavage during apoptosis and necrosis. Journal of Neurotrauma, 16(10), 999.

Pike, B.R., Zhao, X., Newcomb, J.K., and Hayes, R.L. (1999). Acute calpain activation followed by delayed caspase-3 activation and apoptotic cell death after stretch injury to septo-hippocampal cultures. Journal of Neurochemistry, 72 (Suppl.), S53A.

Hayes, R.L., Zhao, X., Newcomb, J.K., Markgraf, C.G., and **Pike**, B.R. (1999). Calpain is activated for up to one month in the thalamus after moderate or severe traumatic brain injury. Journal of Neurotrauma, 16(10), 1000.

Zhao, X., **Pike**, B.R., Newcomb, J.K., and Hayes, R.L. (1999). TNF-α stimulates caspase-3 activation and apoptotic cell death in primary septo-hippocampal cultures. Journal of Neurochemistry, 72 (Suppl.), S53B.

Pike, B.R., Zhao, X., Newcomb, J.K., & Hayes, R.L. (1998). Caspase-3 activation after stretch injury in primary septo-hippocampal cultures: relationship to cell viability and morphology. Society for Neuroscience Abstracts, 24(2), 1731.

Pike, B.R., Zhao, X., Newcomb, J.K., & Hayes, R.L. (1998). Caspase-3 activation after stretch injury in primary septo-hippocampal cultures: relationship to cell viability and morphology. Journal of Neurotrauma, 15(10), 891.

Adams, F.S., Scheule, R.K., Pike, B.R., Yu, G-J., & Yang, K. (1998). The application of cationic lipid #67 for CNS gene therepy. Society for Neuroscience Abstracts, 24(2), 1726.

Adams, F.S., Scheule, R.K., Pike, B.R., Yu, G-J., & Yang, K. (1998). The application of cationic lipid #67 for CNS gene therepy. Journal of Neurotrauma, 15(10), 853.

Zhao, X., Pike, B.R., Newcomb, J.K., Wang, K.K.W., and Hayes, R.L. (1998). Mechanisms of pharmacological protection from stretch-induced cell injury in primary cell cultures. Journal of Neurotrauma, 15(10), 904.

Hayes, R.L., Zhao, X., Newcomb, J.K., Pike, B.R., Posmantur, R.M., and Wang, K.K.W. (1998). Novel characteristics of glutamate-induced cell death in primary septo-hippocampal cultures: relationship to calpain and caspase-3 activation. Journal of Neurotrauma, 15(10), 873.

Newcomb, J.K., Zhao, X., Pike, B.R., Wang, K.K.W., and Hayes, R.L. (1998). Proteolytic mechanisms of cell injury following glucose-oxygen deprivation in primary septo-hippocampal cell cultures. Journal of Neurotrauma, 15(10), 887.

Hayes, R.L., Zhao, X., Pike, B.R., Newcomb, J.K., Posmantur, R.M., Wang, K.K.W., & Clifton, G.L. (1998). A comparative study of apoptosis and necrosis in mixed septo-hippocampal cultures. Journal of Neurochemistry, 70 (Suppl. 1), S11.

Pike, B.R., Zhao, X., Wang, K.K.W., Liu, S.J., Newcomb, J.K., Gegeny, T., Posmantur, R.M., Clifton, G.L., & Hayes, R.L. (1997). Calpain and caspase proteolysis of α-spectrin following traumatic brain injury. Society for Neuroscience Abstracts, 23, 2194.

Pike, B.R., Zhao, X., Wang, K.K.W., Liu, S.J., Newcomb, J.K., Gegeny, T., Posmantur, R.M., Clifton, G.L., & Hayes, R.L. (1997). Calpain and caspase proteolysis of α-spectrin following traumatic brain injury. Journal of Neurotrauma, 14(10), 763.

Zhao, X., Pike, B.R., Newcomb, J.K., Posmantur, R.M., Wang, K.K.W., Clifton, G.L., & Hayes, R.L. (1997). The effects of apoptosis or necrosis on septo-hippocampal glial-neuronal cultures. Society for Neuroscience Abstracts, 23, 2194.

Zhao, X., Pike, B.R., Newcomb, J.K., Posmantur, R.M., Wang, K.K.W., Clifton, G.L., & Hayes, R.L. (1997). Apoptosis and necrosis in septo-hippocampal glial-neuronal cultures: a comparative study. Journal of Neurotrauma, 14(10), 778.

Hayes, R.L., Pike, B.R., Zhao, X., Newcomb, J.K., & Clifton, G.L. (1997). Proteolysis of the specific and endogenous calpain inhibitor (calpastatin) following traumatic brain injury. Journal of Neurotrauma, 14(10), 762.

Newcomb, J.K., Zhao, X., Pike, B.R., Clifton, G.L., & Hayes, R.L. (1997). Evidence of apoptosis following controlled cortical impact injury in the rat. Journal of Neurotrauma, 14(10), 763.

Pike, B.R., Zhao, X., Wang, K.K.W., Liu, S.J., Newcomb, J.K., Gegeny, T., Clifton, G.L., & Hayes, R.L. (1997). Regional and temporal characterization of calpain-mediated α-spectrin proteolysis following traumatic brain injury. Journal of Neurochemistry, 69(Suppl.), S144.

Zhao, X., Pike, B.R., Liu, S.J., Newcomb, J.K., Posmantur, R., Wang, K.K.W., Clifton, G.L., & Hayes, R.L. (1997). Subcellular localization and duration of μ-calpain and m-calpain activity following traumatic brain injury in the rat: a casein zymography study. Journal of Neurochemistry, 69(Suppl.), S143.

Pike, B.R., Hamm, R.J., Zhu, J.P., Phillips, L.L., Temple, M.T., & Buck, D.L. (1996). Chronic post-injury administration of a partial muscarinic M_1 agonist improves cognitive outcome and reduces decreases in septal cholinergic acetyltransferase (ChAT) immunoreactivity (IR). Society for Neuroscience Abstracts, 22, 2154.

Temple, M.D., Hamm, R.J., Pike, B.R., Buck, D.L., & Lyeth, B.G. (1996). Time-dependent, chronic administration of D-cycloserine, an NMDA partial agonist, improves cognitive recovery following traumatic brain injury. Society for Neuroscience Abstracts, 22, 2153.

6

Temple, M.D., Hamm, R.J., **Pike**, B.R., O'Dell, D.M., Phillips, L.L., & Lyeth, B.G. (1996). Chronic, post-injury administration of D-cycloserine (DCS), an N-methyl-D-aspartate (NMDA) partial agonist, enhances cognitive recovery following traumatic brain injury (TBI). Journal of Neurotrauma, 13, 597.

Pike, B.R., Hamm, R.J., Temple, M.D., O'Dell, D.M., & Lyeth, B.G. (1995). Activation of the post-traumatic cholinergic system improves cognitive performance in rats: Effects of Lu 25-109-T, a partial muscarinic M_1 agonist with M_2 antagonist effects. Journal of Neurotrauma, 12, 991.

Wiley, J.L., Compton, A.D., Temple, M.D., **Pike**, B.R., O'Dell, D.M., & Hamm, R.J. (1995). Reduced sensorimotor reactivity following traumatic brain injury in rats. Journal of Neurotrauma, 12, 992.

O'Dell, D.M., Hamm, R.J., Temple, M.D., **Pike**, B.R., & Lyeth, B.G. (1995). Pre-injury administration of diazepam is neuroprotective in traumatically brain injured rats. Journal of Neurotrauma, 12, 964.

Pike, B.R., Hamm, R.J., O'Dell, D.M., Temple, M.D., & Lyeth, B.G., (1995). Tacrine slows cognitive recovery following traumatic brain injury and a muscarinic M_2 antagonist reduces its effect. Society for Neuroscience Abstracts, 21, 2120.

Pike, B.R., Hamm, R.J., O'Dell, D.M., Temple, M.D., & Lyeth, B.G. (1995). Post-injury treatment of cognitive impairment: Time dependent effects of a cholinergic M_2 antagonist. Journal of Neurotrauma, 12, 452.

Pike, B.R., Hamm, R.J., O'Dell, D.M., Temple, M.D., & Lyeth, B.G. (1995). The effects of early and delayed administration of a selective muscarinic M_2 receptor antagonist (BIBN 99) on cognitive performance following experimental brain injury in rats. Journal of Neurotrauma, 12, 135.

Pike, B.R., Hamm, R.J., O'Dell, D.M., Temple, M.D., & Lyeth, B.G. (1995). Chronic post-injury administration of BIBN 99, a selective muscarinic M2 receptor antagonist, attenuates cognitive impairment following traumatic brain injury in the rat. Life Sciences, 56, 1048.

O'Dell, D.M., Hamm, R.J., **Pike**, B.R., Temple, M.D., & Lyeth, B.G. (1995). Chronic post-injury administration of tetrahydroaminoacradine does not promote cognitive recovery in injured rats. Journal of Neurotrauma, 12, 393.

Temple, M.D., **Pike**, B.R., Hamm, R.J., & Ellis, E.E. (1995). The effect of post-injury administration of PEG-SOD or lidocaine on behavioral recovery following fluid percussion brain injury in rats. Journal of Neurotrauma, 12, 145.

O'Dell, D.M., Hamm, R.J., **Pike**, B.R., Temple, M.D., & Lyeth, B.G. (1995). Immediate but not delayed chronic treatment with Suritozole (MDL 26,479) attenuates cognitive deficits following traumatic brain injury in the rat. Journal of Neurotrauma, 12, 133.

Hamm, R.J., O'Dell, D., **Pike**, B., Temple, M., & Lyeth, B.G. (1994). Chronic administration of pentylenetetrazol after traumatic brain injury improves cognitive performance of injured rats. Society For Neuroscience Abstracts, 20, 193.

Temple, M.D., Hamm, R.J., O'Dell, D.M., **Pike**, B.R., & Lyeth, B.G. (1994). Evaluation of working memory following traumatic brain injury using the Morris water maze. Society For Neuroscience Abstracts, 20, 197.

Pike, B.R., Hamm, R.J., O'Dell, D.M., & Lyeth, B.G. (1994). The effect of pre- and post-injury treatment with scopolamine and MK-801 on cognitive impairment following traumatic brain injury in rats. Journal Of Neurotrauma, 11(1), 123.

Pike, B.R, Hamm, R.J., O'Dell, D.M., Lyeth, B.G., & Jenkins, L.W. (1993). Traumatic brain injury enhances the amnesic effect of a glutamatergic antagonist and pre-injury treatment blocks the effect. Society For Neuroscience Abstracts, 19, 1883.

Temple, M.D., Hamm, R.J., O'Dell, D.M., **Pike**, B.R., Lyeth, B.G., & Jenkins, L.W. (1993). The effect of an enriched environment on recovery of cognitive function after traumatic brain injury. Society For Neuroscience Abstracts, 19, 1878.

O'Dell, D.M., Hamm, R.J., **Pike**, B.R., Lyeth, B.G., & Jenkins, L.W. (1994). Gustatory neophobia after traumatic brain injury in rats: Evidence of amygdala damage. Journal Of Neurotrauma, 11(1),121.

Hamm, R.J., O'Dell, D.M., **Pike**, B.R., Lyeth, B.G., & Jenkins, L.W. (1992). Selective cognitive impairment following traumatic brain injury in rats. Society For Neuroscience Abstracts, 18, 169.

Hamm, R.J., O'Dell, D.M., **Pike**, B.R., Lyeth, B.G., & Jenkins, L.W. (1992). An analysis of the relative effectiveness of three measures of motor impairment following traumatic brain injury. <u>Journal Of Neurotrauma</u>, <u>9</u>(4), 388.

Temporal and Spatial Profile of Bid Cleavage After Experimental Traumatic Brain Injury

*Gerhard Franz, *Ronny Beer, *Denis Intemann, †Stanislaw Krajewski, †John C. Reed,
*Klaus Engelhardt, ‡Brian R. Pike, ‡Ronald L. Hayes, §Kevin K. Wang, *Erich Schmutzhard,
and *Andreas Kampfl

*Department of Neurology, University Hospital Innsbruck, Innsbruck, Austria; †The Burnham Institute, La Jolla, California;
‡Department of Neuroscience, Evelyn F. and William L. McKnight Brain Institute of the University of Florida, Gainesville,
Florida; and §Department of Neuroscience Therapeutics, Pfizer Inc., Ann Arbor, Michigan, U.S.A.

Summary: Apoptosis plays an essential role in the cascade of CNS cell degeneration after traumatic brain injury. However, the underlying mechanisms are poorly understood. The authors examined the temporal profile and cell subtype distribution of the proapoptotic protein Bid from 6 hours to 7 days after cortical impact injury in the rat. Increased protein levels of tBid were seen in the cortex ipsilateral to the injury site from 6 hours to 3 days after trauma. Immunohistologic examinations revealed expression of tBid in neurons, astrocytes, and oligodendrocytes from 6 hours to 3 days after impact injury, and concurrent assessment of DNA damage using TUNEL identified tBid-immunopositive cells with apoptoticlike morphology in the traumatized cortex. Moreover, Bid cleavage and activation of caspase-8 and caspase-9 occurred at similar time points and in similar brain regions (i.e., cortical layers 2 to 5) after impact injury. In contrast, there was no evidence of caspase-8 or caspase-9 processing or Bid cleavage in the ipsilateral hippocampus, contralateral cortex, and hippocampus up to 7 days after the injury. The results provide the first evidence of Bid cleavage in the traumatized cortex after experimental traumatic brain injury *in vivo,* and demonstrate that tBid is expressed in neurons and glial cells. Further, findings indicate that cleavage of Bid may be associated with the activation of the initiator caspase-8 and caspase-9. Finally, these data support the hypothesis that cleavage of Bid contributes to the apoptotic degeneration of different CNS cells in the injured cortex. **Key Words:** Apoptosis—Bid—Caspases—Neurons—Glia—Traumatic brain injury.

Apoptosis is a feature of acute neurodegenerative diseases, including cerebral ischemia and traumatic brain injury (TBI) (Conti et al., 1998; Faden, 1996; McIntosh et al., 1998; Rink et al., 1995). Moreover, members of the caspase family of cysteine proteases have been implicated as important regulators of apoptosis following TBI. For example, caspase-3 is the major executioner caspase involved in neuronal and glial apoptosis after

TBI *in vivo* (Beer et al., 2000*b*; Clark et al., 2000; Yakovlev et al., 1997) and *in vitro* (Pike et al., 2000).

Two major caspase-3–activating pathways have been identified. The extrinsic pathway involves cell surface receptors such as Fas. Binding of the Fas ligand to Fas allows the recruitment and activation of the initiator caspase-8 (Li et al., 1998), which in turn activates executioner caspase-3 and caspase-7 (Stennicke et al., 1998; van de Craen et al., 1999). Importantly, recent data have emphasized a contributory role for the extrinsic pathway in TBI-induced CNS apoptosis (Beer et al., 2000*a*; 2001; Keane et al., 2001).

The intrinsic apoptotic pathway is initiated by the release of cytochrome *c* to the cytosol. Cytochrome *c* then binds to the adaptor protein Apaf-1, which allows the recruitment and activation of the initiator caspase-9 in the presence dATP (Crompton, 2000; Green and Reed, 1998). Activated caspase-9 then results in caspase-3 processing (Slee et al., 1999). A role for caspase-9 activation in CNS apoptosis in TBI *in vivo* has been established recently (Yakovlev et al., 2001).

One proapoptotic member of the Bcl2 family, referred to as Bid, may play an important role in the sequence of events leading to caspase activation (Crompton, 2000). For example, recent *in vitro* studies have shown that Bid is a specific substrate of caspase-8 in the Fas apoptotic signaling pathway (Li et al., 1998). While inactive full-length (p22) Bid is present in the cytosol, tBid (p15; a truncated form of Bid) translocates to the mitochondria and induces conformational changes in Bax and Bak, triggering cytochrome *c* release into the cytosol with subsequent activation of caspase-9 (Grinberg et al., 2002; Krajewska et al., 2002; McDonnell et al., 1999). Thus, Bid represents an important mediator of cross-talk between the death receptor and the mitochondria pathways.

Although previous findings regarding the processing of caspase-8, caspase-9, and caspase-3 would suggest a contributory role of Bid-induced apoptosis of CNS cells after brain trauma, no studies to date have examined the temporal and spatial profile of Bid cleavage after TBI *in vivo*. To further investigate the processing of Bid after experimental TBI, rodents were subjected to a widely used model of experimental mechanical brain injury: lateral cortical impact injury (Dixon et al., 1991; Franz et al., 1999). Western blot analyses of cortical and hippocampal samples were used to determine the expression and cleavage of Bid after TBI. Immunohistochemical examinations were performed to investigate the cell subtype distribution of tBid, and terminal deoxynucleotidyl transferase-mediated 2′-deoxyuridine 5′-biotin nick end labeling (TUNEL) was used to assess whether tBid-immunopositive cells exhibit morphological features of apoptosis-related DNA damage. Finally, Western blotting and immunolabeling for tBid, caspase-8, and activated caspase-9 was performed to address whether these proteins are expressed at similar time points and in similar brain regions after experimental TBI *in vivo*.

MATERIALS AND METHODS

Rat model of traumatic brain injury

A controlled cortical impact device was used to induce a moderate level of TBI as described previously (Beer et al., 2001; Dixon et al., 1991; Franz et al., 1999). Briefly, adult male Sprague-Dawley rats (250 to 350 g) were intubated and anesthetized with 2% halothane in a 2:1 mixture of $N_2O:O_2$. Core body temperature was monitored continuously by a rectal thermistor probe and maintained at 36.5°C to 37.5°C. Animals were mounted in a stereotaxic frame on the injury device in a prone position, and were secured by ear and incisor bars. The head was held in a horizontal plane with respect to the interaural lines. A midline incision was made, the soft tissues were reflected, and two 7-mm craniotomies were made between lambda and bregma and centered 5 mm laterally on either side of the central suture. The dura was kept intact over the cortex. Injury was induced by impacting the right cortex (ipsilateral cortex) with a 6-mm-diameter tip at a rate of 4 m/sec. The injury device was set to produce a tissue deformation of 2 mm. Velocity was measured directly by the linear velocity displace-

ment transducer (Model 500 HR; Shaevitz, Detroit, MI, U.S.A.), which produces an analog signal that was recorded by a PC-based data acquisition system for analysis of time/displacement parameters of the impactor. After cortical impact, animals were extubated and immediately assessed for recovery of reflexes (Dixon et al., 1991). Sham-injured animals underwent identical surgical procedures but did not receive an impact injury. Naive animals were not exposed to any injury-related surgical procedures. A total of 56 animals were used in this study (naive, n = 8; sham-injured rats, n = 8; injured rats, n = 40). All animal studies carefully conformed to the guidelines outlined in the *Guide for the Care and Use of Laboratory Animals* from the Austrian Department of Health and Science, and were approved by the University of Innsbruck Medical School Animal Welfare Committee. Importantly, all efforts were made to minimize animal suffering and to reduce the number of animals used.

Sample preparation, sodium dodecyl sulfate-polyacrylamide gel electrophoresis, immunoblotting, and quantification

All animals (n = 28) received a lethal dose of intraperitoneal phenobarbital (20 mg/kg; Tyrol Pharma, Austria) and were killed by decapitation 6 hours or 1, 2, 3, or 7 days after TBI (n = 4 for each time point after injury; n = 2 for sham-injured and naive animals). Sham-injured animals were killed 6 hours and 2 days after sham surgery, respectively. Both cortices and hippocampi (ipsilateral and contralateral to the injury site) were removed. Excision of both cortices beneath the craniotomies extended approximately 4 mm laterally, approximately 7 mm rostrocaudally, and to a depth extending to the white matter. All samples were immediately frozen in liquid N_2. The microdissected tissue was homogenized at 4°C in ice-cold homogenization buffer containing 20 mmol/L piperazine-N,N′-bis (2-ethanesulfonic acid) (pH 7.1), 2 mmol/L ethylene glycol-bis (β-aminoethyl ether)-N,N,N′,N′-tetraacetic acid, 1 mmol/L ethylenediamine tetraacetic acid, 1 mmol/L dithiothreitol, 0.3 mmol/L phenylmethylsulfonylfluoride, and 0.1 mmol/L leupeptin. Chelators and protease inhibitors (Sigma, St. Louis, MO, U.S.A.) were added to prevent endogenous *in vitro* activation of proteases and subsequent artifactual degradation of Bid and caspases during tissue processing.

Protein concentrations were determined by bicinchoninic acid microprotein assays (Sigma) with albumin standards. Protein-balanced samples were prepared for polyacrylamide gel electrophoresis. Sixty micrograms of protein per lane was routinely resolved on 16% Tris/glycine gels (Invitrogen, Groningen, The Netherlands). After separation, proteins were immediately transferred to nitrocellulose membranes using Western blotting as described previously (Beer et al., 2001). Coomassie blue (Bio-Rad, Hercules, CA, U.S.A.) and Ponceau red (Sigma) staining were routinely performed to confirm successful transfer of protein and to insure that equal amounts of protein were loaded in each lane. Five-percent nonfat milk in phosphate-buffered saline (PBS) with 0.05% Tween 20 was used to reduce nonspecific binding. Immunoblots were probed with a mouse monoclonal antibody (diluted 1:1000; Santa Cruz Biotechnology, Santa Cruz, CA, U.S.A.) reacting with the p20 subunit and precursor of caspase-8 (Beer et al., 2001), a rabbit polyclonal antiserum (diluted 1:2500) against the large subunit (p35) of caspase-9 (The Burnham Institute, La Jolla, CA, U.S.A.; Krajewski et al., 1999), a rabbit polyclonal antibody (diluted 1:2500; Pharmingen, San Diego, CA, U.S.A.) directed against full-length Bid, or a polyclonal anti-Bid antiserum (diluted 1:2500; The Burnham Institute) recognizing cleaved tBid (Krajewska et al., 2002). Specificity of the anti-Bid antisera was

confirmed by preabsorption with recombinant full-length or truncated Bid (obtained by incubation of recombinant Bid with recombinant active caspase-8), respectively. After incubation with primary antibodies overnight at 4°C, nitrocellulose membranes (Amersham Pharmacia Biotech, Uppsala, Sweden) were incubated with secondary antibodies linked to horseradish peroxidase (Amersham Pharmacia Biotech) for 1 hour at ambient temperature. Enhanced chemiluminescence reagents (Amersham Pharmacia Biotech) were used to visualize the immunolabeling on X-ray film. In each blot, the constitutively expressed protein α-tubulin (Sigma) was used as an internal standard to further indicate that sample processing was performed correctly.

Immunohistochemistry

Animals from all treatment groups (n = 28) received a lethal injection of intraperitoneal phenobarbital (20 mg/kg) before perfusion. Rats were transcardially perfused through the left ventricle (120 mL 0.9% saline and 200 mL 4% paraformaldehyde) at 6 hours or 1, 2, 3, or 7 days after TBI (n = 4 for each time point after injury; n = 4 for sham and naive animals). The brains were removed, grossly sectioned coronally at 2-mm intervals, and routinely embedded in paraffin. Sections were then cut at 3 to 4 microns on a rotary microtome, mounted on aminoalkylsilated glass slides, and processed for immunohistochemical staining as described previously (Beer et al., 2000a,b; 2001). Consecutive sections from the primary injury zone were probed with anticaspase-8 (rabbit polyclonal antiserum, The Burnham Institute) (Beer et al., 2001), anticaspase-9 p35 (rabbit polyclonal antiserum, The Burnham Institute) (Krajewski et al., 1999) and anti-Bid (rabbit polyclonal antiserum, The Burnham Institute) (Krajewska et al., 2002). Antibodies were diluted 1:5000 in 10% fetal calf serum in PBS and permitted to bind overnight at 4°C. Biotinylated goat antirabbit secondary antibody (Vector Laboratories, Burlingame, CA, U.S.A.) was then applied at a dilution of 1:200 in 3% rat serum in PBS for 1 hour at ambient temperature followed by avidinperoxidase (Sigma), diluted 1:100 in PBS, also for 1 hour at ambient temperature. The reaction was visualized by treatment with 0.05% 3,3-diaminobenzidine tetrahydrochloride solution in PBS containing 0.05% H_2O_2. The color reaction was stopped with several washes of PBS. Immunostaining results were confirmed by preimmune serum from the same animals and by preabsorption of the polyclonal antibodies with the relevant recombinant protein. In addition, sections without primary antibodies were similarly processed to control for binding of the secondary antibody. On control sections, no specific immunoreactivity was detected.

For double immunostaining using brightfield chromagens, sections were pretreated with the rabbit polyclonal antiserum against Bid as described previously. Sections were then incubated with a mouse monoclonal anti-NeuN (neuron-specific nuclear protein) antibody (Wolf et al., 1996) (Chemicon, Temecula, CA, U.S.A.) for neuronal staining. For staining of astrocytes and oligodendrocytes, a mouse monoclonal anti–glial fibrillary acid protein (GFAP) antibody (Debus et al., 1983) (Roche Molecular Biochemicals, Mannheim, Germany) or an anti-CNPase (2′,3′-cyclic-nucleotide-3′-phosphodiesterase) monoclonal antibody (Sprinkle, 1989) (Sternberger Monoclonals Inc., Lutherville, MD, U.S.A.) was used. All antibodies were diluted 1:500 in 10% fetal calf serum in PBS and were allowed to bind overnight at 4°C. Sections were rinsed and incubated with a biotinylated horse antimouse antibody (Vector Laboratories) at a dilution of 1:200 for 1 hour at ambient temperature, followed by incubation with an alkaline phosphatase avidin-biotin substrate and then reaction with blue chromagen

(Vector Blue; Vector Laboratories). The color reaction was stopped with several washes of PBS. Sections were dehydrated with graded ethanol, cleared in a xylene substitute (Histoclear; National Diagnostics, Atlanta, GA, U.S.A.), mounted in Permount (Fisher Scientific, Nepean, Ontario, Canada), and coverslipped. Control experiments were performed in which the primary antibodies were omitted. No staining was observed under these conditions.

For histochemical detection of DNA fragmentation on selected representative sections, TUNEL was performed as described by Gavrieli et al. (1992) with minor modifications (Beer et al., 2000a; 2001). The TUNEL reaction was visualized by treatment for 5 minutes with 5-bromo-4-chloro-3-indolyl phosphate/nitro blue tetrazolium substrate system (Dako Corporation, Carpinteria, CA, U.S.A.). For double-label experiments, sections were then processed for Bid immunohistochemistry as described earlier. Immunohistochemical staining was visualized by exposure to 3-amino-9-ethylcarbazole in N,N′-dimethylformamide (Sigma). Primary antibody, labeling mix, or secondary antibody was omitted in control sections. Sections were mounted using an aqueous mounting fluid (Dako Corporation) and examined under the light microscope.

Statistical analysis

Semiquantitative evaluation of immunoreactivity detected by Western blotting was performed using computer-assisted two-dimensional densitometric scanning on a Macintosh computer using the public domain NIH Image program (developed at the US National Institutes of Health and available at http://rsb.info.nih.gov/nih-image/). Relative band densities on Western blots (n = 1 per blot) were expressed as arbitrary densitometric units for each time point. This procedure was performed for the data from four independent experiments, for a total of four different animals per time point. Data acquired in arbitrary densitometric units were transformed to percentages of the densitometric levels observed for scans from sham animals on the same blot. Group differences were determined by analysis of variance and the Tukey *post hoc* honestly significant difference test. Values are mean ± SD of four independent experiments. Differences were considered significant when $P < 0.05$.

RESULTS

Western blotting

Cortical impact injury leads to cleavage of Bid in the ipsilateral cortex. To determine whether Bid is cleaved after TBI, brain extracts from cortex and hippocampus ipsilateral and contralateral to the injury site were examined by Western blotting for the expression of full-length Bid (22 kd) and tBid (15 kd). In the ipsilateral cortex, cortical impact resulted in decreased protein levels of full-length Bid from 6 hours to 3 days after trauma (Fig. 1A), and the lowest immunoreactivity was observed at 1 day after injury (64% decrease relative to sham-injured animals). Concomitantly, tBid immunoreactivity increased within 6 hours after TBI, peaked at 1 day after the impact (793% increase relative to sham animals), and was still significantly increased 2 days and 3 days after impact injury (Fig. 1B). After 7 days, no statistically significant increase in tBid immunoreactivity was evident when compared with levels of sham-injured control animals. In the ipsilateral hippocampus, contralateral
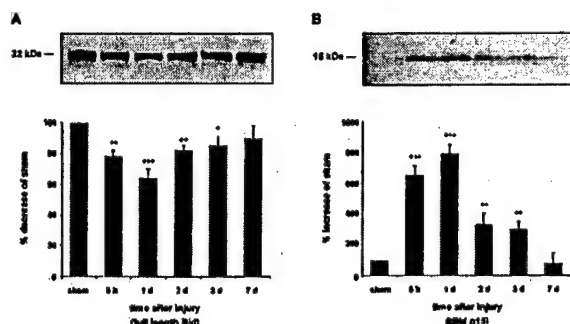
FIG. 1. Time course of Bid protein expression **(A)** and cleavage **(B)** after traumatic brain injury (TBI). Samples from single-control (sham-injured) and single-injured animals were prepared for Western blotting 6 hours to 7 days after TBI. Immunoreactivity is expressed as arbitrary densitometric units. Data were transformed to percentages of the densitometric levels observed on scans from sham-injured animals visualized on the same blot. Values are mean ± SD of four independent experiments. **(A)** Ipsilateral cortex: immunoblots showed processing of full-length Bid (22 kd) at 6 hours ($++P < 0.01$), 1 day ($+++P < 0.001$), 2 days ($++P < 0.01$), and 3 days ($+P < 0.05$) after TBI. **(B)** Immunoreactivity of cleaved Bid (tBid, 15 kd) increased significantly 6 hours after TBI ($+++P < 0.001$), peaked at 1 day after injury ($+++P < 0.001$), and remained significantly increased up to 3 days after trauma ($++P < 0.01$).

cortex, and hippocampus, TBI resulted in no apparent alteration in immunoreactivity of full-length and cleaved Bid (data not shown).

Proteolytic processing of caspase-8 and caspase-9 occurs in the injured cortex. Because Bid cleavage infers with the activation of caspase-8 and caspase-9, processing of these two caspases was examined by Western blot analysis. Using a monoclonal anticaspase-8 antibody that recognizes both procaspase-8 (p55) and its large subunit (p20), an increase of p55 and p20 caspase-8 immunoreactivity was observed in the ipsilateral cortex from 6 hours to 3 days after TBI (Fig. 2A). Immunoreactivity for caspase-8 p20 increased significantly within 6 hours, peaked at 1 day after the impact (860% increase as compared with sham animals), and was still significantly increased at 2 days and 3 days after impact injury. After 7 days, no significant increase was evident in the p55 and p20 fragments when compared with levels in sham-injured control animals. These results are consistent with a previous report on caspase-8 expression and proteolysis after experimental TBI (Beer et al., 2001). Further, immunoblots of cortical samples ipsilateral to the injury site showed an increase in the immunoreactivity for the large subunit (p35) of activated caspase-9 from 6 hours to 3 days after TBI. Densitometric measures of caspase-9 p35 protein levels from injured animals revealed a 325% increase relative to sham levels at 6 hours after TBI (Fig. 2B). The increase of caspase-9 p35 immunoreactivity reached a maximum level 2 days after impact injury (840% increase relative to sham-injured animals) and declined to a 520% increase relative

to the sham group at 3 days after TBI. At 7 days after trauma, no statistically significant difference in caspase-9 p35 immunoreactivity was observed between cortical samples ipsilateral to the injury site and cortical samples from sham-injured animals.

No significant increases in caspase-8 and caspase-9 p35 immunoreactivity were seen between sham-injured and injured animals in cortical samples contralateral to the injury site and hippocampal samples ipsilateral and contralateral to the injury site 6 hours to 7 days after TBI (data not shown).

Immunohistochemistry

Immunohistochemical staining for tBid, caspase-8, and caspase-9, and cell subtype distribution of tBid after traumatic brain injury. Ipsilateral and contralateral cortical and hippocampal tissues were examined rostrocaudally from +0.2 to −3.8 mm bregma. No immunoreactivity for tBid (Fig. 3A), caspase-8, and activated caspase-9 was present in the tissue from sham-injured or naive (data not shown) control rats. Positive immunoreactivity for tBid (Figs. 3B and 3E), caspase-8 (Fig. 3C), and processed caspase-9 (Fig. 3D) was found throughout the ipsilateral cortex at the primary injury zone (from −1.5 to −3.4 mm bregma, cortical layers 2 to 5) from 6 hours to 3 days after the trauma (time point = 1 day after trauma, −3.4 mm bregma). Immunoreactivity for tBid, caspase-8, and activated caspase-9 was absent in contralateral cortical samples and hippocampal samples ipsilateral and contralateral to the injury site at all time points investigated (data not shown).
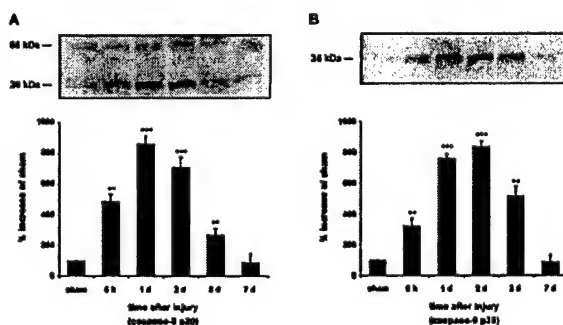

FIG. 2. Time course of caspase-8 p20 **(A)** and caspase-9 p35 **(B)** protein expression after traumatic brain injury (TBI). Samples from single-control (sham-injured) and single-injured animals were prepared for Western blotting 6 hours to 7 days after TBI. Immunoreactivity is expressed as arbitrary densitometric units. Data were transformed to percentages of the densitometric levels observed on scans from sham-injured animals visualized on the same blot. Values are mean ± SD of four independent experiments. Ipsilateral cortex: the proteolytically active fragments of caspase-8 p20 **(A)** and caspase-9 p35 **(B)** increased significantly within 6 hours after TBI ($++P < 0.01$). **(A)** Caspase-8 p20 immunoreactivity peaked at 1 day after injury ($+++P < 0.001$) and remained increased until 3 days after trauma ($++P < 0.01$). **(B)** Caspase-9 p35 immunoreactivity peaked at 2 days after TBI ($+++P < 0.001$) and remained significantly increased 3 days after impact injury ($++P < 0.01$).
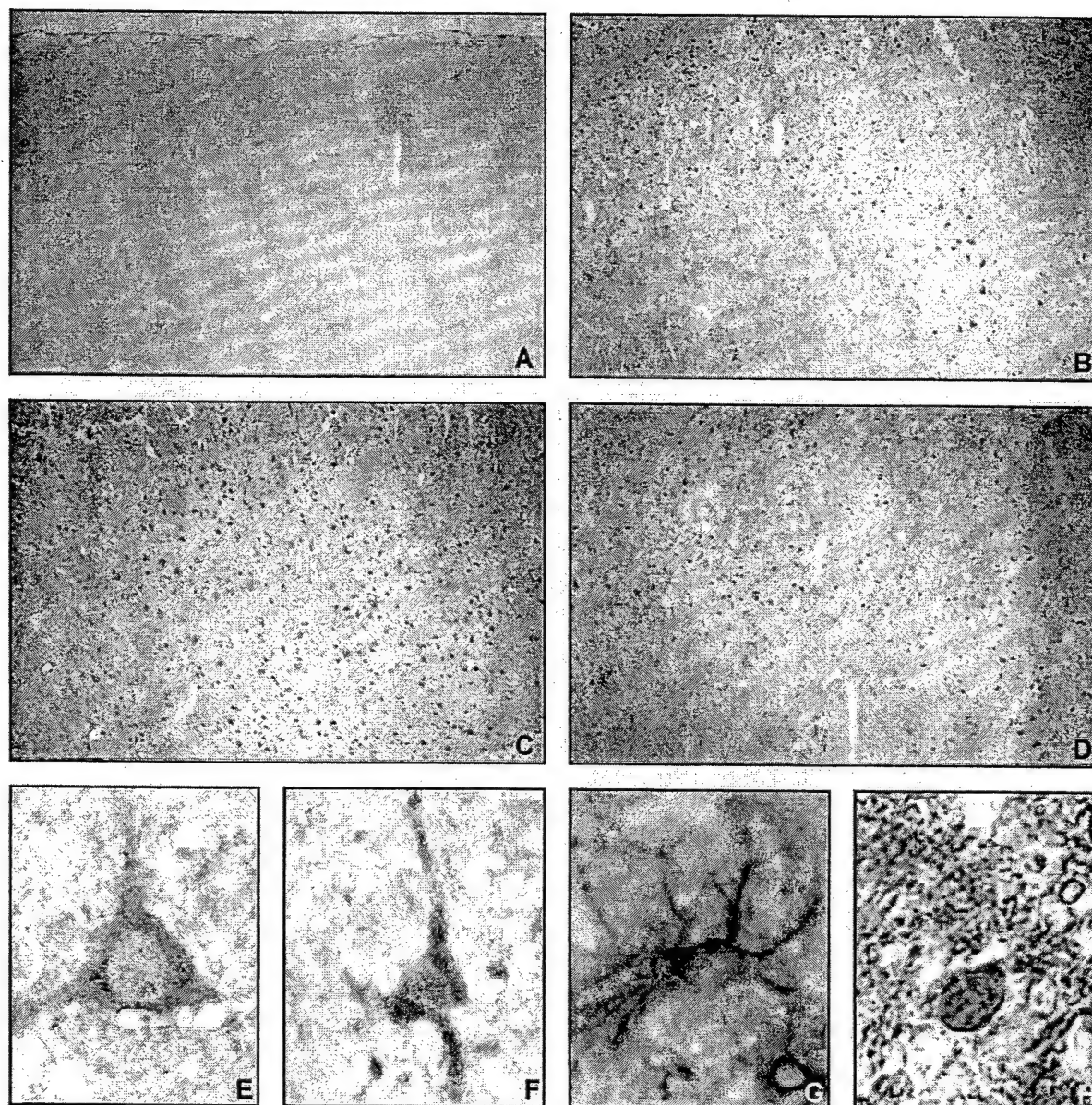
FIG. 3. Immunohistochemical analysis of tBid, caspase-8 p20, caspase-9 p35, and cell-subtype distribution of tBid in the traumatized cortex (−3.4 mm bregma) 1 day after traumatic brain injury (TBI). Sham-injured controls showed no specific immunolabeling for tBid **(A)**. Intermediate **(B)** and high-magnification **(E)** photomicrographs showed specific tBid expression in the ipsilateral cortex after impact injury. Cells immunopositive for caspase-8 p20 **(C)** and caspase-9 p35 **(D)** were found within similar brain region on consecutive sections (± 10 µm). Double-immunostaining experiments with tBid (brown, **F–H**) and NeuN (blue, **F**), GFAP (blue, **G**), and CNPase (blue, **H**) provided evidence that tBid is expressed in cortical neurons **(F)**, astrocytes **(G)**, and oligodendrocytes **(H)** after TBI. Magnifications: A, 40×; B–D, 100×; E–H, 1000×.

To further investigate whether tBid is expressed in neurons or glial cells, we performed double-labeling experiments for tBid and the neuronal cell-specific marker NeuN, the astrocytic marker GFAP, and the oligodendroglial marker CNPase, respectively. These immunohistochemical analyses of tBid-positive cells from 6 hours to 3 days after TBI (Fig. 3F–H; time point = 1 day after trauma, −3.4 mm bregma) identified labeling with NeuN, GFAP, and CNPase, and demonstrated the expression of tBid in neurons (Fig. 3F), astrocytes (Fig. 3G), and oligodendrocytes (Fig. 3H).

tBid-immunopositive cells exhibit nuclear apoptoticlike morphology. To further verify an apoptotic component of posttraumatic cell death and to determine the role of tBid in trauma-induced apoptosis, sections immunopositive for tBid were processed for TUNEL to assess

DNA damage. Double-labeling experiments (Fig. 4) demonstrated that a substantial proportion of TUNEL-positive cells with shrunken morphology, condensed nuclei, and chromatin margination (Fig. 4, arrows) also expressed tBid in layers 2 to 5 at the primary injury zone (time point = 1 day after trauma, bregma –3.4 mm). However, cells with tBid immunoreactivity or gross apoptoticlike morphology alone were also detected (Fig. 4).

DISCUSSION

Our results provide the first evidence for Bid expression and activation after experimental TBI. In the cortex ipsilateral to the injury site, increased immunoreactivity for activated tBid was detected from 6 hours to 3 days after TBI, and immunohistochemistry demonstrated expression of tBid in neurons, astrocytes, and oligodendrocytes at similar time points. In addition, our data revealed expression of tBid in CNS cells with apoptoticlike morphology in the traumatized cortex. Finally, our data suggest that caspase-8, caspase-9, and Bid are activated in similar brain regions of the injured cortex from 6 hours to 3 days after experimental brain trauma.

Only limited data exist regarding the putative role of Bid for apoptotic degeneration in chronic and acute neurologic disorders. For example, cleaved Bid has been implicated in apoptosis of neurons in Parkinson disease (Viswanath et al., 2001) and experimental epilepsy (Henshall et al., 2001). Further, tBid may also mediate apoptotic neuronal cell death after focal cerebral ischemia (Plesnila et al., 2001). In this regard, it is noteworthy that cortical impact injury may produce focal ischemia in the cortex ipsilateral to the injury site (Bryan et al., 1995). Thus, reduced cerebral blood flow may have contributed to Bid activation in our experiments.
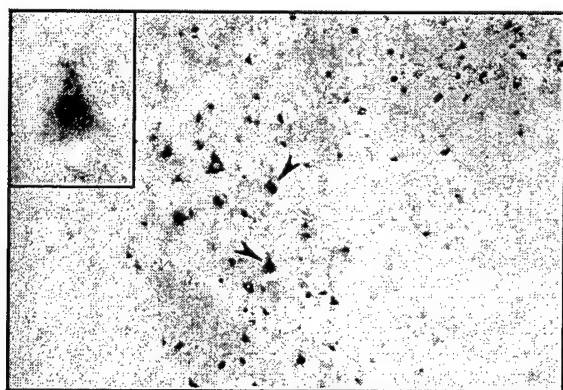

FIG. 4. Appearance of tBid in TUNEL-positive cells in the traumatized cortex (–3.4 mm bregma) 1 day after traumatic brain injury. Combined immunohistochemistry for tBid (red color) and TUNEL (dark blue color) showed processing of Bid in cells with gross nuclear apoptoticlike morphology. The TUNEL-positive cells exhibited chromatin condensation and nuclear fragmentation (arrows). Magnification: 200x; insert, 1,000x.

Bid is a specific substrate of the initiator caspase-8 in the Fas apoptotic signaling pathway (Li et al., 1998). Importantly, we and others have documented increased expression of Fas and activation of caspase-8 after experimental brain trauma (Beer et al., 2000a; 2001; Keane et al., 2001). Our data now indicate that activated caspase-8 and tBid are expressed at similar time points and in similar cortical regions after cortical impact injury, which may suggest a contributory role of activated caspase-8 in the cleavage and activation of Bid. However, a current report also provided evidence that other proteases such as calpain may cleave Bid to an active fragment capable of mediating cytochrome c release in experimental myocardial ischemia (Chen et al., 2001). Therefore, future studies are needed to further investigate the potential role of other proteases in Bid processing after experimental brain injury, as calpain may play an important role in the degeneration of CNS cells after brain trauma (Kampfl et al., 1997; Saatman et al., 2000) and cerebral ischemia (Neumar et al., 1996) in vivo.

Our double-labeling experiments revealed the expression of tBid in neurons, astrocytes, and oligodendrocytes. Interestingly, expression of tBid has recently been shown in neurons and astrocytes after oxygen/glucose deprivation in vitro (Plesnila et al., 2001). Importantly, our results are the first to indicate that tBid is expressed in neurons and glial cells after up to 3 days after experimental brain injury in vivo, and that tBid is seen in CNS cells with apoptoticlike morphology. These results may suggest that even delayed treatment paradigms targeting Bid cleavage may prevent apoptotic cell death after acute brain injuries in vivo. In this regard, it is noteworthy that a recent report revealed that Bid-deficient neurons are more resistant to death after oxygen/glucose deprivation in vitro (Plesnila et al., 2001).

Current data suggest that tBid causes cytochrome c release from mitochondria, which results in the activation of caspase-9 and subsequently caspase-3 (Budihardjo et al., 1999). However, only limited data exist regarding the release of cytochrome c and the activation of caspase-9 after TBI in vivo (Buki et al 2000; Keane et al 2001; Yakovlev et al., 2001). Interestingly, the present study found that tBid and activated caspase-9 are expressed in similar brain regions at similar time points after cortical impact injury in the rat. These data may support the hypothesis that tBid contributes to the activation of caspase-9 in the traumatized cortex from 6 hours to 3 days after TBI. However, future studies are needed to further elucidate the exact role of tBid in caspase-9 activation after different acute CNS injuries in vitro and in vivo.

Our study failed to detect tBid, caspase-8, caspase-9, and apoptotic CNS morphology in the hippocampus ipsilateral to the injury site at the investigated time points. Previous reports clearly describe features of apoptotic

neuronal degeneration in the hippocampus (Clark et al., 2000; Yakovlev et al., 1997). However, previous studies in our laboratory (Beer et al., 2000a,b; 2001; Franz et al., 1999) have shown that cortical impact injury may not necessarily be associated with hippocampal neuronal degeneration. Probable reasons for discrepancies in the appearance of hippocampal damage may be subtle methodological differences in animal models of TBI. For example, differences in angulation and velocity of the impact devices could account for the absence of hippocampal degeneration.

In summary, our data suggest that activation of Bid occurs in the traumatized cortex after cortical impact injury in the rat, and that Bid cleavage is associated with caspase-8 and caspase-9 activation. As Bid is strategically located upstream of mitochondria and caspase-3 processing, it may represent an attractive therapeutic target for CNS diseases in which apoptotic cell death is prominent. However, this implicates the need for further investigations of the significance of Bid cleavage inhibition on functional outcome after TBI.

REFERENCES

Austrian Department of Health and Science (1989) Guide for the care and use of laboratory animals. *Federal Law Gazette* 501

Beer R, Franz G, Krajewski S, Pike BR, Hayes RL, Reed JC, Wang KK, Klimmer C, Schmutzhard E, Poewe W, Kampfl A (2001) Temporal and spatial profile of caspase 8 expression and proteolysis after experimental traumatic brain injury. *J Neurochem* 78:862–873

Beer R, Franz G, Schöpf M, Reindl M, Zelger B, Schmutzhard E, Poewe W, Kampfl A (2000a) Expression of Fas and Fas ligand after experimental traumatic brain injury in the rat. *J Cereb Blood Flow Metab* 20:669–677

Beer R, Franz G, Srinivasan A, Hayes RL, Pike BR, Newcomb JK, Zhao X, Schmutzhard E, Poewe W, Kampfl A (2000b) Temporal profile and cell subtype distribution of activated caspase-3 following experimental traumatic brain injury. *J Neurochem* 75:1264–1273

Budihardjo I, Oliver H, Lutter M, Luo X, Wang X (1999) Biochemical pathways of caspase activation during apoptosis. *Annu Rev Cell Dev Biol* 15:269–290

Bryan RM, Cherian L, Robertson C (1995) Regional cerebral blood flow after controlled cortical impact injury in rats. *Anesth Analg* 80:687–695

Buki A, Okonkwo DO, Wang KK, Povlishock JT (2000) Cytochrome c release and caspase activation in traumatic axonal injury. *J Neurosci* 20:2825–2834

Chen M, He H, Zhan S, Krajewski S, Reed JC, Gottlieb RA (2001) Bid is cleaved by calpain to an active fragment *in vitro* and during myocardial ischemia/reperfusion. *J Biol Chem* 276:30724–30728

Clark RS, Kochanek PM, Watkins SC, Chen M, Dixon CE, Seidberg NA, Melick J, Loeffert JE, Nathaniel PD, Jin KL, Graham SH (2000) Caspase-3 mediated neuronal death after traumatic brain injury in rats. *J Neurochem* 74:740–753

Conti AC, Raghupathi R, Trojanowski JQ, McIntosh TK (1998) Experimental brain injury induces regionally distinct apoptosis during the acute and delayed post-traumatic period. *J Neurosci* 18:5663–5672

Crompton M (2000) Bax, Bid and the permeabilization of the mito-chondrial outer membrane in apoptosis. *Curr Opin Cell Biol* 12:414–419

Debus E, Weber K, Osborn M (1983) Monoclonal antibodies specific for glial fibrillary acidic (GFA) protein and for each of the neurofilament triplet polypeptides. *Differentiation* 25:193–203

Dixon CE, Clifton GL, Lighthall JW, Yaghmai AA, Hayes RL (1991) A controlled cortical impact model of traumatic brain injury in the rat. *J Neurosci Methods* 39:253–262

Faden AI (1996) Pharmacologic treatment of acute traumatic brain injury. *JAMA* 276:569–570

Franz G, Reindl M, Patel SC, Beer R, Unterrichter I, Berger T, Schmutzhard E, Poewe W, Kampfl A (1999) Increased expression of apolipoprotein D following experimental traumatic brain injury. *J Neurochem* 73:1615–1625

Gavrieli Y, Sherman Y, Ben-Sasson SA (1992) Identification of programmed cell death *in situ* via specific labeling of nuclear DNA fragmentation. *J Cell Biol* 119:493–501

Green DR, Reed JC (1998) Mitochondria and apoptosis. *Science* 281:1309–1312

Grinberg M, Sarig R, Zaltsman Y, Frumkin D, Grammatikakis N, Reuveny E, Gross A (2002) tBID homooligomerizes in the mitochondrial membrane to induce apoptosis. *J Biol Chem* 277:12237–12245

Henshall DC, Bonislawski DP, Skradski SL, Lan JQ, Meller R, Simon RP (2001) Cleavage of bid may amplify caspase-8-induced neuronal death following focally evoked limbic seizures. *Neurobiol Dis* 8:568–580

Kampfl A, Posmantur RM, Zhao X, Schmutzhard E, Clifton GL, Hayes RL (1997) Mechanisms of calpain proteolysis following traumatic brain injury: implications for pathology and therapy: a review and update. *J Neurotrauma* 14:121–134

Keane RW, Kraydieh S, Lotocki G, Alonso OF, Aldana P, Dietrich WD (2001) Apoptotic and antiapoptotic mechanisms after traumatic brain injury. *J Cereb Blood Flow Metab* 21:1189–1198

Krajewska M, Mai JK, Zapata JM, Ashwell KW, Schendel SL, Reed JC, Krajewski S (2002) Dynamics of expression of apoptosis-regulatory proteins Bid, Bcl-2, Bcl-X, Bax and Bak during development of murine nervous system. *Cell Death Differ* 9:145–157

Krajewski S, Krajewska M, Ellerby LM, Welsh K, Xie Z, Deveraux QL, Salvesen GS, Bredesen DE, Rosenthal RE, Fiskum G, Reed JC (1999) Release of caspase-9 from mitochondria during neuronal apoptosis and cerebral ischemia. *Proc Natl Acad Sci U S A* 96:5752–5757

Li H, Zhu H, Xu CJ, Yuan J (1998) Cleavage of BID by caspase 8 mediates the mitochondrial damage in the Fas pathway of apoptosis. *Cell* 94:491–501

McDonnell JM, Fushmann D, Milliman CL, Korsmeyer SJ, Cowburn D (1999) Solution structure of the proapoptotic molecule Bid: a structural basis for apoptotic agonists and antagonists. *Cell* 96:625–634

McIntosh TK, Saatman KE, Raghupathi R, Graham DI, Smith DH, Lee VM, Trojanowski JQ (1998) The Dorothy Russell Memorial Lecture. The molecular and cellular sequelae of experimental traumatic brain injury: pathogenetic mechanisms. *Neuropathol Appl Neurobiol* 24:251–267

Neumar RW, Hagle SM, DeGracia DJ, Krause GS, White BC (1996) Brain mu-calpain autolysis during global cerebral ischemia. *J Neurochem* 66:421–424

Pike BR, Zhao X, Newcomb JK, Glenn CC, Anderson DK, Hayes RL (2000) Stretch injury causes calpain and caspase-3 activation and necrotic and apoptotic cell death in septo-hippocampal cell cultures. *J Neurotrauma* 17:283–298

Plesnila N, Zinkel S, Le DA, Amin-Hanjani S, Wu Y, Qiu J, Chiarugi A, Thomas SS, Kohane DS, Korsmeyer SJ, Moskowitz MA (2001) BID mediates neuronal cell death after oxygen/glucose deprivation and focal cerebral ischemia. *Proc Natl Acad Sci U S A* 98:15318–15323

Rink A, Fung KM, Trojanowski JQ, Lee VM, Neugebauer E, McIntosh TK (1995) Evidence of apoptotic cell death after experimental traumatic brain injury in the rat. *Am J Pathol* 147:1575–1583

Saatman KE, Zhang C, Bartus RT, McIntosh TK (2000) Behavioral efficacy of posttraumatic calpain inhibition is not accompanied by

reduced spectrin proteolysis, cortical lesion, or apoptosis. *J Cereb Blood Flow Metab* 20:66–73

Slee EA, Harte MT, Kluck RM, Wolf BB, Casiano CA, Newmeyer DD, Wang HG, Reed JC, Nicholson DW, Alnemri ES, Green DR, Martin SJ (1999) Ordering the cytochrome c-initiated caspase cascade: hierarchical activation of caspases-2, -3, -6, -7, -8, and -10 in a caspase-9-dependent manner. *J Cell Biol* 144:281–292.

Sprinkle TJ (1989) 2′,3′-cyclic nucleotide 3′ phosphodiesterase, an oligodendrocyte-Schwann cell and myelin-associated enzyme of the nervous system. *Crit Rev Neurobiol* 4:235–301

Stennicke HR, Jurgensmeier JM, Shin H, Deveraux Q, Wolf BB, Yang X, Zhou Q, Ellerby HM, Ellerby LM, Bredesen D, Green DR, Reed JC, Froelich CJ, Salvesen GS (1998) Pro-caspase-3 is a major physiologic target of caspase-8. *J Biol Chem* 273:27084–27090

Van de Craen M, Declercq W, Van den Brande I, Fiers W, Vandenabeele P (1999) The proteolytic procaspase activation network: an *in vitro* analysis. *Cell Death Differ* 6:1117–1124

Viswanath V, Wu Y, Boonplueang R, Chen S, Stevenson FF, Yantiri F,

Yang L, Beal MF, Andersen JK (2001) Caspase-9 activation results in downstream caspase-8 activation and bid cleavage in 1-methyl-4-phenyl-1,2,3,6-tetrahydropyridine-induced Parkinson's disease. *J Neurosci* 21:9519–9528

Wolf HK, Buslei R, Schmidt-Kastner R, Schmidt-Kastner PK, Pietsch T, Wiestler OD, Bluhmke I (1996) NeuN: a useful neuronal marker for diagnostic histopathology. *J Histochem Cytochem* 44:1167–1171

Yakovlev AG, Knoblach SM, Fan L, Fox GB, Goodnight R, Faden AI (1997) Activation of CPP32-like caspases contributes to neuronal apoptosis and neurological dysfunction after traumatic brain injury. *J Neurosci* 17:7415–7424

Yakovlev AG, Ota K, Wang G, Movsesyan V, Bao WL, Yoshihara K, Faden AI (2001) Differential expression of apoptotic protease-activating factor-1 and caspase-3 genes and susceptibility to apoptosis during brain development and after traumatic brain injury. *J Neurosci* 21:7439–7446

Accumulation of non-erythroid αII-spectrin and calpain-cleaved αII-spectrin breakdown products in cerebrospinal fluid after traumatic brain injury in rats

Brian R. Pike,* Jeremy Flint,* Satavisha Dutta,† Erik Johnson*, Kevin K. W. Wang† and Ronald L. Hayes*

*Department of Neuroscience, Evelyn F. and William L. McKnight Brain Institute of the University of Florida, Gainesville, Florida, USA

†Department of Neuroscience Therapeutics, Pfizer Inc, Ann Arbor, Michigan, USA

Abstract

Although a number of increased CSF proteins have been correlated with brain damage and outcome after traumatic brain injury (TBI), a major limitation of currently tested biomarkers is a lack of specificity for defining neuropathological cascades. Identification of surrogate biomarkers that are elevated in CSF in response to brain injury and that offer insight into one or more pathological neurochemical events will provide critical information for appropriate administration of therapeutic compounds for treatment of TBI patients. Non-erythroid αII-spectrin is a cytoskeletal protein that is a substrate of both calpain and caspase-3 cysteine proteases. As we have previously demonstrated, cleavage of αII-spectrin by calpain and caspase-3 results in accumulation of protease-specific spectrin breakdown products (SBDPs) that can be used to monitor the magnitude and temporal duration of protease activation. However, accumulation of αII-spectrin and αII-SBDPs in CSF after TBI has never been examined. Following a moderate level (2.0 mm) of controlled cortical impact TBI in rodents, native αII-spectrin protein was decreased in brain tissue and increased in CSF from 24 h to 72 h after injury. In addition, calpain-specific SBDPs were observed to increase in both brain and CSF after injury. Increases in the calpain-specific 145 kDa SBDP in CSF were 244%, 530% and 665% of sham-injured control animals at 24 h, 48 h and 72 h after TBI, respectively. The caspase-3-specific SBDP was observed to increase in CSF in some animals but to a lesser degree. Importantly, levels of these proteins were undetectable in CSF of uninjured control rats. These results indicate that detection of αII-spectrin and αII-SBDPs is a powerful discriminator of outcome and protease activation after TBI. In accord with our previous studies, results also indicate that calpain may be a more important effector of cell death after moderate TBI than caspase-3.

Keywords: calpain, caspase-3, cell death, cerebrospinal fluid, spectrin, traumatic brain injury.

J. Neurochem. (2001) **78**, 1297–1306.

The incidence of traumatic brain injury (TBI) in the United States of America is conservatively estimated to be more than 2 million persons annually with approximately 500 000 hospitalizations (Goldstein 1990). Of these, about 70 000–90 000 head injury survivors are permanently disabled. The annual economic cost to society for care of head-injured patients is estimated at $25 billion (Goldstein 1990). Thus, accurate and reliable measurement of outcome following head injury is of great interest to both head injury survivors and clinicians. Assessment of pathology and neurological impairment immediately after TBI is crucial for determination of appropriate clinical management and for predicting long-term outcome. The outcome measures most often used in head-injured patients are the Glasgow coma scale (GCS), the Glasgow outcome scale (GOS), and computed tomography (CT) scans to detect intracranial pathology.

However, despite dramatically improved emergency triage systems based on these outcome measures, most TBI survivors suffer long-term (for a number of years) impairment, and a large number of TBI survivors are severely affected by TBI despite predictions of 'good recovery' on the GOS (Marion 1996). Because of the limitations of current clinical assessments of TBI severity, there has been an increased interest in the development of neurochemical markers for determining injury severity and for clinical evaluation of pathophysiological mechanisms operative in traumatized brain.

For example, TBI results in neuronal tissue death that can cause a variety of neurochemicals such as amino acids, ions and lactate, as well as a number of cellular proteins and enzymes, to be released into the blood and CSF (Goodman and Simpson 1996). Although assessment of cardiac and liver protein levels in the blood has routinely been used in medical practice for years (e.g. creatine kinase MB or troponin-T), assessment of CNS proteins in blood or CSF is far less developed. Thus, recent studies have measured a variety of neurochemical substances in the CSF or blood in attempt to identify specific surrogate markers of cellular damage and outcome after TBI and other CNS disorders (Haber and Grossman 1980; Inao *et al.* 1988; Robinson *et al.* 1990; Lyeth *et al.* 1993; Raabe and Seifert 1999; Raabe *et al.* 1999; Zemlan *et al.* 1999; Clark *et al.* 2000a; Tapiola *et al.* 2000). For example, creatine kinase BB, lactate dehydrogenase, myelin basic protein, and neuron-specific enolase have been measured in blood or CSF in various CNS disorders including TBI. However, these proteins are non-specific to the brain, offer no insight as to mechanism of injury, and/or prediction of outcome utilizing these proteins has not proven reliable (Goodman and Simpson 1996). Other proteins detected in CSF after brain injury such as S-100B are highly specific to the CNS and have been more robustly correlated with outcome (Raabe and Seifert 1999; Raabe *et al.* 1999). Although brain-specific surrogate biomarkers like S-100B may be useful indicators of outcome after brain injury, detection of these proteins in blood or CSF offers no insight into neurochemical alterations that mediate brain damage after TBI. Thus, identification of neurochemical markers that are specific to the CNS and that provide information about specific ongoing neurochemical events would prove immensely beneficial for both prediction of outcome and for guidance of targeted therapeutic delivery.

Non-erythroid αII-spectrin is the major structural component of the cortical membrane cytoskeleton, is particularly abundant in axons and presynaptic terminals (Riederer *et al.* 1986; Goodman *et al.* 1995), and is a major substrate for both calpain and caspase-3 cysteine proteases (Wang *et al.* 1998). The calpain-mediated cleavage of αII-spectrin occurs between Tyr^{1176} and Gly^{1177} resulting in the formation of calpain-signature spectrin breakdown products (SBDPs) of

150 and 145 kDa (Harris *et al.* 1988). The caspase-3-mediated cleavages of αII-spectrin occur at Asp^{1185}, Ser^{1186}, Asp^{1478} and Ser^{1479} resulting in the formation of caspase-3-signature SBDPs of 150 and 120 kDa, respectively (Wang *et al.* 1998). Importantly, numerous investigations have documented increased pathological activation of calpain and/or caspase-3 proteases after TBI (Saatman *et al.* 1996a, 2000; Kampfl *et al.* 1997; Newcomb *et al.* 1997; Posmantur *et al.* 1997; Yakovlev *et al.* 1997; Pike *et al.* 1998a; Clark *et al.* 1999, 2000b; LaPlaca *et al.* 1999; Okonkwo *et al.* 1999; Zhang *et al.* 1999; Beer *et al.* 2000; Buki *et al.* 2000). In addition, our laboratory and others have provided extensive evidence that αII-spectrin is processed by calpains and/or caspase-3 to signature cleavage products *in vivo* after TBI (Beer *et al.* 2000; Newcomb *et al.* 1997; Pike *et al.* 1998a; Buki *et al.* 2000) and in *in vitro* models of mechanical stretch injury (Pike *et al.* 2000b), necrosis (Zhao *et al.* 1999), apoptosis (Nath *et al.* 1996a, 1996b; Pike *et al.* 1998b), glutamate or NMDA excitotoxicity (Nath *et al.* 2000; Zhao *et al.* 2000), and oxygen-glucose deprivation (Nath *et al.* 1998; Newcomb *et al.* 1998). Moreover, use of selective αII-SBDP antibodies has been used to demonstrate that brain regions with the highest accumulation of SBDPs also have the highest levels of neuronal cell death (Roberts-Lewis *et al.* 1994; Newcomb *et al.* 1997). Thus, the ubiquitous distribution of αII-spectrin in the brain coupled with the ability to utilize signature αII-spectrin proteolytic fragments generated by pathological activation of calpain and/or caspase-3 after TBI makes αII-spectrin a potentially important biomarker of brain damage. To test this hypothesis, the present investigation examined alterations in brain levels of αII-spectrin and αII-SBDPs after controlled cortical impact TBI in rodents, and compared these changes to accumulation of αII-spectrin and αII-SBDPs in CSF in the same animals.

Materials and methods

Surgical Preparation and controlled cortical impact traumatic brain injury

As previously described (Dixon *et al.* 1991; Pike *et al.* 1998a), a cortical impact injury device was used to produce TBI in rodents. Cortical impact TBI results in cortical deformation within the vicinity of the impactor tip associated with contusion, and neuronal and axonal damage that is constrained in the hemisphere ipsilateral to the site of injury (Gennarelli 1994; Meaney *et al.* 1994). Adult male (280–300 g) Sprague-Dawley rats (Harlan; Indianapolis, IN, USA) were initially anesthetized with 4% isoflurane in a carrier gas of 1 : 1 O_2/N_2O (4 min) followed by maintenance anesthesia of 2.5% isoflurane in the same carrier gas. Core body temperature was monitored continuously by a rectal thermistor probe and maintained at 37 ± 1°C by placing an adjustable temperature controlled heating pad beneath the rats. Animals were mounted in a stereotactic frame in a prone position and secured by ear and

incisor bars. A midline cranial incision was made, the soft tissues were reflected, and a unilateral (ipsilateral to site of impact) craniotomy (7 mm diameter) was performed adjacent to the central suture, midway between bregma and lambda. The dura mater was kept intact over the cortex. Brain trauma in rats ($n = 9$) was produced by impacting the right cortex (ipsilateral cortex) with a 5-mm diameter aluminum impactor tip (housed in a pneumatic cylinder) at a velocity of 3.5 m/s with a 2.0-mm compression and 150 ms dwell time (compression duration). Velocity was controlled by adjusting the pressure (compressed N_2) supplied to the pneumatic cylinder. Velocity and dwell time were measured by a linear velocity displacment transducer (Lucas Shaevitz™ model 500 HR; Detroit, MI, USA) that produces an analogue signal that was recorded by a storage-trace oscilloscope (BK Precision, model 2522B; Placentia, CA, USA). Sham-injured animals ($n = 4$) underwent identical surgical procedures but did not receive an impact injury. Appropriate pre- and post-injury management was maintained to insure that all guidelines set forth by the University of Florida Institutional Animal Care and Use Committee and the National Institutes of Health guidelines detailed in the Guide for the Care and use of Laboratory Animals were complied with.

CSF and cortical tissue preparation

The CSF and brain cortices were collected from animals at various intervals after sham-injury or TBI. At the appropriate time-points, TBI or sham-injured animals were anesthetized as described above and secured in a stereotactic frame with the head allowed to move freely along the longitudinal axis. The head was flexed so that the external occipital protuberance in the neck was prominent and a dorsal midline incision was made over the cervical vertebrae and occiput. The atlanto-occipital membrane was exposed by blunt dissection and a 25G needle attached to polyethylene tubing was carefully lowered into the cisterna magna. Approximately 0.1–0.15 mL of CSF was collected from each rat. Following CSF collection, animals were removed from the stereotactic frame and immediately killed by decapitation. Ipsilateral and contralateral (to the impact site) cortices were then rapidly dissected, rinsed in ice cold PBS, and snap frozen in liquid nitrogen. Cortices beneath the craniotomies were excised to the level of the white matter and extended ~4 mm laterally and ~7 mm rostrocaudally. The CSF samples were centrifuged at 4000 g for 4 min at 4°C to clear any contaminating erythrocytes. Cleared CSF and frozen tissue samples were stored at −80°C until ready for use. Cortices were homogenized in a glass tube with a Teflon dounce pestle in 15 volumes of an ice-cold triple detergent lysis buffer (20 mMH EPES, 1 mMEDTA , 2 mMEGTA , 150 mM NaCl, 0.1% SDS, 1.0% IGEPAL 40, 0.5% deoxycholic acid, pH 7.5) containing a broad range protease inhibitor cocktail (cat. #1-836-145Roche Molecular Biochemicals, Indianapolis, IN, USA).

Immunoblot analyses of CSF and cortical tissues

Protein concentrations of tissue homogenates and CSF were determined by bicinchoninic acid microprotein assays (Pierce Inc., Rockford, IL, USA) with albumin standards. Protein balanced samples were prepared for sodium dodecyl sulfate–polyacrylamide gel electrophoresis (SDS–PAGE) in twofold loading buffer containing 0.25 M Tris (pH 6.8), 0.2 M DTT, 8% SDS, 0.02%

bromophenol blue, and 20% glycerol in distilled H_2O. Samples were heated for 10 min at 100°C and centrifuged for 1 min at 8160 g in a microcentrifuge at ambient temperature. Forty micrograms of protein per lane was routinely resolved by SDS–PAGE on 6.5% Tris/glycine gels for 1 h at 200 V. Following electrophoresis, separated proteins were laterally transferred to polyvinylidene fluoride (PVDF) membranes in a transfer buffer containing 0.192 M glycine and 0.025 M Tris (pH 8.3) with 10% methanol at a constant voltage of 100 V for 1 h at 4°C. Blots were blocked for 1 h at ambient temperature in 5% non-fat milk in TBS and 0.05% Tween-20. Panceau Red (Sigma, St Louis, MO, USA) was used to stain membranes to confirm successful transfer of protein and to insure that an equal amount of protein was loaded in each lane.

Antibodies and immunolabeling of PVDF membranes

Immunoblots containing brain or CSF protein were probed with an anti-α-spectrin (fodrin) monoclonal antibody (FG 6090 Ab; clone AA6; cat. # FG 6090; Affiniti Research Products Limited, Mamhead Castle, Mamhead, Exeter, UK) that detects intact non-erythroid αII-spectrin (280 kDa) and 150, 145 and 120 kDa cleavage fragments to αII-spectrin. A cleavage product of 150 kDa is initially produced by calpains or caspase-3 proteases (each proteolytic cleavage yields a unique amino-terminal region; Nath *et al.* 1996b; Wang *et al.* 1998). The calpain-generated 150 kDa product is further cleaved by calpain to yield a specific calpain signature product of 145 kDa (Harris *et al.* 1988; Nath *et al.* 1996a,b) whereas the caspase-3 generated 150 kDa product is further cleaved by caspase-3 to yield a specific caspase-3 signature product of 120 kDa (Nath *et al.* 1998; Wang *et al.* 1998). To further confirm the specificity of calpain-cleaved spectrin in CSF after TBI, a second antibody (anti-SBDP150; rabbit polyclonal) that recognizes only the calpain-cleaved N-terminal region (GMMPR) of the 150 kDa αII-spectrin breakdown product (SBDP) was also used (Saido *et al.* 1993; Nath *et al.* 1996b). Some immunoblots were immunolabeled with an antibody that recognizes erythroid αI-spectrin (Cat.# BYA10881; Accurate Chemical & Scientific Corp, Westbury, NY, USA). Following an overnight incubation at 4°C with the primary antibodies (FG 6090 Ab, 1 : 4000 for brain tissue and 1: 2000 for CSF; SBDP150 Ab, 1 : 1000; BYA10881, 1 : 400), blots were incubated for 1 h at ambient temperature in 3% non-fat milk that contained a horseradish peroxidase-conjugated goat anti-mouse IgG (1 : 10 000 dilution) or goat-anti-rabbit IgG (1 : 3000). Enhanced chemiluminescence (ECL; Amersham) reagents were used to visualize immunolabeling on Kodak Biomax ML chemiluminescent film.

Statisitical analyses

Semi-quantitative evaluation of protein levels detected by immun-blotting was performed by computer-assisted densitometric scanning (AlphaImager 2000; Digital Imaging System, San Leandro, CA, USA). Data were acquired as integrated densitometric values and transformed to percentages of the densitometric levels obtained on scans from sham-injured animals visualized on the same blot. Data was evaluated by least squares linear regression followed by ANOVA. All values are given as mean ± SEM. Differences were considered significant if $p < 0.05$.

Results

Proteolysis of αII-spectrin in the cortex by calpain, but not caspase-3 after TBI

In the ipsilateral cortex, TBI resulted in decreased protein levels of αII-spectrin (280 kDa) that were associated with concomitant accumulation of calpain-generated 150 and 145 kDa αII-SBDPs (Fig. 1). However, there was little to no detectable increase in the caspase-3-genearated 120 kDa αII-SBDP. These results replicate our previous investigation that reported calpain but not caspase-3 processing of

αII-spectrin following a moderate level of lateral controlled cortical impact TBI (Pike *et al.* 1998a). Decreased αII-spectrin (280 kDa) protein levels were 65%, 48% and 39% of sham-injured protein levels at 24 h, 48 h, and 72 h after TBI, respectively (Fig. 2). Increased 150 kDa αII-SBDP levels were 189%, 157%, and 153% of sham-injured levels at 24 h, 48 h and 72 h after TBI, respectively, while increased 145 kDa αII-SBDP levels were 237%, 203% and 198% of sham-injured levels at 24 h, 48 h and 72 h after TBI, respectively (Fig. 2).

In the contralateral cortex, traumatic brain injury resulted in no apparent alteration in protein levels of αII-spectrin (280 kDa) or in any apparent accumulation of calpain-generated 150 or 145 kDa αII-SBDPs, or in caspase-3 generated 120 kDa αII-SBDP as compared to sham-injured control animals (Fig. 1). These results are also in accord with our previous report that calpain-mediated processing of αII-spectrin is predominately confined to ipsilateral brain regions after moderate lateral controlled cortical impact TBI (Newcomb *et al.* 1997; Pike *et al.* 1998a).
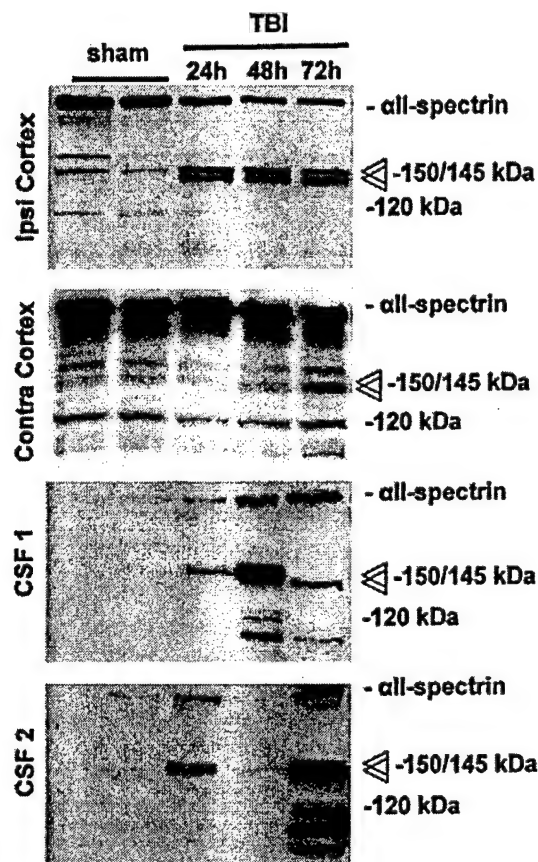

Fig. 1 Traumatic brain injury (TBI) results in prominent accumulation of αII-spectrin (280 kDa) and calpain-cleaved 150 kDa and 145 kDa αII-SBDPs in CSF (FG 6090 Ab). The caspase-3 generated 120 kDa fragment was also apparent in CSF of some animals. TBI caused proteolysis of constitutively expressed brain αII-spectrin (280 kDa) in ipsilateral but not contralateral cortex. Increases in the caspase-3-mediated 120 kDa αII-SBDP were not as apparent in ipsilateral or contralateral cortex after TBI. Immunolabeling of additional unknown bands at ~110 kDa and 95 kDa were also detected in CSF at 48 h and 72 h after injury. CSF1 and CSF2 are from two separate series of animals shown to illustrate that there was more variability in CSF levels of SBDPs than in brain levels, which may reflect individual differences in injury severity.
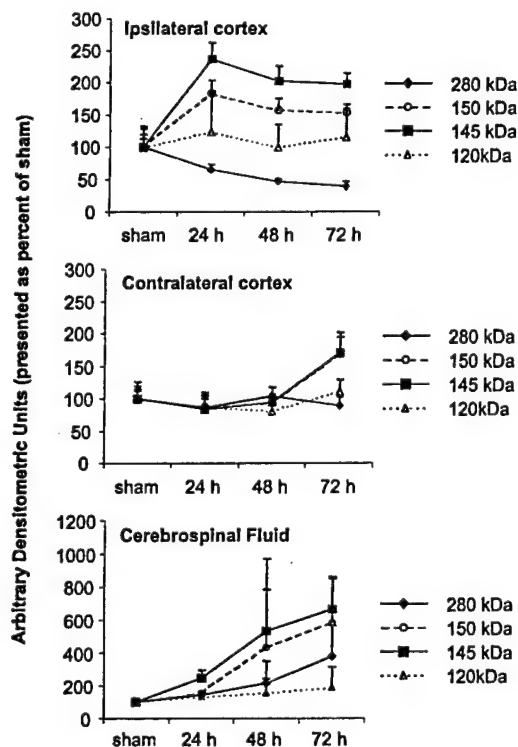

Fig. 2 Mean arbitrary densitometric units obtained from 280 kDa αII-spectrin and the 150 kDa and 145 kDa αII-SBDPs were converted to percent of sham-injured values. Decreases in 280 kDa αII-spectrin and increases in 150 kDa and 145 kDa αII-SBDPs (ipsilateral cortex) were associated with concomitant increases of these proteins in the CSF. Mean accumulation of the caspase-3 generated 120 kDa fragment in these tissues was relatively flat.
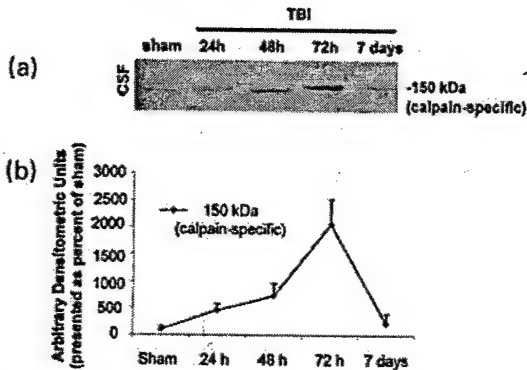
Fig. 3 N-terminal fragment-specific detection of calpain-generated SBDP150 in CSF after traumatic brain injury (SBDP150 Ab). (a) As with the FG 6090 Ab, the SBDP150 Ab detected a progressive increase in the calpain-cleaved 150 kDaA SBDP from 24 h to 72 h after TBI. Levels of 150 kDa SBDP had resolved to sham-injured control levels by seven days after TBI. (b) Mean arbitrary densitometric units of SBDP150 levels detected with anti-SBDP150 Ab.

Accumulation of calpain-mediated αII-SBDPs in CSF after TBI

Immunoblot analyses of CSF levels of non-erythroid αII-spectrin and αII-SBDPs (FG 6090 Ab) showed no detectable levels of these proteins in CSF of sham-injured control animals (Fig. 1). However, after TBI, accumulation of αII-spectrin (280 kDa) and calpain-generated 150 and 145 kDa SBDPs were markedly increased at 24 h, 48 h and 72 h, after injury (Fig. 1). In addition, there was an increase in the caspase-3-generated 120 kDa fragment in one animal at 48 h after TBI, and in another animal at 72 h after TBI (Fig. 1). Accumulation of αII-spectrin (280 kDa) protein levels was 143%, 212%, and 379% of sham-injured animals at 24 h, 48 h, and 72 h after TBI, respectively (Fig. 2). Similarly, accumulation of 150 kDa αII-SBDP after TBI was 155%, 434%, and 583% of sham-injured levels at 24 h, 48 h, and 72 h, respectively, while accumulation of 145 kDa αII-SBDP after TBI was 244%, 530%, and 665% of sham-injured levels at 24 h, 48 h and 72 h, respectively (Fig. 2). In contrast, although accumulation of the caspase-3 cleaved 120 kDa fragment was detected in two animals, the average response was relatively flat. In addition, several lower molecular weight species of αII-spectrin were detected. The protease(s) responsible for these lower molecular weight fragments are currently unknown. However, future identification of these bands may provide important new information regarding other neurochemical events in the brain after TBI.

To provide further confirmation of calpain-generated αII-SBDP accumulation in CSF after TBI, an additional group of animals ($n = 5$ per time-point) was injured as described above and immunoblots of CSF samples were probed with anti-SBDP150 Ab. In this experiment, an additional time-point (7 days post-TBI) was also examined. The SBDP150 Ab specifically recognizes only the calpain-cleaved 150 kDa αII-spectrin fragment and does not recognize the intact 280 kDa protein or other proteolytic fragments (Saido et al. 1993; Nath et al. 1996b). Results with the SBDP150 Ab were nearly identical to those obtained with the FG-6090 Ab (Fig. 3). The calpain-cleaved 150 kDa SBDP was nearly undetectable in CSF of sham-injured animals, and a progressive increase in immunoreactivity was observed from 24 h to 72 h after TBI. Importantly, this experiment also demonstrated that levels of calpain-cleaved 150 kDa SBDP were decreased back to sham-injured control levels by seven days after TBI (Fig. 3).

Linear regression analyses of Cortical versus CSF levels of αII-spectrin and αII-SBDPs

Least squares linear regression was calculated to determine the relationship between brain and CSF levels of αII-spectrin and αII-SBDPs over days post-injury. The slope of the regression lines for αII-spectrin and αII-SBDPs in brain and CSF were analyzed by ANOVA.

For cortical levels of 280 kDa αII-spectrin protein, the slope of the regression line was relatively steep and negative indicating large decreases over days in cortical levels of native αII-spectrin protein (Fig. 4). In contrast, the slope of the regression line for CSF levels of 280 kDa αII-spectrin was relatively steep and positive indicating large increases over days in CSF levels of αII-spectrin protein after TBI. In addition, ANOVA indicated that there was a significant difference ($F = 19.95$, $p < 0.001$) between cortical and CSF slopes for 280 kDa αII-spectrin protein level. This significance indicates that as brain levels of αII-spectrin decrease over days, CSF levels of αII-spectrin increase over days.

For cortical and CSF levels of 150 kDa αII-SBDP, both slopes of the regressions lines were positive indicating large increases in the calpain-cleaved 150 kDa αII-SBDP in brain and CSF over days (Fig. 4). ANOVA indicated no significant difference ($F = 1.86$, $p = 0.1873$) between slopes indicating that the relative accumulation of 150 kDa αII-SBDP in cortex and CSF were similar. However, the slope for CSF 150 kDa αII-SBDP was relatively steeper than the slope for cortical 150 kDa αII-SBDP. This result reflects the densitometric data (Fig. 2) indicating that, in the cortex, peak levels of the 150 kDa αII-SBDP accumulated rapidly (24 h) and were maintained at 48 h and 72 h post-injury. This result also reflects densitometric data (Fig. 2) indicating that CSF levels of the 150 kDa αII-SBDP accumulated more slowly early after injury (24 h) with a greater rate of further accumulation at 48 h and 72 h post-injury. Observed statistical differences in accumulation rates can be appreciated visually in the immunoblot data (Fig. 1). The stability of αII-spectrin and αII-SBDPs in CSF may be increased due to lack of endogenous proteases. For example,
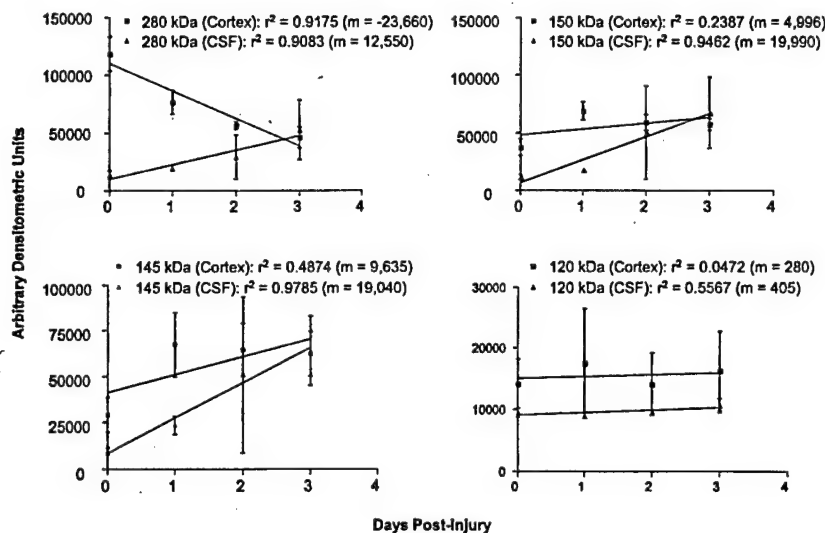
Fig. 4 Cortical versus CSF levels of αII-spectrin (280 kDa) and αII-SBDPs (150, 145, and 120 kDa) over days post-injury. Least squares regression lines of brain and CSF spectrin and SBDP levels were plotted on the same graph. Pearson correlation coefficients for each regression line are indicated. Results indicate that parenchymal decreases in levels of native αII-spectrin (280 kDa) are associated with increases in CSF accumulation while increased parenchymal levels of calpain-mediated αII-SBDPs (150 and 145 kDa) are associated with increased CSF accumulation. On average, there were no changes in parenchymal or CSF levels of the caspase-3-mediated 120 kDa αII-SBDP, although individual rats at different time points showed some increase in CSF levels of the 120 kDa product.

when CSF from TBI animals was stored in individual aliquots at either − 85°C or at ambient laboratory temperature (~26°C) without protease inhibitors for 48 h, αII-SBDP levels from ambient temperature aliquots were only decreased by 28% compared to aliquots stored at − 85°C (Fig. 5). Importantly, the relative stability of αII-SBDP protein in CSF at ambient temperature further indicates this protein as a useful biomarker after TBI.

For cortical and CSF levels of calpain-cleaved 145 kDa αII-SBDP, both slopes of the regression lines were steep and positive indicating large increases in the 145 kDa αII-SBDP in brain and CSF over days (Fig. 4). ANOVA indicated no

significant difference $(F = 0.69, \quad p = 0.4153)$ between slopes indicating that the relative accumulation of 145 kDa αII-SBDP in cortex and CSF were similar as compared to the respective controls. Comparison of slopes for 150 kDa and 145 kDa αII-SBDPs in the brain revealed that the slope of the brain 145 kDa αII-SBDP over days was considerably steeper than the slope of the brain 150 kDa αII-SBDP. This result indicates that brain 145 kDa αII-SBDP protein levels accumulate at a greater rate over days than brain 150 kDa αII-SBDP protein levels. This observation is most likely the result of lower basal levels of brain 145 kDa αII-SBDP than brain 150 kDa αII-SBDP in sham-injured animals and of continued calpain digestion of the larger 150 kDa αII-SBDP to the smaller 145 kDa αII-SBDP over time.

For cortical and CSF levels of caspase-3-cleaved 120 kDa αII-SBDP, both slopes were nearly horizontal, indicating no increased accumulation of caspase-3-generated 120 kDa αII-SBDP over days after TBI (Fig. 4). In addition, ANOVA indicated no significant difference between slopes $(F = 0.002, p = 0.9621)$.

Erythroid αI-spectrin versus non-erythroid αII-spectrin
After head injury, the most likely source of CSF contamination will be from blood. Both neurons and blood contain the erythroid form αI-spectrin protein. However, erythrocytes do not contain non-erythroid αII-spectrin protein. To demonstrate that the source of αII-spectrin immunoreactivity in the CSF is not blood borne, we probed

48 h storage temperature
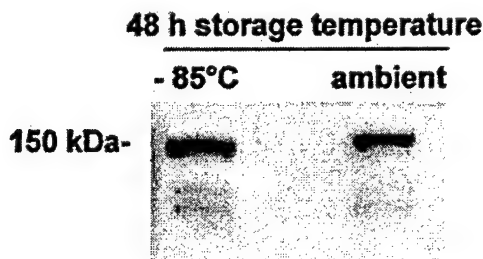
- 85°C   ambient

Fig. 5 Stability of αII-SBDP in CSF after prolonged storage in the absence of protease inhibitors at ambient laboratory temperature. The αII-SBDP protein levels only decreased by 28% when stored at ambient temperature (~26°C) for 48 h compared to identical samples stored at − 85°C for 48 h. These results indicate that αII-SBDPs in CSF are relatively stable at room temperature. This is an important practical consideration for clinical utility.
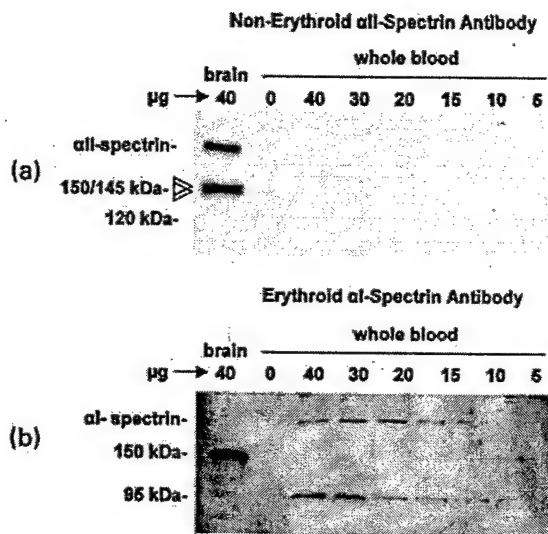
Fig. 6 (a) Non-erythroid αII-spectrin protein is not detected in whole blood. After TBI, the most probable source of non-CNS accumulation of proteins in the CSF is from blood. This immunoblot demonstrates that non-erythroid αII-spectrin is detectable in brain protein homogenates but not in blood protein homogenates. (b) In contrast, use of an erythroid αI-spectrin antibody on the same blot that has been stripped and re-probed reveals immunoreactivity for both blood and brain spectrin. These results demonstrate that potential blood contamination of CSF samples does not affect detection of brain-derived αII-spectrin.

immunoblots containing various concentrations of whole blood proteins and brain protein with either an erythroid anti-αI-spectrin antibody or with an anti-αII-spectrin antibody (Fig. 6a,b). As predicted, no immunoreactivity was observed at any concentration of whole blood protein (0–40 μg) while brain spectrin was highly reactive to the non-erythroid anti-αII-spectrin antibody. In contrast, both the brain and blood protein samples were immunoreactive to the erythroid anti-αI-spectrin antibody. This result clearly indicates that use of the non-erythroid, but not the erythroid, anti-spectrin antibody can be used to discriminate non-blood borne spectrin protein in CSF samples.

Discussion

This paper provides the first evidence for accumulation of non-erythroid αII-spectrin protein and calpain-mediated αII-SBDPs in CSF after TBI. Detection of calpain-specific proteolytic fragments to αII-spectrin were confirmed with two antibodies, one that recognizes both intact αII-spectrin and calpain-specific SBDPs (FG 6090 Ab), and one that recognizes only the N-terminal region of calpain-cleaved 150 kDa SBDP (SBDP150 Ab). Results of this investigation indicate that CSF detection of αII-spectrin and αII-SBDPs can provide both a sensitive surrogate biochemical measure

of TBI pathology and provide important information about specific neurochemical events that have occurred in the brain after TBI. To our knowledge, this is the first investigation of any CNS pathology to indicate that identification of accumulated CSF proteins or protein metabolic products can be used to infer specific neurochemical events (i.e. calpain activation) in the brain. Thus, use of αII-SBDPs as surrogate biochemical markers of TBI has important clinical ramifications for assessment of outcome after injury and for determination of specific pathological proteolytic cascades known to occur after TBI. Although other CNS proteins have been detected in CSF after brain injury (e.g. S-100B) and have been correlated with outcome, these proteins offer no insight into pathological mechanisms that have occurred in the brain after TBI. Obviously, identification of metabolic products with known neurochemical etiology will be beneficial for appropriate application of targeted therapeutics (such as calpain inhibitors) after TBI.

Calpain and caspase-3 cysteine proteases are important mediators of cell death and dysfunction in numerous CNS diseases and injuries including TBI. The calpains have historically been associated with necrotic (oncotic) cell death although recent evidence indicates a role in apoptotic cell death as well (Linnik et al. 1996; Nath et al. 1996a,b; Newcomb et al. 1998; Pike et al. 1998b). Numerous investigations have reported calpain activation after TBI (Saatman et al. 1996a, 2000; Kampfl et al. 1997; Newcomb et al. 1997; Posmantur et al. 1997; Pike et al. 1998a) and inhibitors of calpains have been shown to confer neuroprotection after TBI (Posmantur et al. 1997; Saatman et al. 1996b, 2000). Caspase-3 is a critical executioner of apoptosis and caspase-3 activation has been reported in in vitro (Shah et al. 1997; Allen et al. 1999; Pike et al. 2000b) and in vivo (Beer et al. 2000; Yakovlev et al. 1997; Pike et al. 1998a; Clark et al. 2000b) models of TBI. However, it should be noted that at least in our hands, the magnitude of calpain activation after TBI is much greater than that of caspase-3, and that at the moderate level of brain injury employed in the current study, caspase-3 is only transiently elevated in deep, non-cortical brain regions (Pike et al. 1998a). This result most likely accounts for the detection of relatively minimal amounts of the 120 kDa caspase-3-mediated αII-SBDP in CSF after TBI. In contrast to our injury model, Beer et al. (2000) have observed prominent levels of caspase-3 activation in the cortex after cortical impact TBI. However, while our cortical impact model is typically characterized by prominent tissue necrosis and progressive cortical cavitation to the gray–white interface (Kampfl et al. 1996; Newcomb et al. 1997; Dixon et al. 1998; Newcomb et al. 1999; Pike et al. 2000a), the model employed by Beer et al. (2000) was not. Thus, differences in injury magnitude may be important factors affecting calpain and/or caspase-3 activation after TBI, and

this hypothesis warrants further investigation. However, it should be pointed out that although caspase-3 activation has not been a prominent feature in our model of cortical impact TBI, we have detected substantial levels of apoptotic cell death in the cortex after TBI (Newcomb *et al.* 1999). This apparent discrepancy between apoptotic cell death and caspase-3 activation raises the intriguing possibility that apoptosis may occur via a caspase-3-independent pathway after TBI. This observation also warrants further examination.

That different injury magnitudes may result in differential activation of calpain or caspase-3 proteases has important implications for targeted therapeutic intervention after TBI, and importantly, further validates the utility of using surrogate markers of TBI that have known neurochemical etiologies. For example, the current investigation detected CSF accumulation of the calpain-mediated αII-SBDP and not the caspase-3-mediated αII-SBDP. Based on this evidence, administration of calpain but not caspase-3 inhibitors would be predicted to have the most beneficial effect on outcome. However, other injury magnitudes may result in more caspase-3 activation indicating use of caspase-3 inhibitors or a combination of calpain/caspase-3 protease inhibitors. Thus, surrogate measures of TBI will result in selective pharmaceutical therapies based on clinical assessment of neuropathology, and this approach is a superior strategy to promiscuous prophylactic administration of unnecessary and potentially harmful compounds.

The most probable source of peripheral contamination of the CSF after TBI will be blood born. Indeed, we did detect visible red blood cell contamination of CSF after experimental TBI (which was removed by centrifugation). However, our control experiments with brain and whole blood immnuoblots (Fig. 6a,b) clearly demonstrated that the non-erythroid anti-αII-spectrin antibody did not detect any αII-spectrin protein in whole blood samples. Conversely, the erythroid αI-spectrin antibody labeled both brain and blood samples. These results indicate that the major source of potential peripheral CSF contamination after TBI, blood, is not detected by the non-erythroid anti-αII-spectrin antibody. This finding supports the utility of αII-spectrin and αII-SBDPs as surrogate biomarkers of injury after TBI, and importantly, as biomarkers of calpain and/or caspase-3 activation after TBI.

One caveat to the current investigation is the finding that there was more variability in levels of CSF SBDPs than there were in brain levels of SBDPs. This variability is indicated by the larger error bars in Fig. 2 and 4 and can be observed in individual animals in Fig. 1. The reason for the larger variability in CSF protein accumulation is unknown, but may reflect differences in individual animal's CSF circulation after TBI. For example, differences in increased intracranial pressure after TBI may restrict passage of CSF through various foramina that may preclude detection of

secreted proteins into the cisterna magna (source of CSF in the present study). Additional studies should examine differences in intraventricular versus intracisternal levels of accumulated SBDPs.

Nonetheless, future studies focused on development of neuron-specific antibodies targeted against calpain-specific and caspase-3-specific αII-SBDPs (such as the SBDP150 Ab) will further strengthen the utility and specificity of αII-SBDPs as surrogate markers of brain injury. In addition, development of enzyme-linked immunosorbent assays (ELISA) will allow greater quantification of calpain and caspase-3 SBDPs and provide a more rapid and practical approach to CSF detection of these proteins.

Acknowledgements

References

Allen J. W., Knoblach S. M. and Faden A. I. (1999) Combined mechanical trauma and metabolic impairment in vitro induces NMDA receptor-dependent neuronal cell death and caspase-3-dependent apoptosis. *FASEB J.* **13**, 1875–1882.

Beer R., Franz G., Srinivasan A., Hayes R. L., Pike B. R., Newcomb J. K., Zhao X., Schmutzhard E., Poewe W. and Kampfl A. (2000) Temporal profile and cell subtype distribution of activated caspase-3 following experimental traumatic brain injury. *J. Neurochem.* **75**, 1264–1273.

Buki A., Okonkwo D. O., Wang K. K. and Povlishock J. T. (2000) Cytochrome C release and caspase activation in traumatic axonal injury. *J. Neurosci.* **20**, 2825–2834.

Clark R. S., Kochanek P. M., Chen M., Watkins S. C., Marion D. W., Chen J., Hamilton R. L., Loeffert J. E. and Graham S. H. (1999) Increases in Bcl-2 and cleavage of caspase-1 and caspase-3 in human brain after head injury. *FASEB J.* **13**, 813–821.

Clark R. S., Kochanek P. M., Adelson P. D., Bell M. J., Carcillo J. A., Chen M., Wisniewski S. R., Janesko K., Whalen M. J. and Graham S. H. (2000a) Increases in Bcl-2 protein in cerebrospinal fluid and evidence for programmed cell death in infants and children after severe traumatic brain injury. *J. Pediatr.* **137**, 197–204.

Clark R. S., Kochanek P. M., Watkins S. C., Chen M., Dixon C. E., Seidberg N. A., Melick J., Loeffert J. E., Nathaniel P. D., Jin K. L. and Graham S. H. (2000b) Caspase-3 mediated neuronal death after traumatic brain injury in rats. *J. Neurochem.* **74**, 740–753.

Dixon C. E., Clifton G. L., Lighthall J. W., Yaghmai A. A. and Hayes R. L. (1991) A controlled cortical impact model of traumatic brain injury in the rat. *J. Neurosci. Meth.* **39**, 253–262.

Dixon C. E., Markgraf C. G., Angileri F., Pike B. R., Wolfson B., Newcomb J. K., Bismar M. M., Blanco A. J., Clifton G. L. and Hayes R. L. (1998) Protective effects of moderate hypothermia on behavioral deficits but not necrotic cavitation following cortical impact injury in the rat. *J. Neurotrauma* **15**, 95–103.

Gennarelli T. A. (1994) Animate models of human head injury. *J. Neurotrauma* **11**, 357–368.

Goldstein M. (1990) Traumatic brain injury: a silent epidemic. *Ann. Neurol.* **27**, 327.

Goodman S. R., Zimmer W. E., Clark M. B., Zagon I. S., Barker J. E. and Bloom M. L. (1995) Brain spectrin: of mice and men. *Brain Res. Bull.* **36**, 593–606.

Goodman J. C. and Simpson R. K. Jr (1996) Biochemical monitoring in head injury. In: R. K. Narayan, J. E. Wilberger and J. T. Povlishock, eds. *Neurotrauma*, pp. 577–591. McGraw-Hill, New York.

Haber B. and Grossman R. G. (1980) Acetylcholine metabolism in intracranial and lumbar spinal cerebrospinal fluid and in blood. In: J. H. Wood, ed. *Neurobiology and Cerebrospinal Fluid*, pp. 345–350. Plenum, New York.

Harris A. S., Croall D. E. and Morrow J. S. (1988) The calmodulin-binding site in alpha-fodrin is near the calcium-dependent protease-I cleavage site. *J. Biol. Chem.* **263**, 15754–15761.

Inao S., Marmarou A., Clarke G. D., Anderson B. J., Fatouros P. P. and Young H. F. (1988) Production and clearance of lactate from brain tissue, cerebrospinal fluid, and serum following experimental brain injury. *J. Neurosurg.* **69**, 736–744.

Kampfl A., Posmantur R., Nixon R., Grynspan F., Zhao X., Liu S. J., Newcomb J. K., Clifton G. L. and Hayes R. L. (1996) Mu-calpain activation and calpain-mediated cytoskeletal proteolysis following traumatic brain injury. *J. Neurochem.* **67**, 1575–1583.

Kampfl A., Posmantur R. M., Zhao X., Schmutzhard E., Clifton G. L. and Hayes R. L. (1997) Mechanisms of calpain proteolysis following traumatic brain injury: implications for pathology and therapy: implications for pathology and therapy: a review and update. *J. Neurotrauma.* **14**, 121–134.

LaPlaca M. C., Raghupathi R., Verma A., Pieper A. A., Saatman K. E., Snyder S. H. and McIntosh T. K. (1999) Temporal patterns of poly (ADP-ribose) polymerase activation in the cortex following experimental brain injury in the rat. *J. Neurochem.* **73**, 205–213.

Linnik M. D., Markgraf C. G., Mason P. J., Velayo N. and Racke M. M. (1996) Calpain inhibition attenuates apoptosis in vitro and decreases infarct size in vivo. In: *Pharmacology of Cerebral Ischemia*. J. Krieglstein, ed. CRC Press, Boca Raton:pp. 33.–40.

Lyeth B. G., Jiang J. Y., Robinson S. E., Guo H. and Jenkins L. W. (1993) Hypothermia blunts acetylcholine increase in CSF of traumatically brain injured rats. *Mol. Chem. Neuropath.* **18**, 247–256.

Marion D. W. (1996) Outcome from severe head injury. In: R. K. Narayan, J. E. Wilberger and J. T. Povlishock, eds. *Neurotrauma*, pp. 767–777. McGraw-Hill, New York.

Meaney D. F., Ross D. T., Winkelstein B. A., Brasko J., Goldstein D., Bilston L. B., Thibault L. E. and Gennarelli T. A. (1994) Modification of the cortical impact model to produce axonal injury in the rat cerebral cortex. *J. Neurotrauma* **11**, 599–612.

Nath R., McGinnis K. J., Nadimpalli R., Stafford D. and Wang K. K. W. (1996a) Effects of ICE-like proteases and calpain inhibitors on neuronal apoptosis. *Neuroreport* **8**, 249–255.

Nath R., Raser K. J., Stafford D., Hajimohammadreza I., Posner A., Allen H., Talanian R. V., Yuen P., Gilbertson R. B. and Wang K. K. (1996b) Non-erythroid α-spectrin breakdown by calpain andinterleukin 1β-converting-enzyme-like protease (s) in apoptotic cells: contributory roles of both protease families in neuronal apoptosis. *Biochem. J.* **319**, 683–690.

Nath R., Probert A., McGinnis K. M. and Wang K. K. W. (1998) Evidence for activation of caspase-3-like protease in excitotoxin- and hypoxia/hypoglycemia-injured neurons. *J. Neurochem.* **71**, 186–195.

Nath R., Scott M., Nadimpalli R., Gupta R. and Wang K. K. (2000) Activation of apoptosis-linked caspase(s) in NMDA-injured brains in neonatal rats. *Neurochem. Int.* **36**, 119–126.

Newcomb J. K., Kampfl A., Posmantur R. M., Zhao X., Pike B. R., Liu S. J., Clifton G. L. and Hayes R. L. (1997) Immunohistochemical study of calpain-mediated breakdown products to alpha-spectrin following controlled cortical impact injury in the rat. *J. Neurotrauma.* **14**, 369–383.

Newcomb J. K., Zhao X., Pike B. R., Wang K. K. W. and Hayes R. L. (1998) Proteolytic mechanisms of cell injury following glucose-oxygen deprivation in primary septo-hippocampal cell cultures. *J. Neurotrauma.* **15**, 887.

Newcomb J. K., Zhao X., Pike B. R. and Hayes R. L. (1999) Temporal profile of apoptotic-like changes in neurons and astrocytes following controlled cortical impact injury in the rat. *Exp. Neurol.* **158**, 76–88.

Okonkwo D. O., Buki A., Siman R. and Povlishock J. T. (1999) Cyclosporin A limits calcium-induced axonal damage following traumatic brain injury. *Neuroreport.* **10**, 353–358.

Pike B. R., Zhao X., Newcomb J. K., Posmantur R. M., Wang K. K. W. and Hayes R. L. (1998a) Regional calpain and caspase-3 proteolysis of α-spectrin after traumatic brain injury. *Neuroreport.* **9**, 2437–2442.

Pike B. R., Zhao X., Newcomb J. K., Wang K. K. W., Posmantur R. M. and Hayes R. L. (1998b) Temporal relationships between de novo protein synthesis, calpain and caspase 3-like protease activation, and DNA fragmentation during apoptosis in septo-hippocampal cultures. *J. Neurosci. Res.* **52**, 505–520.

Pike B. R., Johnson E., Flint J., Glenn C. C. and Hayes R. L. (2000a) Prolonged calpain activation in regions of tissue atrophy after traumatic brain injury. *Restor. Neurol. Neurosci.* **16** (3, 4), 166.[abstract].

Pike B. R., Zhao X., Newcomb J. K., Glenn C. C., Anderson D. K. and Hayes R. L. (2000b) Stretch injury causes calpain and caspase-3 activation and necrotic and apoptotic cell death in septo-hippocampal cell cultures. *J. Neurotrauma.* **17**, 283–298.

Posmantur R., Kampfl A., Siman R., Liu J., Zhao X., Clifton G. L. and Hayes R. L. (1997) A calpain inhibitor attenuates cortical cytoskeletal protein loss after experimental traumatic brain injury in the rat. *Neuroscience.* **77**, 875–888.

Raabe A. and Seifert V. (1999) Fatal secondary increase in serum S-100B protein after severe head injury. *J. Neurosurgery.* **91**, 875–877.

Raabe A., Grolms C., Sorge O., Zimmermann M. and Seifert V. (1999) Serum S-100B protein in severe head injury. *Neurosurgery.* **45**, 477–483.

Riederer B. M., Zagon I. S. and Goodman S. R. (1986) Brain spectrin (240/235) and brain spectrin (240/235E): two distinct spectrin subtypes with different locations within mammalian neural cells. *J. Cell Biol.* **102**, 2088–2097.

Roberts-Lewis J. M., Savage M. J., Marcy V. R., Pinsker L. R. and Siman R. (1994) Immunolocalization of μ-calpain mediated spectrin degradation to vulnerable neurons in ischemic gerbil brain. *J. Neurosci.* **14**, 3934–3944.

Robinson S. E., Martin R. M., Davis T. R., Gyenes C. A., Ryland J. E. and Enters E. K. (1990) The effect of acetylcholine depletion on behavior following traumatic brain injury. *Brain Res.* **509**, 41–46.

Saatman K. E., Bozyczko-Coyne D., Marcy V., Siman R. and McIntosh T. K. (1996a) Prolonged calpain-mediated spectrin breakdown occurs regionally following experimental brain injury in the rat. *J. Neuropathol. Exp. Neurol.* **55**, 850–860.

Saatman K. E., Murai H., Bartus R. T., Smith D. H., Hayward N. J., Perri B. R. and McIntosh T. K. (1996b) Calpain inhibitor AK295 attenuates motor and cognitive deficits following experimental brain injury in the rat. *Proc. Natl Acad. Sci. USA* **93**, 3428–3433.

Saatman K. E., Zhang C., Bartus R. T. and McIntosh T. K. (2000)

Behavioral efficacy of posttraumatic calpain inhibition is not accompanied by reduced spectrin proteolysis, cortical lesion, or apoptosis. *J. Cereb. Blood Flow Metab.* **20**, 66–73.

Saido T. C., Yokota M., Nagao S., Yamaura I., Tani E., Tsuchiya T., Suzuki K. and Kawashima S. (1993) Spatial resolution of fodrin proteolysis in postischemic brain. *J. Biol. Chem.* **268**, 25239–25243.

Shah P. T., Yoon K. W., Xu X. M. and Broder L. D. (1997) Apoptosis mediates cell death following traumatic injury in rat hippocampal neurons. *Neuroscience.* **79**, 999–1004.

Tapiola T., Pirttila T., Mikkonen M., Mehta P. D., Alafuzoff I., Koivisto K. and Soininen H. (2000) Three-year follow-up of cerebrospinal fluid tau, β-amyloid 42 and 40 concentrations in Alzheimer's disease. *Neurosci. Lett.* **280**, 119–122.

Wang K. K. W., Posmantur R. M., Nath R., McGinnis K. M., Whitton M., Talanian R. V., Glantz S. B. and Morrow J. S. (1998) Simultaneous degredation of αII and βII spectrin by caspase-3 (CPP32) in apoptotic cells. *J. Biol. Chem.* **273**, 22490–22497.

Yakovlev A. G., Knoblach S. M., Fan L., Fox G. B., Goodnight R. and Faden A. I. (1997) Activation of CPP32-like caspases contributes to neuronal apoptosis and neurological dysfunction after traumatic brain injury. *J. Neurosci.* **17**, 7415–7424.

Zemlan F. P., Rosenberg W. S., Luebbe P. A., Cambell T. A., Dean G. E., Weiner N. E., Cohen J. A., Rudick R. A. and Woo D. (1999) Quantification of axonal damage in traumatic brain injury: affinity purification and characterization of cerebrospinal fluid tau proteins. *J. Neurochem.* **72**, 741–750.

Zhang C., Raghupathi R., Saatman K. E., LaPlaca M. C. and McIntosh T. K. (1999) Regional and temporal alterations in DNA fragmentation factor (DFF)-like proteins following experimental brain trauma in the rat. *J. Neurochem.* **73**, 1650–1659.

Zhao X., Pike B. R., Newcomb J. K., Wang K. K., Posmantur R. M. and Hayes R. L. (1999) Maitotoxin induces calpain but not caspase-3 activation and necrotic cell death in primary septo-hippocampal cultures. *Neurochem. Res.* **24**, 371–382.

Zhao X., Newcomb J. K., Pike B. R., Wang K. K., d'Avella D. and Hayes R. L. (2000) Novel characteristics of glutamate-induced cell death in primary septohippocampal cultures: relationship to calpain and caspase-3 protease activation. *J. Cereb. Blood Flow Metab.* **20**, 550–562.

Concurrent Assessment of Calpain and Caspase-3 Activation After Oxygen–Glucose Deprivation in Primary Septo-Hippocampal Cultures

Jennifer K. Newcomb-Fernandez, Xiurong Zhao, *Brian R. Pike, †Kevin K. W. Wang, ‡Andreas Kampfl, ‡Ronald Beer, *S. Michelle DeFord, and *Ronald L. Hayes

*University of Texas Health Science Center-Houston, Department of Neurosurgery, The Vivian L. Smith Center for Neurologic Research, Houston, Texas, *Evelyn F. and William L. McKnight Brain Institute of the University of Florida, Department of Neuroscience, Gainesville, Florida, and †Park-Davis Pharmaceutical Research, Warner-Lambert Company, Ann Arbor, Michigan, U.S.A.; and ‡University Hospital Innsbruck, Department of Neurology, Innsbruck, Austria*

Summary: The contributions of calpain and caspase-3 to apoptosis and necrosis after central nervous system (CNS) trauma are relatively unexplored. No study has examined concurrent activation of calpain and caspase-3 in necrotic or apoptotic cell death after any CNS insult. Experiments used a model of oxygen–glucose deprivation (OGD) in primary septo-hippocampal cultures and assessed cell viability, occurrence of apoptotic and necrotic cell death phenotypes, and protease activation. Immunoblots using an antibody detecting calpain and caspase-3 proteolysis of α-spectrin showed greater accumulation of calpain-mediated breakdown products (BDPs) compared with caspase-3–mediated BDPs. Administration of calpain and caspase-3 inhibitors confirmed that activation of these proteases contributed to cell death, as inferred by lactate dehydrogenase release. Oxygen–glucose deprivation resulted in expression of apoptotic and necrotic cell death phenotypes, especially in neurons. Immunocytochemical studies of calpain and caspase-3 activation in apoptotic cells indicated that these proteases are almost always concurrently activated during apoptosis. These data demonstrate that calpain and caspase-3 activation is associated with expression of apoptotic cell death phenotypes after OGD, and that calpain activation, in combination with caspase-3 activation, could contribute to the expression of apoptotic cell death by assisting in the degradation of important cellular proteins. **Key Words:** Apoptosis—Calpain—Caspases—Necrosis—Stroke—TBI.

Increased activation of calpain and caspase-3 occurs in many central nervous system (CNS) injuries and diseases. Caspase-3 is considered a key executioner in the apoptotic cell death cascade and shares numerous substrates with the Ca^{2+}-dependent protease calpain, including the cytoskeletal protein α-spectrin (Wang, 2000). Studies examining animal models of ischemia have reported increased calpain (Bartus et al., 1995; Roberts-

Lewis et al., 1994; Yokota et al., 1995; Rami et al., 2000) or caspase-3 (Chen et al., 1998; Namura et al., 1998) activation after injury. Furthermore, inhibition of calpain (Hong et al., 1994; Markgraf et al., 1998) or caspase-3 (Fink et al., 1998; Himi et al., 1998) reduced infarct volume, substrate proteolysis, DNA fragmentation, and hippocampal cell death after focal and global ischemia. Activation of these proteases also has been observed in animal models of traumatic brain injury (TBI) (Newcomb et al., 1997; Pike et al., 1998a; Saatman et al., 1996; Yakovlev et al., 1997; Clark et al., 2000; Beer et al., 2000; Buki et al., 2000). Inhibition of calpain (Post-mantur et al., 1997) or caspase-3 (Yakovlev et al., 1997) is protective in these models, although conflicting data has been reported (Clark et al., 2000; Saatman et al., 2000). However, few investigations have examined concurrent activation of calpain and caspase-3 after CNS injury or disease (Buki et al., 2000; Nath et al., 1998; Pike et al., 1998a).

Although apoptosis and necrosis occur after ischemia (Linnik et al., 1993) and TBI (Colicos and Dash, 1996; Newcomb et al., 1999; Rink et al., 1995), the relation between protease activation and the expression of apoptotic and necrotic cell death phenotypes is relatively unexplored. Traditionally, calpain activation has been associated with necrosis, and caspase-3 activation with apoptosis. Although caspase-3 activation has not been detected in models of necrosis (Wang et al., 1996; Zhao et al., 1999), calpain activation has been implicated in various models of apoptosis (Nath et al., 1996; Pike et al., 1998b; Squier et al., 1994; Vanags et al., 1996). However, inconsistencies in criteria associated with cell death phenotypes have complicated data interpretation (Charriaut-Marlangue and Ben-Ari, 1995).

Oxygen–glucose deprivation (OGD) is a widely used *in vitro* model of ischemia, which produces apoptotic (Kalda et al., 1998) and necrotic (Gwag et al., 1995; Goldberg and Choi, 1993) cell death phenotypes and increased calpain and caspase-3 activity (Nath et al., 1998). Currently, no study has investigated the concurrent activation of calpain and caspase-3 in archetypal necrotic and apoptotic cell death phenotypes after any CNS insult. The current study sought to determine the contributions of these proteases to apoptotic and necrotic cell death after OGD. The current findings demonstrate that coactivation of calpain and caspase-3 is usually associated with the expression of apoptotic cell death phenotypes after OGD.

MATERIALS AND METHODS

Primary septo-hippocampal cultures

Septi and hippocampi were dissected from 18-day-old rat fetuses, dissociated by trituration, and the dissociated cells were plated on poly-L-lysine coated 24-well culture plates, 6-well culture plates or 12-mm German Glass (Erie Scientific, Portsmouth, NH, U.S.A.) at a density of 4.36×10^5 cells/mL. Cultures were maintained in Delbecco's modified Eagle's medium (DMEM) with 10% fetal bovine serum in a humidified incubator in an atmosphere of 5% CO_2 at 37°C. After 5 days in culture, the media was changed to DMEM with 5% horse serum. Subsequent media changes were performed three times a week. Experiments were performed on days 10 to 11 *in vitro* when astroglia had formed a confluent monolayer beneath morphologically mature neurons. All animal studies conformed to the guidelines outlined in *Guide for the Care and Use of Laboratory Animals* from the National Institutes of Health and were approved by the University of Florida and the University of Texas-Houston Health Science Center Animal Welfare Committee.

Oxygen–glucose deprivation

To achieve oxygen–glucose deprivation (OGD), a technique similar to that described by Copin et al. (1998) was used. Normal media was replaced with low glucose media (Hank's balanced salt solution containing 1.8 mmol/L Ca^{2+}, 0.8 mmol/L Mg^{2+}, and 0.2 g/L d-glucose) and culture plates were placed in an airtight chamber (Billups-Rothenberg, Del Mar, CA, U.S.A.). The chamber was flushed with 95% N_2/5% CO_2 for 3 minutes, sealed, and placed in a 37°C incubator for the appro-

priate duration. Initial experiments that manipulated the amount of time (1 to 10 minutes) the chamber was flushed with 95% N_2/5% CO_2 confirmed that 3 minutes of flushing combined with the low glucose media produced an environment severe enough to result in a consistent model of cell injury. After the insult, low glucose media was replaced with DMEM (serum-free) and cultures were returned to a normoxic environment. Initial experiments deprived cells of oxygen and glucose for various durations (1 to 12 hours) and samples were collected 24 hours after the cultures had returned to a normal environment. These data suggested that 10 hours of OGD resulted in substantial cell death and protease activation. To examine the effects of altering the length of reperfusion (that is, duration of normoxia after OGD) samples were collected at various times (immediately through 48 hours) after 10 hours of OGD. Subsequent experiments focused on 10 hours of OGD combined with 24 hours of reperfusion, unless stated otherwise.

Chemical inducers of apoptotic or necrotic cell death phenotypes

To provide comparisons of OGD with classic apoptotic and necrotic profiles, cultures were treated with staurosporine, a general protein kinase inhibitor, or maitotoxin, a potent marine toxin that activates both voltage-sensitive and receptor-operated calcium channels (Wang et al., 1996). Cultures were challenged with 0.5 μmol/L staurosporine for 24 hours, a dose and duration that produces apoptotic but not necrotic neuronal cell death in this *in vitro* system (Pike et al., 1998b). Separate cultures were treated with maitotoxin (0.1 nmol/L) for 1 hour, a dose and duration that produces an exclusively necrotic cell death profile in neurons and glia and is associated with calpain, but not caspase-3 activation (Zhao et al., 1999).

Pharmacologic inhibition of calpain and caspase activation

Cultures were pretreated 1 hour before and were cotreated during OGD, with various doses of calpain inhibitor-3 (CI-3, [MDL28170], 1 to 300 μmol/L; CalBiochem, San Diego, CA, U.S.A.), the pan-caspase inhibitor (Z-D-DCB, 50 to 200 μmol/L; Bachem, Philadelphia, PA, U.S.A.) or the specific caspase-3 inhibitor (z-DEVD-fmk, 50 to 200 μmol/L; CalBiochem). Stock solutions (50 mmol/L) of CI-3 (in dimethyl sulfoxide), Z-D-DCB (in EtOH), and z-DEVD-fmk (in dimethyl sulfoxide) were added directly to the low glucose media for the 1-hour pretreatment, and then cells were deprived of oxygen. Initial experiments confirmed that incubating cells with low glucose media for 1 hour had no effect on control cells or injury magnitude in cells later exposed to OGD (data not shown). After OGD, low glucose media was replaced with DMEM (serum-free) containing fresh inhibitor. Samples were collected 12 or 24 hours after OGD for lactate dehydrogenase (LDH) release and immunoblot analyses. Western blot analyses confirmed whether the drugs and doses used inhibited activation of calpain and caspase-3–like proteases inferred by α-spectrin proteolysis.

Determination of lactate dehydrogenase activity

Lactate dehydrogenase activity assessed cell viability (Koh and Choi, 1987) in experiments examining the effects of OGD and protease inhibition. Lactate dehydrogenase released from damaged cells was measured by standard kinetic assay for pyruvate (Hoffmann-LaRoche Ltd., Basel, Switzerland). Briefly, culture medium was removed from each well and centrifuged at 5,000 g for 5 minutes. One hundred microliters of supernatant was transferred to each well of 96-well flat bottom plate and 100 μL of detection reagent was added. After incubation, the

absorbance of samples was measured at 490 nm using Bio-Rad model 450 microplate reader (Hercules, CA, U.S.A.).

Annexin V and propidium iodide staining

Control cells and cells exposed to OGD, staurosporine, or maitotoxin were simultaneously stained with Annexin V and propidium iodide (PI) to differentiate apoptotic and necrotic cell death phenotypes. Cells were rinsed with phosphate-buffered saline (PBS) and incubated in staining solution consisting of HEPES buffer, Annexin V fluorescein labeling reagent (Molecular Probes; Eugene, OR, U.S.A.), and PI (Molecular Probes) for 15 minutes in the dark. Stained cells were examined with a Zeiss Axiovert 135 fluorescence microscope (Oberkochen, Germany) fitted with a filter combination that allowed green and red fluorescing cells to be seen simultaneously. The number of apoptotic and necrotic cells was calculated (10 sequential 320× fields were counted and averaged per well) for n = 3 wells per condition.

DNA gel electrophoresis

DNA gel electrophoresis was performed as previously described (Zhao et al., 2000; Gong et al., 1994). At the appropriate time after injury, cells were collected by centrifugation, fixed in 70% cold ethanol, and stored in fixative at −20°C for 24 to 72 hours. After subsequent centrifugation and removal of ethanol, cell pellets were resuspended in phosphate-citrate buffer at room temperature for 1 hour, centrifuged, and the supernatant was concentrated by vacuum in a SpeedVac concentrator (ThermoSavant, Holbrook, NY, U.S.A.). The pellet was incubated in Nonidet NP-40 and DNase-free RNase followed by proteinase K. After the incubation, 6× loading buffer was added and the contents of the tube were transferred to a 1.5% agarose gel. Electrophoresis was performed in 1× 0.1 mol/L Tris, 0.09 mol/L boric acid, 1 mmol/L EDTA, pH 8.4 at 40 V for 2 hours. DNA was visualized and photographed under UV light after staining with 5 μg/mL ethidium bromide.

DNA fragmentation ELISA

Apoptotic cell death also was examined with an assay that allowed specific determination of mono- and oligonucleosomes in the cytoplasmic fraction of cell lysates (Cell Death Detection ELISA Plus; Hoffman-LaRoche Ltd., Basel, Switzerland). At the appropriate time after injury, cells were collected by centrifugation and 2 mL lysis buffer was mixed with the pellet. The solution was incubated for 30 minutes at room temperature and stored at −20°C for 24 to 72 hours. After thawing, diluted samples (5 μL sample + 15 μL lysis buffer) were added to each well of a streptavidin-coated, 96-well microtiter plate (separate studies confirmed that this dilution resulted in a suitable cell concentration, data not shown). Eighty microliters of reagent solution containing incubation buffer, anti–histone-biotin, and anti–DNA-POD was added to each well and incubated with the sample on a shaker for 2 hours. The solution was removed and wells were rinsed with incubation buffer to remove unbound antibody. The amount of POD retained in the immunocomplex—and thus the amount of DNA fragments—was determined colorimetrically with the substrate ABTS using a microplate reader (Bio-Rad Model 450) at 405 nm with a reference filter of 490 nm. Absorbance values were calculated and reported as percent of control.

Assessment of caspase-3 and calpain activity

The cytoskeletal protein α-spectrin contains sequence motifs preferred by calpain and caspase-3 proteases; thus, activation of these proteases can be assessed concurrently by immunoblot identification of calpain and/or caspase-3 signature cleavage products. Although calpains and caspases produce initial fragments of nearly identical size (150 kDa), calpains further process α-spectrin into a distinctive breakdown product (BDP) of 145 kDa (Harris et al., 1988; Nath et al., 1996), whereas caspase-3 produces a unique 120-kDa BDP (Wang et al., 1998b). Notably, the initial 150-kDa fragment produced by calpain differs from that produced by the caspases. Immunocytochemistry using antibodies specific for this calpain-mediated fragment (SBDP 150) or the 120-kDa fragment produced by caspase-3 (SBDP 120) allows detection of calpain- and/or caspase-3–mediated proteolysis of α-spectrin in individual cells. Caspase-3 activation also can be inferred by the appearance of BDPs to the proenzyme, because activation occurs when caspase-3 is proteolyzed into smaller subunits.

Sodium dodecyl sulfate-polyacrylamide gel electrophoresis and immunoblotting. Gel electrophoresis and immunoblotting were performed as described previously (Pike et al., 2000). At the appropriate time after injury, media was removed and cells were collected from each well with lysis buffer and sheared with a 25-gauge needle. Protein content was assayed by the Micro BCA method (Pierce, Rockford, IL, U.S.A.). For protein electrophoresis, equal amounts of total protein (25 μg) were prepared in 4× loading buffer and heated at 95°C for 10 minutes. For analysis of α-spectrin proteolysis, samples were resolved in a vertical electrophoresis chamber using a 4% stacking gel over a 6.5% acrylamide resolving gel. Separated proteins were laterally transferred to a nitrocellulose membrane (0.45 μm). For analysis of caspase-3 proteolysis, samples were resolved using a 4% to 20% gradient acrylamide gel or a Tris-Tricine gel (16.5% + 4% stacking). Separated proteins were laterally transferred to a nitrocellulose membrane (0.2 μm). Nitrocellulose membranes were stained with Panceau red (Sigma, St. Louis, MO, U.S.A.) to ensure even transfer of all samples to the membranes and to confirm that equal amounts of protein were loaded in each lane. Blots were blocked overnight in 5% nonfat milk in 20 mmol/L Tris, 0.15 mol/L NaCl, and 0.005% Tween-20 at 4°C.

Immunoblots were probed with an anti–α-spectrin monoclonal antibody (Affiniti Research Products, U.K.) that detects intact α-spectrin (MW_r = 240 kDa) and 150-, 145-, and 120-kDa BDP, as described previously (Pike et al., 2000). Separate blots were probed with a caspase-3 polyclonal antibody (1:500; Santa Cruz Biotechnology, Santa Cruz, CA, U.S.A.) that detects the caspase-3 proenzyme (32 kDa) and proteolytic fragments. After incubation in primary antibody for 2 hours at room temperature, blots were incubated in peroxidase-conjugated goat anti-rabbit IgG (1:3000) for 1 hour. Enhanced chemiluminescence reagents (ECL; Amersham, Buckinghamshire, U.K.) were used to visualize immunolabeling on Hyperfilm (Hyperfilm ECL; Amersham).

Semiquantitative evaluation of protein levels detected by immunoblotting was performed through computer-assisted, one-dimensional densitometric scanning (AlphaImager 2000 Digital Imaging System; San Leandro, CA, U.S.A.). Data were acquired as integrated densitometric values and transformed to percentages of the densitometric values obtained from control samples. Data from multiple Western blots (n = 4) were combined and analyzed statistically.

Calpain- and caspase-3–mediated α-spectrin BDPs in individual cells. Cells were cultured on German Glass for immunocytochemistry protocols. Control cultures or cells exposed to OGD, staurosporine, or maitotoxin were fixed in 4% paraformaldehyde for 5 minutes and rinsed in PBS. Cells were blocked in 10% normal goat serum in PBS for 30 minutes at 37°C and incubated simultaneously in primary antibodies specific for SBDP 150 (1:100, polyclonal, made in rabbit; gift

from T.C. Saido, Japan, (Saido et al., 1993)) and SBDP 120 (1:100, polyclonal, made in chicken; gift from Kevin Wang, Parke-Davis, Ann Arbor, MI (Buki et al., 2000)) for 30 minutes at 37°C. After rinsing in PBS/0.05% Tween 20, cells were incubated in secondary antibodies linked to Alexa Fluor 488 (1:50, goat α-chicken; Molecular Probes, Eugene, OR, U.S.A.) or Alexa Fluor 568 (1:50, goat α-rabbit; Molecular Probes) for 30 minutes at 37°C. To assess nuclear morphology (that is, characteristics of necrotic or apoptotic alterations) cells were counterstained with the DNA dye, 4' 6-diamidino-2-phenylindole, dihydrochloride (DAPI, 1:500; Molecular Probes). German Glass were mounted onto glass slides with Fluoromount-G (Southern Biotechnology Associates; Birmingham, AL, U.S.A.).

Cells were examined under oil immersion at 1000× magnification with a Zeiss Axiovert 135 fluorescence microscope equipped as described above. DAPI staining was viewed with a UV2A filter (Zeiss). Nuclear morphology was assessed in cells immunoreactive for SBDP 150, or SBDP 120, or both, and cells were categorized (blind to treatment condition) as healthy, apoptotic, or necrotic. Nuclei of healthy cells can be identified by a homogenous and diffuse fluorescent chromatin, whereas cells classified as apoptotic fluoresce intensely and are characterized by highly condensed chromatin, visibly shrunken and often irregular shaped nuclei, margination of chromatin along the periphery of the nuclear envelope, or by the separation of the nucleus into discrete nuclear fragments (apoptotic bodies). In contrast, necrotic cells fluoresce brightly with pyknotic chromatin where nuclei have maintained their basic morphology or have become rounded or swollen in appearance. These cells also fail to exhibit apoptotic morphology (Schmechel, 1999; Purnanam and Boustany, 1999). Using these criteria, the number of healthy, apoptotic, and necrotic SBDP 150 and SBDP 120 immunoreactive cells were quantified in control and OGD cultures.

Analysis of cell types

Control cells or cells exposed to OGD were prepared for immunocytochemistry as described above. Cells were labeled with both neuronal nuclear marker (NeuN) and microtubule-associated protein (MAP)2 or GFAP (glial fibrillary acidic protein) to evaluate neuronal and astroglial morphology, respectively. Using both NeuN and MAP2 allowed clear visualization of the neuronal cell body and processes. All cells were blocked in 10% normal goat serum in PBS and were incubated in primary antibodies specific for NeuN (1:1000, monoclonal; Chemicon, Temecula, CA, U.S.A.) and MAP2 (1:1000, monoclonal; Sternberger Monoclonals, Lutherville, MD, U.S.A.) or GFAP (1:1000, monoclonal; Sigma). After rinsing in PBS/0.05% Tween 20, cells were incubated in secondary antibody linked to Alexa Fluor 488 (1:50, goat α-mouse; Molecular Probes). Cells were counterstained with DAPI and mounted onto glass slides with Fluoromount-G.

Samples immunolabeled with NeuN and MAP2 were examined under low magnification to assess neuronal loss after OGD (10 sequential 320× fields were counted and added per sample, n = 6). Samples immunolabeled with GFAP also were examined under low magnification, however quantitative data on loss of GFAP-positive cells could not be obtained because of the high density of these cells and the inability to differentiate individual glia. Under high magnification (1000×), DAPI staining was examined in NeuN- and/or MAP2-positive cells and GFAP-positive cells (50 random immunoreactive cells per sample) to assess the nuclear morphology of neurons and astroglia, respectively. Values for healthy, apoptotic, and necrotic

neurons and astroglia were calculated for control and OGD cells using the criteria described above.

Statistical analysis

Data were evaluated by one-way analysis of variance and *post hoc* least significant difference *t* test. Values are given as mean ± SD. Differences were considered significant at $P \leq 0.05$.

RESULTS

Effects of oxygen–glucose deprivation on primary mixed septo-hippocampal cultures

Effects of oxygen–glucose deprivation duration and reperfusion. An initial set of experiments (data not shown) was conducted to evaluate duration of OGD on cell viability. Primary mixed septo-hippocampal cultures were deprived of oxygen and glucose for 1, 6, 8, 10, or 12 hours and media was collected 24 hours after cultures were returned to normal conditions for analysis of LDH release. Reported as percent of control, significant increases in LDH release ($P < 0.01$) occurred after 6 (204% ± 18.1%), 8 (233% ± 30.1%), 10 (895% ± 43.1%), and 12 (725% ± 70.5%) hours of OGD. Subsequent experiments (data not shown) investigated the effect of reperfusion length on cell viability. Samples were subjected to OGD for 10 hours and media were collected immediately or after 3, 12, 24, or 48 hours of reperfusion for analysis of LDH release. Significant increases in LDH release were evident immediately after injury (172% ± 15.2%, $P < 0.05$) compared with control cultures. Moreover, increasing the length of reperfusion resulted in a time-dependent and significant increase in LDH release ($P < 0.001$) at all later times tested—3 (367% ± 51.7%), 12 (561% ± 5.6%), 24 (674% ± 14.7%), and 48 (784% ± 5.6%) hours after injury, compared with control samples.

Characterization of cell death phenotypes after oxygen-glucose deprivation. To distinguish apoptotic and necrotic cell death, control cells and cells subjected to OGD (10 hours + 24 hours of reperfusion) were stained with Annexin V and PI (data not shown). Staurosporine- (0.5 mmol/L for 24 hours) and maitotoxin- (0.1 nmol/L for 1 hour) treated cells were used as positive controls of apoptosis and necrosis, respectively. Values are reported as total apoptotic or necrotic cells per well (10, 320× fields). Uninjured control cultures contained few apoptotic (78.0 ± 40.0) or necrotic (8.3 ± 2.1) cells. Cultures subjected to OGD contained significantly ($P < 0.001$) more apoptotic (356.3 ± 32.0) and necrotic (180.7 ± 37.4) cells compared with control cultures. In comparison, staurosporine treatment produced a significant increase ($P < 0.001$) in apoptotic cells (389.3 ± 37.5) with fewer necrotic cells (38.3 ± 14.4), whereas maitotoxin treatment resulted in a significant increase ($P < 0.001$) in necrotic cells (597.0 ± 73.4) with fewer apoptotic cells (13.7 ± 3.8) compared with control cultures.

Examination of DAPI staining (10, 1000× fields) revealed morphologic changes in chromatin staining that

were clearly distinguishable from the classic necrotic phenotype (Fig. 1A and 1B). These nonnecrotic changes showed different evolutionary stages of chromatin margination, condensation, and formation of apoptotic bodies. Thus, these nuclear profiles were termed apoptoticlike. Most stained nuclei in control cultures were healthy; however, some apoptoticlike nuclei were observed and were probably because of spontaneous apoptosis (Fig. 1A). Compared with control cultures, OGD cultures contained significantly less healthy nuclei ($P < 0.001$) and significantly more apoptoticlike nuclei ($P < 0.001$). Necrotic nuclei were rarely observed in either control or
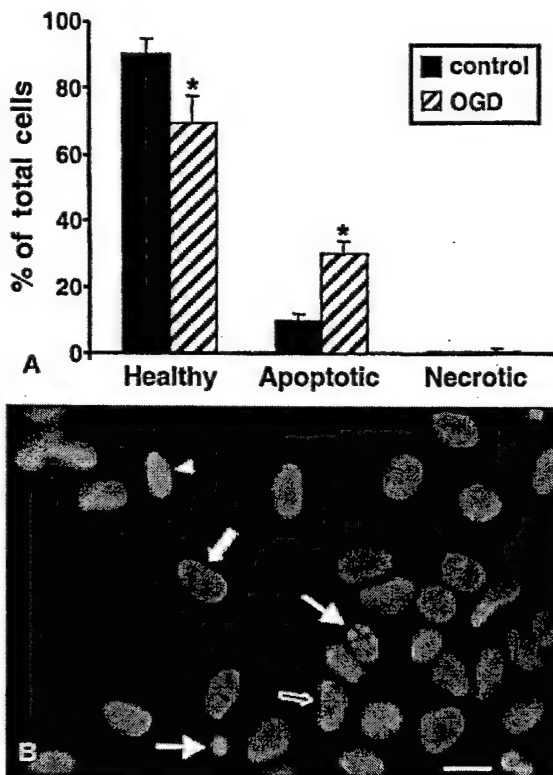

FIG. 1. Analysis of nuclear morphology after oxygen–glucose deprivation (OGD). **(A)** Control cultures and cultures deprived of oxygen and glucose (10 hours + 24 hours of reperfusion) were stained with DAPI, and cells were characterized as healthy, apoptoticlike, or necrotic based on nuclear morphology. Control cultures contained mostly healthy nuclei (90.1% ± 6.1%), although apoptoticlike nuclei (9.6% ± 2.9%) were detected. Compared with control cultures, OGD contained significantly fewer healthy nuclei (69.3% ± 10.5%) and significantly more apoptoticlike nuclei (30.0% ± 5.4%). No significant differences were observed in the percentage of necrotic cells between control (0.3% ± 0.2%) and OGD (0.7% ± 1.0%) cultures. *$P < 0.001$. **(B)** DAPI staining of septo-hippocampal cultures after OGD. Representative image illustrating the typical distribution of cell death phenotypes after OGD (10 hours + 24 hours of reperfusion). Nuclei exhibiting apoptoticlike morphology such as chromatin condensation (arrowhead), irregular-shaped nuclei (open arrow), and the formation of apoptotic bodies (thin arrows) were frequently detected after OGD. Healthy nuclei (wide arrow) also were observed after injury. Scale bar = 1 μm.

OGD cultures. Figure 1B shows a representation of the typical distribution of cell death phenotypes after OGD in this culture system. Nuclei exhibiting apoptoticlike morphology were frequently detected after OGD, as well as cells with healthy nuclei. Surprisingly, examination of DAPI staining in OGD cultures failed to reveal a substantial number of necrotic cells, in contrast with data collected with Annexin V and PI staining. This reduction in necrotic cells may be caused by the frequent rinses and incubations performed during the immunocytochemistry and DAPI staining protocol that may have caused many necrotic cells to detach and go undetected by DAPI in the culture system. However, quite similar data were obtained using these separate techniques to calculate the number of apoptoticlike cells per sample. If values are adjusted to reflect the different field magnifications (320× for Annexin and 1000× for DAPI), the average number of apoptoticlike cells per sample is similar for Annexin (356.3 cells per sample) and DAPI (332.8 cells per sample, data not shown). These data stress the reliability of the authors' assessments of the contribution of apoptosis to cell death in the culture system.

Condensation and aggregation of chromatin, as shown with DAPI staining (Fig. 1B), may occur independently of endonuclease activation (Oberhammer et al., 1993). Therefore, two separate techniques were used to qualitatively (Fig. 2A) and quantitatively (Fig. 2B) assess internucleosomal DNA fragmentation, and thus endonuclease activation, after OGD. DNA electrophoresis (Fig. 2A) revealed a robust ladder pattern, characteristic of internucleosomal DNA fragmentation, after 10 hours of OGD with 12, 24, and 48 hours of reperfusion. Faint bands also were detected after 3 hours of reperfusion. Staurosporine treatment produced a characteristic DNA ladder pattern, whereas control samples and cells subjected to maitotoxin failed to show any internucleosomal fragments.

As an additional indicator of internucleosomal fragmentation, the amount of mono- and oligonucleosomes in the cytoplasmic fraction of cell lysates was quantitatively assessed (Fig. 2B). Control cultures showed little DNA fragmentation, whereas cells deprived of oxygen and glucose for 10 hours contained significantly more mono- and oligonucleosomes after 24 ($P < 0.001$) and 48 ($P < 0.001$) hours of reperfusion, but not after 3 or 12 hours of reperfusion. In comparison, staurosporine treatment resulted in a significant increase ($P < 0.001$) in mono- and oligonucleosomes, whereas samples exposed to maitotoxin were not statistically different from control samples.

Induction of cell death by oxygen–glucose deprivation in neurons and glia. To identify the type of cell (that is, neuron vs. astroglia) affected by OGD, primary mixed septo-hippocampal cultures were stained with NeuN and MAP2 (for neurons) or GFAP (for astroglial)
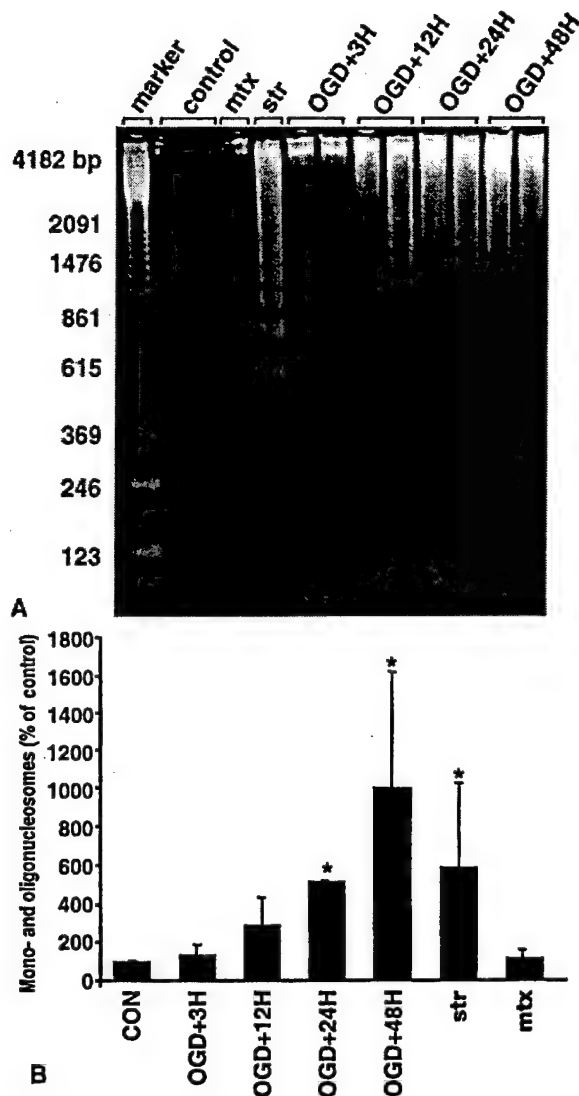
FIG. 2. Assessment of internucleosomal DNA fragmentation after oxygen–glucose deprivation (OGD). **(A)** DNA electrophoresis. Samples collected from control and maitotoxin (mtx)-treated cultures showed no internucleosomal DNA fragmentation, whereas staurosporine (str) treatment produced a characteristic DNA ladder pattern. Cultures subjected to OGD for 10 hours and collected 3 hours after injury exhibited a faint ladder. Prominent DNA laddering was observed 12, 24, and 48 hours after injury. **(B)** DNA fragmentation assay. DNA fragmentation was quantitatively assessed by detection of mono- and oligonucleosomes in the cytoplasmic fraction of cell lysates. Analysis of control cultures demonstrated little DNA fragmentation, similar to cells deprived of oxygen and glucose for 10 hours after 3 (129% ± 46.8%) or 12 (287% ± 163.0%) hours of reperfusion. However, a significant increase in mono- and oligonucleosomes was detected in cells deprived of oxygen and glucose for 10 hours after 24 (513% ± 5.6%) and 48 (998% ± 606.9%) hours of reperfusion. Staurosporine (str) treatment resulted in a significant increase (582% ± 441.7%) in mono- and oligonucleosomes, whereas samples exposed to maitotoxin (mtx) were not statistically different from control samples (111% ± 58.1%). *P < 0.001.

and counterstained with DAPI (Fig. 3). Low magnification examination of NeuN and MAP2 staining in OGD cultures revealed a significant loss (68% ± 9.3% of control values, $P < 0.001$) of immunoreactive (IR) neurons (data not shown). Examination of GFAP staining in cells subjected to OGD showed that OGD had a modest effect on astroglia that was not readily apparent under low magnification.

High magnification (1000×) examination of NeuN, or MAP2 IR cells, or both (Fig. 3), showed that the majority of positive cells in control cultures possessed large cell bodies and several intact processes that were intensely labeled for both neuronal markers (Fig. 3A). These cells contained healthy, oval-shaped nuclei with diffuse chromatin distribution (Fig. 3B). In contrast, NeuN and MAP2 staining of OGD cultures showed a substantial number of neurons with shrunken cell bodies and fragmented processes (Fig. 3C). Nuclei of these neurons were shrunken, irregularly shaped, and possessed highly condensed chromatin (Fig. 3D). Apoptoticlike nuclei that were not IR for NeuN or MAP2 also were observed (Fig. 3D). These cells may have been apoptotic astroglia, or more likely, neurons in an advanced stage of apoptosis in which the phenotype is most apparent and degeneration of cellular proteins may compromise the retention of epitopes necessary for cell type identification. Quantitative analysis of DAPI staining in NeuN, or MAP2 IR cells, or both (50 random IR cells per sample), demonstrated that the majority of positive cells in control cultures exhibited healthy nuclear morphology (83.3% ± 4.4%). Although cells with apoptoticlike nuclei (16.7% ± 1.8%) were occasionally observed, neurons with necrotic nuclei were not detected in this set of control cultures. Analysis of DAPI staining in OGD cultures revealed a significantly lower percentage of healthy nuclei (57.3% ± 9.3%, $P < 0.001$) and significantly higher percentage of apoptoticlike nuclei (40.3% ± 8.6%, $P < 0.001$), compared with control cultures. Although OGD cultures also contained more necrotic nuclei (2.3% ± 1.5%) than control cultures, necrotic cells were rarely observed.

Examination of GFAP staining in control and OGD cultures showed that most GFAP-positive cells were healthy astroglia with large cell bodies, extensive processes, and diffuse and even immunoreactivity (Fig. 3E and 3G, respectively). Astroglial nuclei were large and oval-shaped with even chromatin distribution (Fig. 3F and 3H). Although most IR cells in OGD cultures appeared healthy, cells with shrunken cell bodies, broken processes, and aggregated GFAP immunoreactivity also were observed (Fig. 3G).

These cells possessed shrunken nuclei with highly condensed chromatin and apoptotic bodies (Fig. 3H). Quantitative assessment of DAPI staining in GFAP IR cells (50 random IR cells per sample) showed that most GFAP-positive cells in control (98.3% ± 12.7%) and
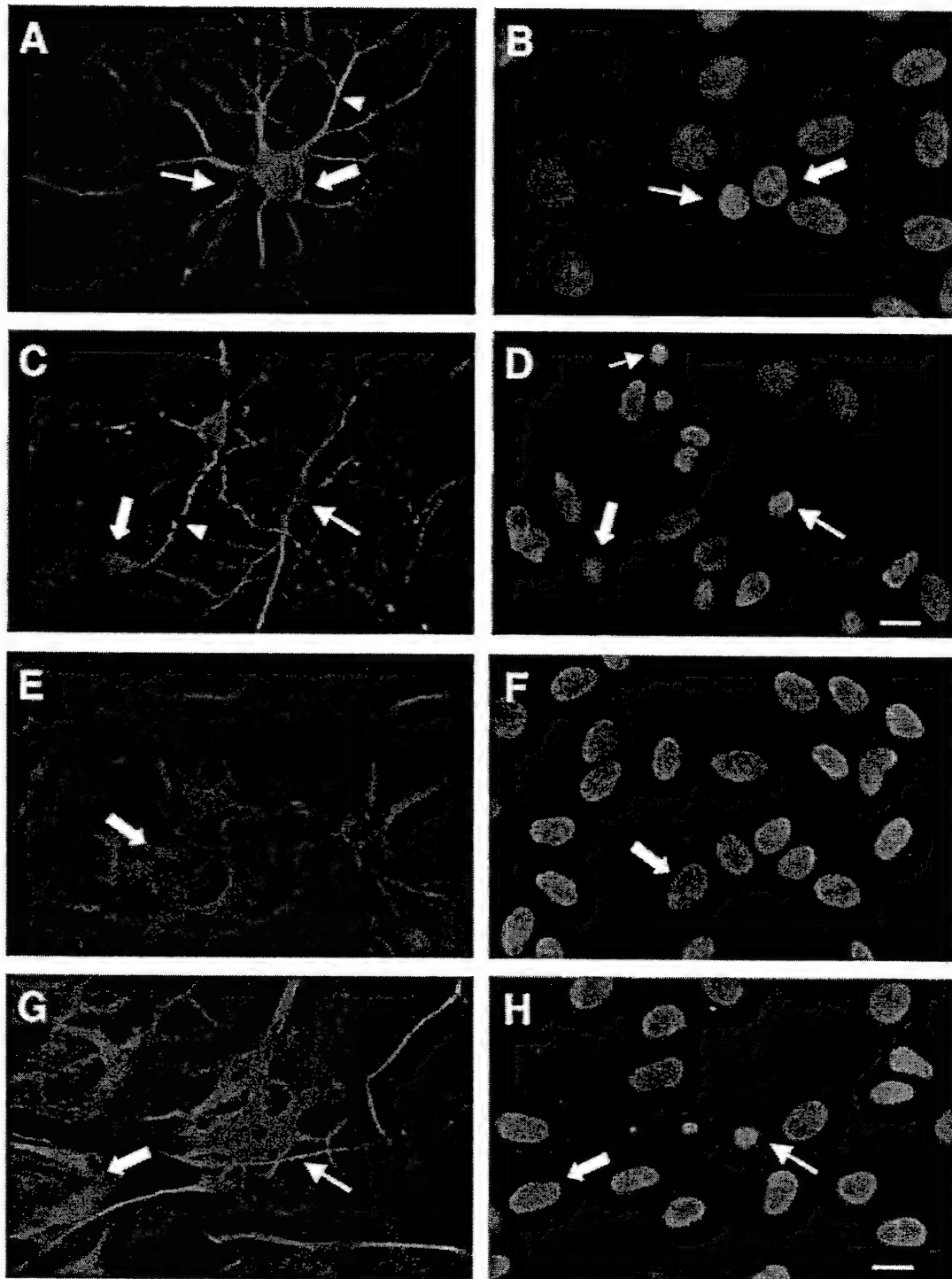
FIG. 3. Neuronal and glial morphology after oxygen–glucose deprivation (OGD). Cultures were immunolabeled with NeuN and MAP2 or GFAP (glial fibrillary acidic protein) and were counterstained with DAPI to assess morphologic and nuclear changes after OGD (10 hours + 24 hours of reperfusion). Cells were examined under high magnification (1000×). (A) NeuN/MAP2 immunoreactive (IR) cells in control cultures possessed large cell bodies (thin arrow, wide arrow) and several intact processes (arrowhead) that were intensely labeled for both neuronal markers. (B) These cells contained healthy, oval-shaped nuclei with diffuse chromatin distribution (thin arrow, wide arrow). (C) Cultures deprived of oxygen and glucose showed a substantial number of neurons with shrunken cell bodies (thin arrow, wide arrow) and fragmented processes (arrowhead). (D) Neuronal nuclei were shrunken, irregularly shaped and possessed highly condensed chromatin (thin arrow, wide arrow). Apoptotic nuclei not IR for NeuN or MAP2 also were observed (small arrow). (E) Control cultures contained healthy astroglia with large cell bodies, extensive processes, and diffuse and even immunoreactivity (arrow). (F) Nuclei were large and oval-shaped with even chromatin distribution (arrow). (G) OGD cultures contained a majority of healthy GFAP-positive cells (wide arrow), but cells with shrunken cell bodies, broken processes, and aggregated GFAP immunoreactivity also were observed (thin arrow) and characterized as apoptoticlike. (H) Nuclei in healthy astroglia resembled those detected in control cultures (wide arrow). Apoptotic astroglia contained shrunken nuclei with highly condensed chromatin and apoptotic bodies (thin arrow). Scale bars = 1 μm.

OGD (91.4% ± 27.2%) cultures possessed healthy nuclei. DAPI staining revealed some effects of OGD, including a decreased percentage of healthy nuclei and an increased percentage of apoptoticlike nuclei (8.4% ± 2.0%), compared with control cells (1.6% ± 1.5%), but these differences were not statistically significant. Necrotic nuclei were rarely observed in either control (0.2% ± 0.5%) or OGD (0.2% ± 0.5%) cultures.

Calpain and caspase-3 proteolysis of α-spectrin after oxygen–glucose deprivation

Western blots. Activation of calpain and caspase-3 after OGD was assessed with Western blots examining proteolysis of α-spectrin (Fig. 4A and 4B). After 10 hours of OGD, samples were collected immediately (0 hour), 3, 12, 24, or 48 hours after cultures were returned to a normal environment. Control samples and samples

deprived of oxygen and glucose for 10 hours and collected immediately after injury showed no evidence of calpain-mediated proteolysis of α-spectrin. However, 3 hours after reperfusion, proteolysis of α-spectrin into 150-kDa and calpain-mediated 145-kDa BDPs was significantly increased over control values ($P < 0.001$). Degradation of α-spectrin continued and proteolysis into the 145-kDa BDP also was increased after 12, 24, and 48 hours of reperfusion ($P < 0.001$). Modest degradation of native α-spectrin was observed after 48 hours of reperfusion ($P < 0.01$). Slight increases in caspase-3–mediated proteolysis were detected after injury, but formation of the 120-kDa BDP was variable and did not differ significantly from control. However, immunoblots detected proteolysis of the caspase-3 proenzyme to the activated isoform (Fig. 4C), suggesting that analyses of autolytic
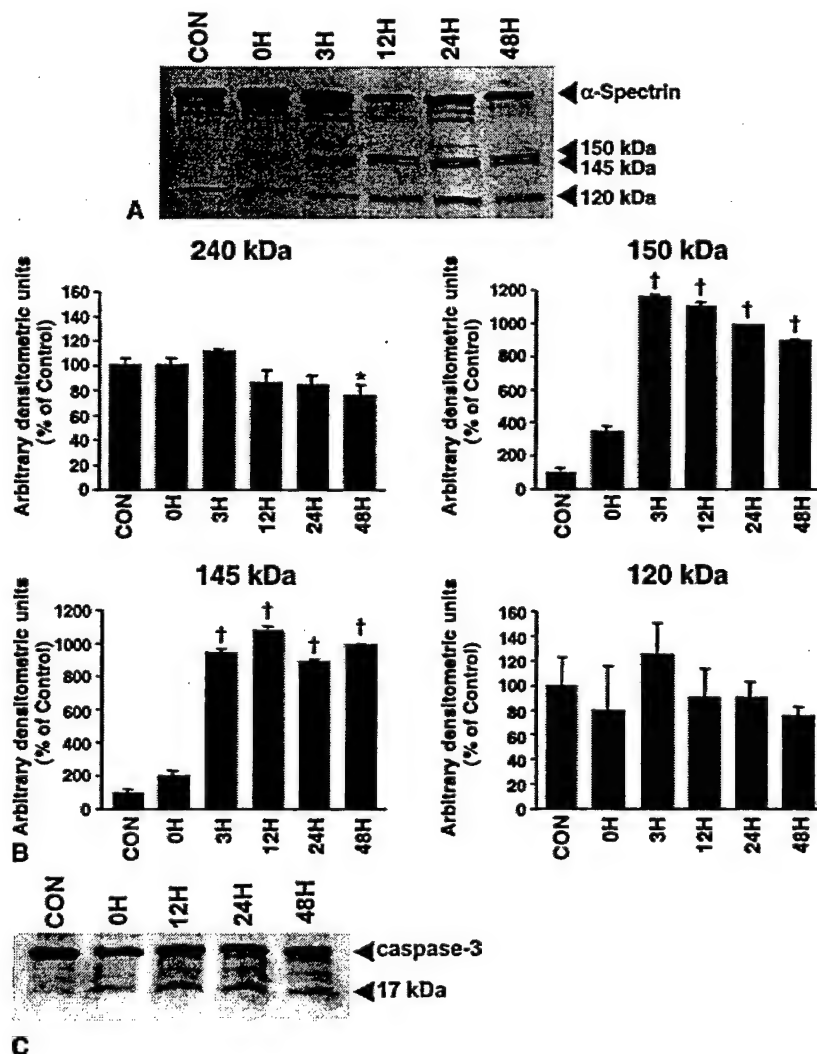

FIG. 4. Calpain- and caspase-3–mediated proteolysis of α-spectrin after oxygen–glucose deprivation (OGD). **(A)** Representative Western blot showing calpain- and caspase-3–mediated proteolysis of α-spectrin after OGD. Control samples and samples collected immediately (0 hour) after injury showed no evidence of calpain-mediated proteolysis of α-spectrin. Accumulation of the 150- and 145-kDa BDPs was detected 3, 12, 24, and 48 hours after OGD. Moderate increases in the caspase-3–mediated BDP were detected after injury, but formation of the 120-kDa BDP was variable. **(B)** Calpain- and caspase-3–mediated proteolysis of α-spectrin semiquantitative analysis. Data from multiple Western blots analyzing α-spectrin proteolysis were acquired as integrated densitometric values and transformed to percentages of the densitometric values obtained from control samples. Formation of the 150- and 145-kDa BDPs was increased after OGD with 3, 12, 24, and 48 hours of reperfusion, whereas modest degradation of native α-spectrin (240 kDa) was detected after 48 hours of reperfusion. Accumulation of the caspase-3–mediated 120-kDa BDP was variable. *$P < 0.01$. †$P < 0.001$. **(C)** Activation of caspase-3 after OGD. Proteolysis of caspase-3 (32 kDa) to the activated isoform (17 kDa) was examined after 10 hours of OGD and 0, 12, 24, or 48 hours of reperfusion. Degradation of the proenzyme (32 kDa) was evident 12, 24, and 48 hours after injury. Proteolysis of caspase-3 into the 17-kDa subunit was detected with all lengths of reperfusion examined.

activation of the caspase-3 proenzyme may be more sensitive than analyses of processing of cytoskeletal protein substrates.

Immunocytochemistry. Primary mixed septo-hippocampal cultures were double-labeled with antibodies specific for calpain (SBDP 150) and caspase-3 (SBDP 120) mediated α-spectrin proteolytic fragments and were counterstained with DAPI (Fig. 5). Across all treatment conditions, cells with evidence of nuclear damage exhibited strong immunoreactivity, whereas most healthy cells showed faint or no immunoreactivity. Cultures deprived of oxygen and glucose had significantly increased cellular colocalization of SBDP 150 and SBDP 120 (93.5 ± 16.7 cells per sample, $P < 0.001$), compared with control cultures (23 ± 8.6 cells per sample). Although OGD cultures contained substantially more IR cells than control cultures, examination of immunocytochemistry showed a similar distribution of protease activation, regardless of treatment condition (Fig. 5A and 5C). Virtually all IR cells in control and OGD cultures showed concurrent calpain and caspase-3 proteolysis in varying magnitudes (Fig. 5A and 5C). Immunolabeling in control (Fig. 5A) and OGD (Fig. 5C) cultures resulted in subcellular localization of BDPs unique from staurosporine (Fig. 5E) or maitotoxin cultures (Fig. 5G). In control and OGD cells, SBDP 150 was localized exclusively within the cell body, that is, near the nuclear membrane. Conversely, SBDP 120 immunoreactivity was detected throughout the entire cell body, specifically along the outer boundary of the cell membrane, and in the proximal processes (Fig. 5A and 5C). The nuclei of IR cells were shrunken, irregularly shaped, possessed condensed chromatin, and were considered apoptoticlike (Fig. 5B and 5D). Staurosporine injured cells were immunoreactive for both SBDP 120 and SBDP 150 in cells exhibiting apoptoticlike nuclear morphology (Fig. 5E and 5F). Notably, different relative magnitudes of caspase-3 and calpain activation were evident in individual cells, but distinct localization of BDPs was not as apparent as the immunoreactivity in control and OGD cells. Maitotoxin-injured cells showed predominantly calpain-mediated BDPs in cells exhibiting the classic necrotic nuclear morphology of rounded, brightly fluoresced nuclei with pyknotic chromatin (Fig. 5G and 5H).

Quantitative analysis of DAPI staining in cells immunoreactive for SBDP 150 or SBDP 120 (data not shown) revealed that the majority of IR cells possessed apoptoticlike nuclei in control (95.7% ± 38.7%) and OGD (97.9% ± 17.2%) cultures. Few IR cells exhibiting a necrotic cell death phenotype were observed in control (1.4% ± 3.7%) or OGD (1.4% ± 1.5%) cultures. Occasionally, IR cells with healthy nuclei were present in control (2.9% ± 3.2%) and OGD (0.7% ± 1.0%) cultures. However, these cells may have been in the initial stages of cell death in which nuclear changes were not yet apparent.

Effects of calpain and caspase inhibitors

Preliminary experiments using protease inhibitors in cultures subjected to 10 hours of OGD and 24 hours of reperfusion data failed to show protection against cell death when LDH release was assayed (data not shown). These data suggested that 24 hours of reperfusion was too long a period to allow the inhibitors to be effective, or that the inhibitors became toxic after such long periods. Moreover, the current data demonstrated robust cell death, DNA fragmentation (Fig. 2), and protease activation (Fig. 4) with 10 hours of OGD and 12 hours of reperfusion. In an attempt to show protection and therefore involvement of calpain and caspase-3, cells were subjected to 10 hours of OGD with 12 hours of reperfusion in the presence of protease inhibitors. Lactate dehydrogenase analysis (Fig. 6A) showed significant decreases in release with CI-3 (100 μmol/L; $P < 0.001$) compared with vehicle-treated cultures. The specific caspase-3 inhibitor, DEVD-fmk (100 μmol/L, $P < 0.05$), also inhibited LDH release; however, decreases were not statistically significant compared with vehicle-treated cultures. The pan-caspase inhibitor, Z-D-DCB (100 μmol/L), had no effect on LDH release. Dimethyl sulfoxide also decreased LDH release, but this effect was not significantly different from the OGD and media cultures.

Consistent with the LDH data, Western blot analyses of these samples (Fig. 6B) showed that CI-3 decreased proteolysis of native 240 kDa α-spectrin and almost completely blocked the formation of the 150/145 kDa doublet. Z-D-DCB also inhibited formation of the 145 kDa BDP to a small extent, but had only a minor effect on the caspase-3–mediated BDP (120 kDa). Surprisingly, DEVD-fmk dramatically reduced the calpain-mediated BDP, but only had a modest effect on the 120 kDa band. Subsequent experiments investigating combined inhibition using CI-3 and DEVD-fmk failed to show a synergistic mechanism. Future experiments should examine more extensive dosing protocols.

DISCUSSION

Although numerous studies have investigated calpain and caspase-3 activation after acute CNS trauma, no study has examined the relation between protease activation and expression of cell death phenotypes. In the current study, the authors detected prominent expression of apoptoticlike cell death phenotypes following a model of OGD, especially in neurons. Moreover, coactivation of calpain and caspase-3 was almost always detected in cells exhibiting apoptoticlike cell death phenotypes.

Oxygen–glucose deprivation resulted in both apoptosis and necrosis in this culture system. Although apop-
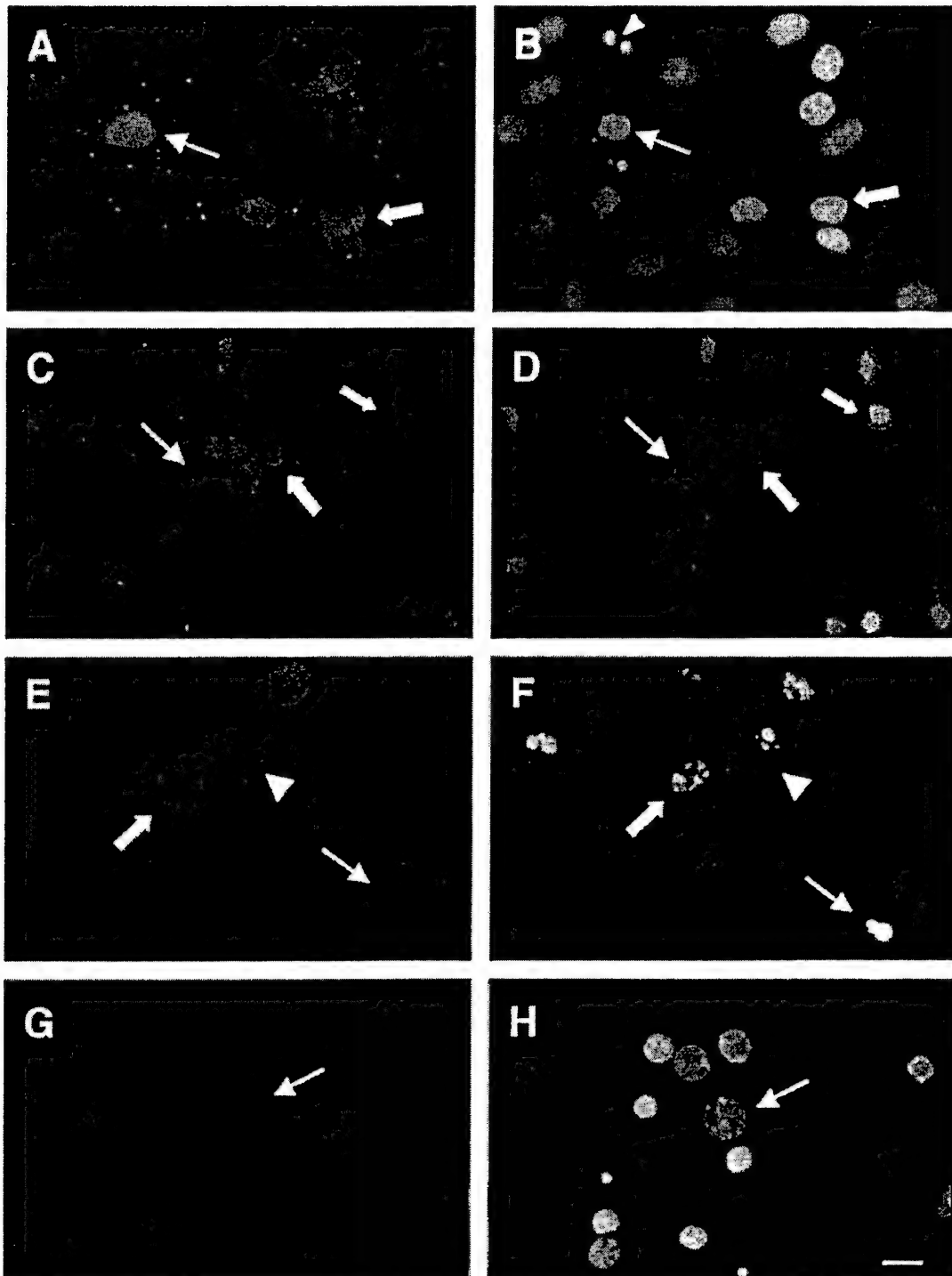
FIG. 5. Calpain and caspase-3 proteolysis of α-spectrin in individual cells following oxygen–glucose deprivation (OGD). Primary mixed septo-hippocampal cultures were immunolabeled with antibodies specific for calpain- (SBDP 150, red fluorescence) and caspase-3 (SBDP 120, green fluorescence)–mediated α-spectrin fragments, and counterstained with DAPI. **(A)** The majority of cells in control cultures were not immunoreactive (IR) for α-spectrin BDPs; however, cells that were IR exhibited both calpain- and caspase-3–mediated BDPs (thin arrow, wide arrow). **(B)** Nuclei of IR cells were shrunken and exhibited chromatin condensation (thin arrow, wide arrow) and apoptotic bodies were also evident (arrowhead). **(C)** OGD cultures also showed concurrent calpain and caspase-3 proteolysis (thin arrow, wide arrows). In addition, IR cells from control (A) and OGD (C) cultures showed subcellular localization of BDPs; SBDP 150 was detected exclusively within the cell body, while SBDP 120 was observed throughout the entire cell body and the proximal processes (A, C, all arrows). **(D)** Nuclei of IR cells in OGD cultures were shrunken, irregularly shaped, and possessed highly condensed chromatin (wide arrows). Nuclei with chromatin margination along the periphery of the nuclear membrane were also detected (thin arrow). **(E)** Stauro-sporine-injured cells were IR for SBDP 120 and SBDP 150 and different relative magnitudes of protease activation were evident in individual cells (thin arrow, wide arrow, arrowhead). **(F)** IR cells exhibited nuclear morphology consistent with apoptosis (thin arrow, wide arrow, arrowhead). **(G)** Maitotoxin-injured cells exhibited calpain-mediated BDPs (arrow). **(H)** Nuclei of IR cells were rounded, brightly fluoresced, exhibited pyknotic chromatin, and were considered necrotic (arrow). Scale bar = 1 μm.
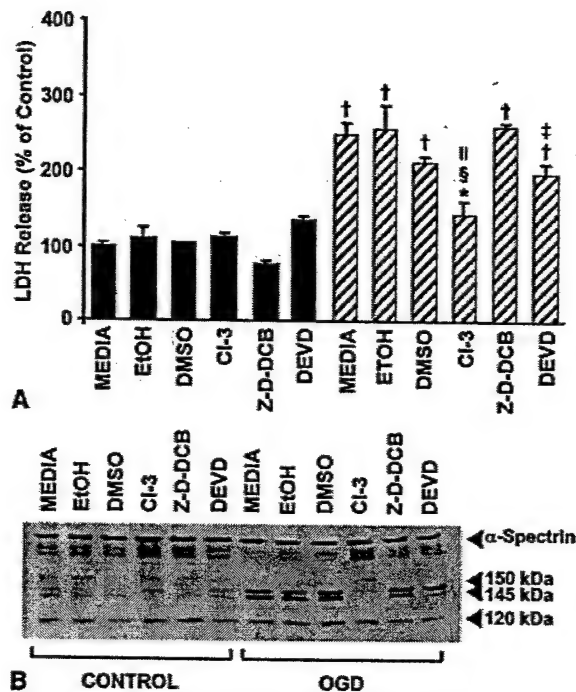
FIG. 6. (A) Effect of protease inhibition on lactate dehydrogenase (LDH) release following oxygen–glucose deprivation (OGD). Cultures were subjected to OGD (10 hours + 12 hours of reperfusion) alone, or combined with varying doses of protease inhibitors. Cell viability was assessed by measuring LDH release and expressed as percent of control. Significant decreases in LDH release were detected with administration of CI-3 (100 μmol/L) compared to vehicle-treated cultures. DEVD-fmk (100 μmol/L) also inhibited LDH release; however, decreases were not statistically significant compared to vehicle-treated cultures. Z-D-DCB (100 μmol/L) had no effect on cell viability. DMSO (2 μL/mL) also decreased LDH release, but its effect was not significantly different from the OGD/media cultures. $*P < 0.05$ and $\dagger P < 0.001$ compared to control; $\ddagger P < 0.05$ and $\S P < 0.001$ compared to OGD/media; $\|P < 0.01$ compared to vehicle-treated OGD. **(B)** Effect of protease inhibition on α-spectrin proteolysis. Western blot analyses of α-spectrin proteolysis assessed inhibition of appropriate proteases. CI-3 (100 μmol/L) decreased proteolysis of native 240 kDa α-spectrin and the formation of the 150/145 kDa doublet. Z-D-DCB (100 μmol/L) had a small effect on the accumulation of the 145 kDa and 120 kDa BDPs. DEVD-fmk (100 μmol/L) substantially reduced the formation of the 145 kDa BDP, but had only a modest effect on the formation of the 120 kDa BDP.

totic and necrotic cell death have been observed in some models of *in vitro* ischemia (Kalda et al., 1998), other models do not observe apoptosis unless glutamate receptor antagonists are used (Gottron et al., 1997; Gwag et al., 1995; Lobner and Choi, 1996). Variations in cell culture methodology, including culture age at time of injury and glial density, may be responsible for these discrepancies. Consistent with the prominent role of apoptosis in development, younger cultures, such as those used in this study, are more susceptible to apoptosis after cyclosporine or staurosporine treatment (McDonald et

al., 1997), whereas older neurons are more vulnerable to *N*-methyl-d-aspartate toxicity (McDonald et al., 1997) and hypoxia (Di Loreto and Balestrino, 1997). In contrast to this article, studies that detected only necrosis after OGD used neuronally enhanced cell cultures (Goldberg and Choi, 1993; Gottron et al., 1997; Lobner and Choi, 1996). Increased sensitivity to glutamate toxicity and OGD has been observed in neuronally enhanced cultures (Zhao et al., 2000; Dugan et al., 1995), suggesting that the absence of glia may intensify a neuron's response to injury. It is conceivable that higher glial concentrations in the current model of OGD blunted the effects of deprivation and resulted in a slower and milder injury. Notably, *in vitro* studies have shown that the same insult can produce apoptosis or necrosis depending on its severity (Bonfoco et al., 1995).

Cell death after OGD was associated with concurrent activation of calpain and caspase-3. Although immunocytochemical experiments revealed robust caspase-3–mediated proteolysis of α-spectrin (120 kDa), Western blots failed to detect consistent increases in this proteolytic fragment. Use of different primary antibodies (monoclonal versus polyclonal) and methods of detection (enhanced chemiluminescence reagents versus fluorescence) may be responsible for these inconsistencies. Western blots using an antibody to the activated caspase-3 17-kDa subunit did provide evidence of caspase-3 activation, confirming immunohistochemical observations of caspase-3 activation and suggesting that Western blot assessments of proenzyme processing may be more sensitive than measures of substrate degradation in some model systems.

Cells phenotypically showing apoptoticlike nuclear profiles exhibited prominent expression of calpain and caspase-3, suggesting that there may be as yet undefined interactions between these two proteases in the expression of the apoptotic phenotype. Calpain and caspase-3 share a variety of substrates that are proteolyzed during apoptosis (Wang, 2000). In addition, these proteases cleave proteins important to each other's regulation—that is, caspase-3–mediated proteolysis of calpastatin, calpain-mediated proteolysis of pro-caspase-3 and pro-caspase-9 (Wang et al., 1998*a*; McGinnis et al., 1999; Wolf et al., 1999). Furthermore, calpains, but not caspases, promote apoptoticlike events during platelet activation (Wolf et al., 1999). Additional evidence for calpain's involvement in apoptotic cell death in CNS injury is provided by recent studies examining *in vivo* TBI and ischemia. Calpain-mediated breakdown products have been detected in the injured cortex after TBI (Beer et al., 2000; Pike et al., 1998*a*), a site associated with prominent apoptotic cell death (Beer et al., 2000; Newcomb et al., 1999), although evidence of caspase-3 activation in this region has yielded conflicting data

(Beer et al., 2000; Pike et al., 1998*a*). These discrepancies may be attributable to differences in injury magnitude, animal age, or species; these issues currently are being addressed in both laboratories. After *in vivo* ischemia, approximately 50% of TUNEL-positive cells failed to show caspase-3 activation (Namura et al., 1998), suggesting that other proteases, such as calpain, are involved in the apoptotic changes observed after injury.

Inhibition of calpain substantially decreased LDH release after OGD with 12 hours of reperfusion, suggesting that calpain activation contributes to cell death in this model. Inhibition of caspase-3 with DEVD-fmk also reduced LDH release, although this drug also showed marked inhibition against calpain activation. Thus, the current study did not allow for comparisons of the relative contribution of these two proteases to cell death in this model. It is unclear why DEVD-fmk showed substantial calpain inhibition and only modest caspase-3 inhibition, but these data suggest that this agent is not a specific inhibitor of caspase-3 activation, at least in this model system. Although not directly addressed in this study, future experiments must more rigorously investigate the relative contribution of calpain and caspase-3 to the expression of apoptotic cell death phenotypes.

Although the current study relied in part on morphologic characteristics of cell death phenotypes, a number of observations suggest that biochemical markers ultimately may be more useful indicators of cell death, especially in acute neurologic insults characterized by heterogeneous or ambiguous cell death phenotypes. In this study, appearance of necrotic cell death depended on method of detection. Using chromatin dyes to distinguish necrotic and apoptotic nuclear morphology is problematic because nuclei may exhibit characteristics either of both types (Colicos and Dash, 1996) or neither type (Zhao et al., 2000) of cell death. In fact, most techniques used to differentiate apoptosis also have been reported to label necrosis, perhaps because late events are similar in both types of cell death (Choi, 1996). Some investigators have argued that necrosis and apoptosis may not be phenotypically distinct events, but rather represent a morphologic continuum (Bonfoco et al., 1995; Portera-Cailliau et al., 1997). This issue is further complicated by evidence showing that the same insult can cause apoptosis and necrosis in different cell populations (Sloviter et al., 1996) or can result in an acute necrotic death with a delayed apoptotic death (Ankarcrona et al., 1995; Pang and Geddes, 1997).

In summary, the current data demonstrate that coactivation of calpain and caspase-3 is a reliable characteristic of apoptotic cell death in the current model system. These observations strongly suggest that calpain activation, in combination with caspase-3 activation, could contribute to the expression of apoptotic cell death by

assisting in the proteolytic degradation of important cellular proteins (Wang, 2000). Finally, interactions between these two cysteine proteases could be important determinants of cell death.

REFERENCES

Ankarcrona M, Dypbukt JM, Bonfoco E, Zhivotovsky B, Orrenius S, Lipton SA, Nicotera P (1995) Glutamate-induced neuronal death: a succession of necrosis or apoptosis depending on mitochondrial function. *Neuron* 15:961–973

Bartus RT, Dean RL, Cavanaugh K, Eveleth D, Carriero DL, Lynch G (1995) Time-related neuronal changes following middle cerebral artery occlusion: implications for therapeutic intervention and the role of calapin. *J Cereb Blood Flow Metab* 15:969–979

Beer R, Franz G, Srinivasan A, Hayes RL, Pike BR, Newcomb JK, Zhao X, Schmutzhard E, Poewe W, Kampfl A (2000) Temporal profile and cell subtype distribution of activated caspase-3 following experimental traumatic brain injury. *J Neurochem* 75:1264–1273

Bonfoco E, Krainc D, Ankarcrona M, Nicotera P, Lipton S (1995) Apoptosis and necrosis: two distinct events induced, respectively, by mild and intense insults with N-methyl-D-aspartate or nitric oxide/superoxide in cortical cell cultures. *Proc Natl Acad Sci U S A* 92:7162–7166

Buki A, Okonkwo DO, Wang KKW, Povlishock JT (2000) Cytochrome c release and caspase activation in traumatic axonal injury. *J Neurosci* 20:2825–2834

Charriaut-Marlangue C, Ben-Ari Y (1995) A cautionary note on the use of TUNEL stain to determine apoptosis. *Neuroreport* 7:61–64

Chen J, Nagayama T, Jin K, Stetler A, Zhu RL, Graham SH, Simon RP (1998) Induction of caspase-3 like protease may mediate delayed neuronal death in the hippocampus after transient cerebral ischemia. *J Neurosci* 18:4914–4928

Choi DW (1996) Ischemia-induced neuronal apoptosis. *Curr Opin Neurobiol* 6:667

Clark RSB, Kochanek PM, Watkins SC, Chen M, Dixon CE, Seidberg NA, Melick J, Loeffert JE, Nathaniel PD, Jin KL, Graham SH (2000) Caspase-3 mediated neuronal death after traumatic brain injury in rats. *J Neurochem* 74:740–753

Colicos MA, Dash PK (1996) Apoptotic morphology of dentate gyrus granule cells following experimental cortical impact injury in rats: possible role in spatial memory deficits. *Brain Res* 739:120–131

Copin JC, Li Y, Reola LF, Chan PH (1998) Trolox and 6, 7-dinitroquinoxaline-2–3dione prevent necrosis but not apoptosis in cultured neurons subjected to oxygen deprivation. *Brain Res* 784:25–36

Di Loreto S, Balestrino M (1997) Development of vulnerability to hypoxic damage in *in vitro* hippocampal neurons. *Int J Dev Neurosci* 15:225–230

Dugan LL, Bruno VMG, Amagasu SM, Giffard RG (1995) Glia modulate the response of murine cortical neurons to excitotoxicity: glia exacerbate AMPA toxicity. *J Neurosci* 15:4545–4555

Fink K, Namura S, Shimizu-Sasamata M, Endres M, Ma J, Dalkara T, Yuan J, Moskowitz MA (1998) Prolonged therapeutic window for ischemic brain damage caused by delayed caspase activation. *J Cereb Blood Flow Metab* 18:1071–1076

Goldberg MP, Choi DW (1993) Combined oxygen and glucose deprivation in cortical cell culture: calcium-dependent and calcium-independent mechanisms of neuronal injury. *J Neurosci* 13:3510–3524

Gong J, Traganos F, Darzynkiewicz Z (1994) A selective procedure for DNA extraction from apoptotic cells applicable for gel electrophoresis and flow cytometry. *Anal Biochem* 218:314–319

Gottron FJ, Ying HS, Choi DW (1997) Caspase inhibition selectively reduces the apoptotic component of oxygen-glucose deprivation-induced cortical neuronal death. *Mol Cell Neurosci* 9:159–169

Gwag BJ, Lobner D, Koh JY, Wie MB, Choi DW (1995) Blockade of glutamate receptors unmasks neuronal apoptosis after oxygen-glucose deprivation *in vitro*. *Neuroscience* 68:615–619

Harris AS, Croall DE, Morrow JS (1988) The calmodulin-binding site in alpha-fodrin is near the calcium-dependent protease-1 cleavage site. *J Biol Chem* 263:15754–15761

Himi T, Ishizaki Y, Murota S (1998) A caspase inhibitor blocks ischemia-induced delayed neuronal death in the gerbil. *Eur J Neurosci* 10:777–781

Hong SC, Goto Y, Lanzino G, Soleau S, Kassell NF, Lee KS (1994) Neuroprotection with a calpain inhibitor in a model of focal cerebral ischemia. *Stroke* 25:663–669

Kalda A, Eriste E, Vassiljev V, Zharkovsky A (1998) Medium transitory oxygen-glucose deprivation induced both apoptosis and necrosis in cerebellar granule cells. *Neurosci Lett* 240:21–24

Koh JY, Choi DW (1987) Quantitative determination of glutamate mediated cortical neuronal injury in cell culture by lactate dehydronase efflux assay. *J Neurosci Meth* 20:83–90

Linnik MD, Zobrist RH, Hatfield MD (1993) Evidence supporting a role for programmed cell death in focal cerebral ischemia in rats. *Stroke* 24:2002–2009

Lobner D, Choi DW (1996) Preincubation with protein synthesis inhibitors protects cortical neurons against oxygen-glucose deprivation-induced death. *Neuroscience* 72:335–341

Markgraf CG, Velayo NL, Johnson MP, McCarty DR, Medhi S, Koehl JR, Chmielewski PA, Linnik MD (1998) Six-hour window of opportunity for calpain inhibition in focal cerebral ischemia in rats. *Stroke* 29:152–158

McDonald JW, Behrens MI, Chung C, Bhattacharyya T, Choi DW (1997) Susceptibility to apoptosis is enhanced in immature cortical neurons. *Brain Res* 759:228–232

McGinnis KM, Gnegy ME, Park YH, Mukerjee N, Wang KKW (1999) Procaspase-3 and poly(ADP)ribose polymerase (PARP) are calpain substrates. *Biochem Biophys Res Comm* 263:94–99

Namura S, Zhu J, Fink K, Endres M, Srinivasan A, Tomaselli KJ, Yuan J, Moskowitz MA (1998) Activation and cleavage of caspase-3 in apoptosis induced by experimental cerebral ischemia. *J Neurosci* 18:3659–3668

Nath R, Raser KJ, Stafford D, Hajimohammadreza I, Posner A, Allen H, Talanian RV, Yuen P, Gilbertsen RB, Wang KKW (1996) Non-erythroid alpha-spectrin breakdown by calpain and interleukin 1 beta-converting-enzyme-like protease(s) in apoptotic cells: contributory roles of both protease families in neuronal apoptosis. *Biochem J* 319:683–690

Nath R, Probert A, McGinnis KM, Wang KKW (1998) Evidence for activation of caspase-3-like protease in excitotoxin- and hypoxia/hypoglycemia-injured neurons. *J Neurochem* 71:186–195

Newcomb JK, Kampfl A, Posmantur RM, Zhao X, Pike BR, Liu SJ, Clifton GL, Hayes RL (1997) Immunohistochemical study of calpain-mediated breakdown products to α-spectrin following controlled cortical impact injury in the rat. *J Neurotrauma* 14:369–383

Newcomb JK, Zhao X, Pike BR, Hayes RL (1999) Temporal profile of apoptotic-like changes in neurons and astrocytes following controlled cortical impact injury in the rat. *Exp Neurol* 158:76–88

Oberhammer F, Fritsch G, Schmied M, Pavelka M, Printz D, Purchio R, Lassman H, Schulte-Hermann R (1993) Condensation of chromatin at the membrane of an apoptotic nuclease is not associated with activation of an endonuclease. *J Cell Sci* 104:317–326

Pang Z, Geddes JW (1997) Mechanisms of cell death induced by the mitochondrial toxin 3-nitropropionic acid: acute excitotoxic necrosis and delayed apoptosis. *J Neurosci* 17:3064–3073

Pike BR, Zhao X, Newcomb JK, Posmantur RM, Wang KKW, Hayes RL (1998a) Regional calpain and caspase-3 proteolysis of α-spectrin after traumatic brain injury. *Neuroreport* 9:2437–2442

Pike BR, Zhao X, Newcomb JK, Wang KKW, Posmantur RM, Hayes RL (1998b) Temporal relationship between *de novo* protein synthesis, calpain and caspase-3 like protease activation, and DNA fragmentation during apoptosis in septo-hippocampal cultures. *J Neurosci Res* 52:505–520

Pike BR, Zhao X, Newcomb JK, Glenn CC, Anderson DK, Hayes RL (2000) Stretch injury causes calpain and caspase-3 activation and necrotic and apoptotic cell death in septo-hippocampal cell cultures. *J Neurotrauma* 17:283–298

Portera-Cailliau C, Price DL, Martin LJ (1997) Excitotoxic neuronal death in the immature brain is an apoptosis-necrosis morphological continuum. *J Comp Neurol* 378:70–87

Posmantur RM, Kampfl A, Simon R, Liu SJ, Zhao X, Clifton GL, Hayes RL (1997) A calpain inhibitor attenuates cortical cytoskeletal protein loss after experimental brain injury in the rat. *Neuroscience* 77:875–888

Purnanam KL, Boustany R-M (1999) Assessment of cell viability and histochemical methods in apoptosis. In: *Apoptosis in neurobiology* (Hannun YA, Boustany R-M, eds), Boca Raton, FL: CRC Press, pp 129–152

Rami A, Agarwal R, Botez G, Winckler J (2000) α-Calpain activation, DNA fragmentation, and synergistic effects of caspase and calpain inhibitors in protecting hippocampal neurons from ischemic damage. *Brain Res* 866:299–312

Rink A, Fung KM, Trojanowski JQ, Lee VMY, Neugebauer E, McIntosh TK (1995) Evidence of apoptotic cell death after experimental traumatic brain injury in the rat. *Am J Path* 147:1575–1583

Roberts-Lewis JM, Savage MJ, Marcy V, Pinsker LR, Simon R (1994) Immunolocalization of μ-calpain mediated spectrin degradation to vulnerable neurons in ischemic gerbil brain. *J Neurosci* 14:3934–3944

Saatman KE, Bozyczko-Coyne D, Marcy V, Simon R, McIntosh TK (1996) Prolonged calpain-mediated spectrin breakdown occurs regionally following experimental brain injury in the rat. *J Neuropathol Exp Neurol* 55:850–860

Saatman KE, Zhang C, Bartus RT, McIntosh TK (2000) Behavioral efficacy of posttraumatic calpain inhibition is not accompanied by reduced spectrin proteolysis, cortical lesion, or apoptosis. *J Cereb Blood Flow Metab* 20:66–73

Saido TC, Yokota M, Nagao S, Yamaura I, Tani E, Tsuchiya T, Suzuki K, Kawashima S (1993) Spatial resolution of fodrin proteolysis in postischemic brain. *J Biol Chem* 268:25239–25243

Schmechel DE (1999) Assessment of ultrastructural changes associated with apoptosis. In: *Apoptosis in neurobiology* (Hannun YA, Boustany R-M, eds), Boca Raton, FL: CRC Press, pp 153–181

Sloviter RS, Dean E, Sollas AL, Goodman JH (1996) Apoptosis and necrosis induced in different hippocampal neuron populations by repetitive perforant path stimulation in the rat. *J Comp Neurol* 366:516–533

Squier MK, Miller AC, Malkinson AM, Cohen JJ (1994) Calpain activation in apoptosis. *J Cell Physiol* 159:229–237

Vanags DM, Porn-Ares MI, Coppola S, Burgess DH, Orrenius S (1996) Protease involvement in fodrin cleavage and phosphatidylserine exposure in apoptosis. *J Biol Chem* 271:31075–31081

Wang KKW, Nath R, Raser KJ, Hajimohammadreza I (1996) Maitotoxin induces calpain activation in SH-SY5Y neuroblastoma cells and cerebrocortical cultures. *Arch Biochem Biophys* 331:208–214

Wang KKW, Posmantur RM, Nadimpalli R, Nath R, Nixon R, Talanian RV, Allen H (1998a) Caspase-mediated fragmentation of calpain inhibitor protein calpastatin during apoptosis. *Arch Biochem Biophys* 356:187–196

Wang KKW, Posmantur RM, Nath R, McGinnis KM, Whitton M, Talanian RV, Glartz SB, Morrow JS (1998b) Simultaneous degradation of αII- and βII-spectrin by caspase 3 (CPP32) apoptotic cells. *J Biol Chem* 273:22490–22497

Wang KKW (2000) Calpain and caspase: can you tell the difference? *Trends Neurosci* 23:20–26

Wolf BB, Goldstein JC, Stennicke HR, Beere H, Amarante-Mendes GP, Salvesen GS, Green DR (1999) Calpain functions in a caspase-independent manner to promote apoptotic-like events during platelet activation. *Blood* 94:1683–1692

Yakovlev AG, Knoblach SM, Fan L, Fox GB, Goodnight R, Faden AI (1997) Activation of CPP32-like caspases contributes to neuronal apoptosis and neurological dysfunction after traumatic brain injury. *J Neurosci* 17:7415–7424

Yokota M, Saido TC, Tani E, Kawashima S, Suzuki K (1995) Three distinct phases of fodrin proteolysis induced in postischemic hippocampus. Involvement of calpain and unidentified protease. *Stroke* 26:1901–1907

Zhao X, Pike BR, Newcomb JK, Wang KKW, Postmantur RM, Hayes RL (1999) Maitotoxin induces calpain but not caspase-3 activation

and necrotic cell death in primary septo-hippocampal cultures. *Neurochem Res* 24:371–382

Zhao X, Newcomb JK, Pike BR, Posmantur RM, Wang KKW, Hayes RL (2000) Novel characteristics of glutamate-induced cell death in primary septo-hippocampal cultures: relationship to calpain and caspase-3 protease activation. *J Cereb Blood Flow Metab* 20:550–562

Temporal and spatial profile of caspase 8 expression and proteolysis after experimental traumatic brain injury

Ronny Beer,* Gerhard Franz,* Stanislaw Krajewski,† Brian R. Pike,‡ Ronald L. Hayes,‡ John C. Reed,† Kevin K. Wang,§ Christian Klimmer,* Erich Schmutzhard,* Werner Poewe* and Andreas Kampfl*

*Department of Neurology, University Hospital Innsbruck, Austria

†The Burnham Institute, La Jolla, California, USA

‡Center for Traumatic Brain Injury Studies, Department of Neuroscience, Evelyn F. and William L. McKnight Brain Institute of the University of Florida, Gainesville, Florida, USA

§Department of Neuroscience Therapeutics, Pfizer Inc., Ann Arbor, Michigan, USA

Abstract

Recent studies have demonstrated that the downstream caspases, such as caspase 3, act as executors of the apoptotic cascade after traumatic brain injury (TBI) *in vivo*. However, little is known about the involvement of caspases in the initiation phase of apoptosis, and the interaction between these initiator caspases (e.g. caspase 8) and executor caspases after experimental brain injuries *in vitro* and *in vivo*. This study investigated the temporal expression and cell subtype distribution of procaspase 8 and cleaved caspase 8 p20 from 1 h to 14 days after cortical impact-induced TBI in rats. Caspase 8 messenger RNA levels, estimated by semiquantitaive RT-PCR, were elevated from 1 h to 72 h in the traumatized cortex. Western blotting revealed increased immunoreactivity for procaspase 8 and the proteolytically active subunit of caspase 8, p20, in the ipsilateral cortex from 6 to 72 h after injury, with a peak at 24 h after TBI. Similar to our previous studies, immunoreactivity for the p18 fragment of activated caspase 3 also increased in the current study from 6 to 72 h after TBI, but peaked at a later timepoint (48 h) as compared with proteolyzed caspase 8 p20. Immuno-

histologic examinations revealed increased expression of caspase 8 in neurons, astrocytes and oligodendrocytes. Assessment of DNA damage using TUNEL identified caspase 8- and caspase 3-immunopositive cells with apoptotic-like morphology in the cortex ipsilateral to the injury site, and immunohistochemical investigations of caspase 8 and activated caspase 3 revealed expression of both proteases in cortical layers 2–5 after TBI. Quantitative analysis revealed that the number of caspase 8 positive cells exceeds the number of caspase 3 expressing cells up to 24 h after impact injury. In contrast, no evidence of caspase 8 and caspase 3 activation was seen in the ipsilateral hippocampus, contralateral cortex and hippocampus up to 14 days after the impact. Our results provide the first evidence of caspase 8 activation after experimental TBI and suggest that this may occur in neurons, astrocytes and oligodendrocytes. Our findings also suggest a contributory role of caspase 8 activation to caspase 3 mediated apoptotic cell death after experimental TBI *in vivo*.

Keywords: apoptosis, astrocyte, caspase 8, neuron, oligodendrocyte, traumatic brain injury.

J. Neurochem. (2001) **78**, 862–873.

Traumatically evoked brain injury is a major cause of morbidity and mortality (Thurman *et al.* 1999). Studies over the last two decades have demonstrated that a significant amount of CNS damage after traumatic brain injury (TBI) occurs as a result of secondary autodestructive insults (Hayes *et al.* 1992; Faden 1996; McIntosh *et al.* 1998). Secondary injury involves a complex cascade of biochemical events that contributes to delayed tissue damage and cell death (Kermer *et al.* 1999; Graham *et al.* 2000). Importantly, recent research reported on a potential role for apoptosis in

cell degeneration after cerebral and spinal cord ischemia (Nitatori et al. 1995; Kato et al. 1997; Charriaut-Marlangue et al. 1998), traumatic spinal cord injury (Crowe et al. 1997; Liu et al. 1997), and TBI in vitro (Shah et al. 1997; Pike et al. 2000) and in vivo (Rink et al. 1995; Conti et al. 1998; Newcomb et al. 1999; Beer et al. 2000b).

Although a potential role for apoptosis in neuronal and glial cell damage after TBI has been suggested, little is known about the molecular mechanisms involved. However, recent evidence implicates a distinct class of proteases, referred to as caspases. So far, 14 mammalian caspases have been described (Nicholson 1999). Based on their proteolytic specifities, caspases further divide into three groups: the inflammatory caspases (e.g. caspase 1), which mediate cytokine maturation (Cerretti et al. 1992); the caspases involved in apoptotic cell death, which segregate into initiator enzymes, such as caspase 8 and caspase 9; executioner caspases, such as caspase 3 (Cohen 1997; Cryns and Yuan 1998). Caspases are synthesized as inactive pro-enzymes that contain three domains (Nicholson 1999), an N-terminal prodomain (approximately 3–24 kDa), a large subunit (approximately 17–21 kDa) and a small subunit (approximately 10–13 kDa). Depending on the cell type, procaspases have been shown to reside in various subcellular localizations (Qin et al. 2001; Shikama 2001) and are activated through proteolytic processing and association of the large and small subunits to form a catalytic heterotetramer (Walker et al. 1994).

Activation of the executioner caspase 3 has been shown in numerous chronic and acute disorders of the nervous system. For example, caspase 3 processing has been demonstrated in Alzheimer's (Stadelmann et al. 1999; Khan et al. 2000) and Parkinson's disease (Mogi et al. 2000). Further, caspase 3 mediated neuronal and glial cell degeneration has been found in experimental models of cerebral and spinal cord ischemia (Hayashi et al. 1998; Namura et al. 1998) and spinal cord injury (Springer et al. 1999). Importantly, recent data have also suggested a contributory role for activated caspase 3 in apoptotic degeneration of neurons, astrocytes and oligodendrocytes after TBI in vivo (Yakovlev et al. 1997; Beer et al. 2000b; Clark et al. 2000).

Current evidence also indicates that in receptor-triggered apoptosis the main pathway for caspase 3 activation is direct activation by caspase 8 (Scaffidi et al. 1998; Stennicke et al. 1998). Importantly, recent data suggest that receptor-mediated apoptosis indeed occurs in acute CNS injuries (Ertel et al. 1997; Felderhoff-Mueser et al. 2000). For example, increased expression of Fas and caspase 8 has been shown after experimental spinal cord ischemia (Matsushita et al. 2000). In addition, increased Fas and Fas ligand immunoreactivity (Beer et al. 2000a) and caspase 3 activation have been reported following TBI in the rat (Beer et al. 2000b; Clark et al. 2000), suggesting a putative link between the activation of caspase 8 and

caspase 3 after TBI in vivo. However, to our knowledge no study to date has concurrently investigated changes in the expression and activity of both caspase 8 and caspase 3 in trauma-induced CNS degeneration.

To further investigate potential changes of caspase 8 and caspase 3 expression after experimental TBI, rodents were subjected to a widely used model of experimental brain injury: lateral cortical impact injury (Dixon et al. 1991; Franz et al. 1999; Beer et al. 2000a,b). The present study employed semiquantitative RT-PCR and western blot analyses of procaspase 8, cleaved caspase 8 p20, and processed caspase 3 to determine the relative temporal profile of caspase 8 to caspase 3 expression and activation from 1 h to 14 days after experimental TBI. Immunohistochemical examinations were performed to investigate the cell subtype distribution of caspase 8 after impact injury in vivo. Further, TUNEL was used to assess whether caspase 8 and caspase 3 immunopositive cells exhibit morphological features of DNA damage consistent with apoptotic phenotype after TBI in the rat.

Materials and methods

Rat model of traumatic brain injury

A controlled cortical impact device was used to induce a moderate level of TBI, as previously described (Dixon et al. 1991; Franz et al. 1999). In brief, adult male Sprague–Dawley rats (250–350 g) were intubated and anesthetized with 2% halothane in a 2 : 1 mixture of N_2O/O_2. Core body temperature was monitored continuously using a rectal thermistor probe and maintained at 36.5–37.5°C by a heating pad. Animals were mounted in a stereotaxic frame on the injury device in a prone position secured by ear and incisor bars. A midline incision was made, the soft tissues were reflected, and two 7-mm craniotomies were made adjacent to the central suture, midway between lambda and bregma. The dura was kept intact over the cortex. Injury was induced by impacting the right (ipsilateral) cortex with a 6-mm diameter aluminum tip at a rate of 4 m/s. The injury device was set to produce a tissue deformation of 2 mm. Impact velocity was measured directly by a linear variable differential transformer (Shaevitz Model 500 HR; Shaevitz, Detroit, MI, USA), which produces an analog signal that was recorded by a PC-based data acquisition system for analysis of time/displacement parameters of the impactor. This magnitude of injury has previously been associated with significant cell degeneration restricted to the contusion site (Franz et al. 1999; Beer et al. 2000a,b). After trauma, animals were extubated and immediately assessed for recovery of reflexes (Dixon et al. 1991). Sham-injured animals underwent identical surgical procedures but did not receive impact injury. Naive animals were not exposed to any injury-related surgical procedures. Ninety animals were used in this study (naive rats, $n = 10$; sham-injured rats, $n = 12$; injured rats, $n = 68$). Animal care and experimental protocols complied with the guidelines outlined in the Guide for the Care and Use of Laboratory Animals, Austrian Department of Health and Science, and were approved by the University of Innsbruck Medical School Animal

Table 1 Systemic parameters

	Prior to craniotomy ($n = 20$)	Post surgery	
		sham ($n = 4$)	injured ($n = 16$)
MABP (mmHg)	101 ± 5	97 ± 8	103 ± 6
pH	7.46 ± 0.01	7.43 ± 0.02	7.44 ± 0.02
PaO_2 (mmHg)	142 ± 4	79 ± 12	85 ± 9
$PaCO_2$ (mmHg)	43 ± 6	41 ± 3	42 ± 5
Rectal temperature (°C)	37.1 ± 0.2	37.3 ± 0.2	36.9 ± 0.1

Values are mean $\pm$ SD; MABP, mean arterial blood pressure.

Welfare Committee. Importantly, all efforts were made to minimize animal suffering and to reduce the number of animals used.

Assessment of physiologic parameters

In a subgroup of animals (sham-injured rats, $n = 4$; injured rats, $n = 16$) systemic parameters were monitored as described by Dixon *et al.* (1991). Briefly, a 22-gauge Teflon catheter was advanced into the abdominal aorta through a left femoral arteriotomy for arterial blood pressure measurement and arterial blood sampling. Blood samples (100 μL) were analyzed for pH, arterial oxygen pressure (PaO_2), and arterial pressure of carbon dioxide ($PaCO_2$), (Table 1) using an AVL Omni 4 (Diamond Diagnostics, Holliston, MA, USA) blood gas analyzer before craniotomy and 5 min after surgery. All parameters were within the normal physiological range (Table 1) (Krinke 2000).

Sample preparation

All animals were given a lethal dose of phenobarbital intraperitoneally (20 mg/kg; Tyrol Pharma, Kundl, Austria) and subsequently killed by decapitation 6 h, 24 h, 48 h, 72 h, 7 days and 14 days after TBI ($n = 4$ for each time after injury, $n = 4$ for naive and sham-injured animals). Both cortices and hippocampi (ipsilateral and contralateral to the injury site) were removed. Excision of both cortices beneath the craniotomies extended ~4-mm laterally, ~7-mm rostrocaudally, and to a depth extending to the white matter. All samples were immediately frozen in liquid nitrogen. The microdissected tissue was homogenized at 4°C in ice-cold homogenization buffer containing 20 mM piperazine-N,N'-bis(2-ethanesulfonic acid) (pH 7.1), 2 mM EGTA, 1 mM EDTA, 1 mM dithiothreitol, 0.3 mM phenylmethylsulfonylfluoride (PMSF), and 0.1 mM leupeptin. Chelators and protease inhibitors (Sigma, St Louis, MO, USA) were added to prevent endogenous *in vitro* activation of proteases and subsequent artifactual degradation of caspase 8 and caspase 3 during tissue processing.

Sodium dodecyl sulfate–polyacrylamide gel electrophoresis, immunoblotting and quantification

Protein concentrations were determined by bicinchoninic acid microprotein assay (Sigma) with albumin standards. Protein-balanced samples were prepared for polyacrylamide gel electrophoresis in two-fold loading buffer containing 0.25 M Tris (pH 6.8), 0.2 M dithiothreitol, 2% sodium dodecyl sulfate, 0.005% bromophenol blue and 5% glycerol in distilled water. Samples were heated for 5 min at 95°C. Sixty micrograms of protein per lane was

routinely resolved on 16% Tris/glycine gels (Invitrogen, Groningen, the Netherlands). After separation, proteins were transferred to nitrocellulose membranes using western blotting with transfer buffer made up of 0.192 M glycine and 0.025 M Tris (pH 8.3). Coomassie blue (Bio-Rad, Hercules, CA, USA) and Ponceau red (Sigma) stainings were performed to confirm that equal amounts of protein were loaded in each lane. Five percent non-fat milk in phosphate buffered saline (PBS) with 0.05% Tween 20 was used to reduce non-specific binding. Immunoblots were probed with either a mouse monoclonal antibody (Santa Cruz Biotechnology, Santa Cruz, CA, USA), reacting with the p20 subunit and precursor of caspase 8, diluted 1 : 1000, or a rabbit polyclonal antiserum (CM1; IDUN Pharmaceuticals, La Jolla, CA, USA; dilution 1 : 5000), directed against the p18 subunit of activated caspase 3. Specifity and sensitivity of CM1 has been described in detail in previous investigations (Namura *et al.* 1998; Srinivasan *et al.* 1998; Beer *et al.* 2000b). After incubation with primary antibodies overnight at 4°C, nitrocellulose membranes (Amersham Pharmacia Biotech, Uppsala, Sweden) were incubated with secondary antibodies linked to horseradish peroxidase (Amersham Pharmacia Biotech) for 1 h at 20°C (automated climate control). Enhanced chemiluminescence reagents (Amersham Pharmacia Biotech) were used to visualize the immunolabeling on X-ray film. In each blot, the constitutively expressed protein α-tubulin (Sigma) was used as an internal standard to further indicate that sample processing was carried out correctly.

Semiquantitative RT-PCR

Total RNA was isolated from frozen ipsilateral and contralateral cortex and hippocampus of naive ($n = 2$), sham-injured ($n = 4$), and injured animals (1 h, 6 h, 24 h, 48 h and 72 h; $n = 4$ for each time point after injury) with Trizol reagent (Life Technologies, Rockville, MD, USA). Ten micrograms of total RNA was treated with 1 U of amplification grade DNase I (Life Technologies) to eliminate residual genomic DNA and was reverse transcribed into first-strand cDNA using Superscript II reverse transcriptase (Life Technologies) with oligo(dT) as primer. The resulting cDNAs were diluted to 100 μL and subjected to PCR analysis. Each PCR mixture contained equal amounts of diluted cDNA corresponding to 200 ng of total RNA, 100 pM of each primer, 10 pM dNTPs, onefold Ampli-Taq reaction buffer and 2.5 U Ampli-Taq-Gold DNA polymerase (PE Biosystems, Foster City, CA, USA). All cDNAs were amplified with primers specific for the housekeeping

gene glyceraldehyde-3-phosphate dehydrogenase (GAPDH; Gen-Bank Acc. No. X02231; 5′-CCCACGGCAAGTTCAACGG-3′ and 5′-CTTTCCAGAGGGGCCATCCA), and caspase 8 (GenBank Acc. No. AF279308; 5′-ACTGGCTGCCCTCAAGTTCCTGTGC-3′ and 5′-TCCCTCACCATTTCCTCTGGGCTGC-3′). PCR amplification was carried out for 34 cycles of 45 s at 94°C, 45 s at 60°C, and 45 s at 72°C, followed by a final step of 10 min at 72°C in the UNO II Thermocycler (Biometra, Göttingen, Germany). The number of cycles and reaction temperature conditions were optimized to provide a linear relationship between the quantity of input template and the quantity of PCR product. PCR products were analyzed by agarose gel electrophoresis in 2% NuSieve agarose gels (FMC BioProducts, Rockland, ME, USA) and visualized by ethidium-bromide staining. The identity of the PCR products obtained was confirmed by Southern blot analysis using an internal oligonucleotide as hybridization probe.

Immunohistochemistry

Prior to perfusion, animals from all treatment groups were given a lethal injection of phenobarbital (20 mg/kg intraperitoneally). Rats were transcardially perfused through the left ventricle (120 mL of 0.9% saline and 200 mL of 4% paraformaldehyde) at 6 h, 24 h, 48 h, 72 h, 7 days and 14 days after TBI ($n = 4$ for each time point after injury; $n = 4$ for sham-injured and naive animals). The brains were removed, grossly sectioned coronally at 2-mm intervals, processed through graded alcohols and xylene substitute (Histo-clear; National Diagnostics, Atlanta, GA, USA), and routinely embedded in paraffin. Sections were cut at 3–4 μm on a rotary microtome, mounted on aminoalkylsilated glass slides, and processed for immunohistochemistry as follows: deparaffinized and rehydrated sections were microwaved in 10 mM sodium citrate buffer, pH 6.0, and allowed to cool to room temperature. Endogenous peroxidase was blocked by treatment with 0.3% H_2O_2 in methanol followed by incubation with 10% fetal calf serum (FCS) in Tris-buffered saline (TBS) for 60 min. Rabbit polyclonal antibodies against caspase 8 (The Burnham Institute, La Jolla, CA, USA) and caspase 3 p18 (IDUN Pharmaceuticals) were diluted 1 : 5000 in 10% FCS and permitted to bind overnight at 4°C.

Rabbit antiserum against caspase 8 was generated as previously described (Krajewska et al. 1997) using recombinant catalytic C-terminal fragment of human caspase 8 protein using construct pET15b MGS H_6-Ser216-TAA. This protein was expressed in BL 21 (DE3) cells by induction with 1 mM IPTG. After cell growth and lysis, the clarified cell lysate was applied to an Ni-NTA column and eluted with an imidazole gradient. The pooled caspase 8 fractions were dialyzed against 50 mM Tris at pH 8.8 and applied to a FPLC Mono Q HR 10/10 column (Amersham Pharmacia Biotech) and eluted with an NaCl gradient. New Zealand white female rabbits were injected subcutaneously with a mixture of recombinant protein (0.1–0.15 mg protein per immunization) and 0.5 mL Freund's complete adjuvant with the dose divided over 10 injection sites, and then boosted three times at weekly intervals followed by another 3–20 boostings at monthly intervals with 0.15 mg each of recombinant protein immunogen in Freund's incomplete adjuvant. Antiserum specificity was confirmed by pre-absorption with full-length or fully cleaved caspase 8 protein, respectively. This polyclonal antibody reacts with the unprocessed zymogen form of caspase 8 and detects the processed large subunit

(p20) of active caspase 8. In addition, specificity of the caspase 8 antiserum has been described recently (Stoka et al. 2001).

Biotinylated goat anti-rabbit (Vector Laboratories, Burlingame, CA, USA) was then applied at a dilution of 1 : 200 in 3% rat serum in TBS for 1 h at room temperature followed by avidin-peroxidase (Sigma), diluted 1 : 100 in TBS, also for 1 h at room temperature. The reaction was visualized by treatment with 0.05% 3,3′-diamino-benzidine tetrahydrochloride solution in TBS containing 0.05% H_2O_2. The color reaction was stopped with several washes of TBS. Immunostaining results were confirmed by the use of pre-immune serum from the same animals and by pre-absorption of the poly-clonal antibodies with the relevant protein.

For double immunostaining using brightfield chromagens, sections were pretreated with the rabbit polyclonal antiserum against caspase 8 as described above. Sections were then incubated with a mouse anti-neuron-specific nuclear protein (NeuN) antibody (Wolf et al. 1996) (Chemicon, Temecula, CA, USA) for neuronal staining. For staining of astrocytes, oligodendrocytes and micro-glia, a mouse anti-GFAP (Debus et al. 1983) (Roche Molecular Biochemicals, Mannheim, Germany), a mouse anti-CNPase (Sprinkle 1989) (Sternberger Monoclonals Inc., Lutherville, MD, USA) and an anti-ED1 monoclonal antibody (Graeber et al. 1990) (Serotec, Kidlington, Oxford, UK) were used. All antibodies were diluted 1 : 500 in 10% FCS in TBS and allowed to bind overnight at 4°C. After being rinsed, sections were incubated with a biotinylated horse anti-mouse antibody (Vector Laboratories) at a dilution of 1 : 200 for 1 h at room temperature followed by incubation with an alkaline phosphatase avidin-biotin substrate and then reaction with blue chromagen (Vector Blue; Vector Labora-tories). Sections were dehydrated through graded ethanol, cleared in a xylene substitute (Histoclear; National Diagnostics, Atlanta, GA, USA), mounted in Permount (Fisher Scientific, Nepean, Ontario, Canada) and coverslipped. Sections without primary antibodies were similarly processed to control for binding of the secondary antibodies. On control sections no specific immuno-reactivity was detected.

Histochemical detection of DNA fragmentation (terminal deoxynucleotidyl transferase-mediated deoxyuridine-biotin nick end labeling)

To confirm the presence of cell degeneration by an apoptotic mechanism, terminal deoxynucleotidyl transferase-mediated deoxy-uridine-biotin nick end labeling (TUNEL) was performed as described by Gavrieli et al. (1992) with minor modifications. Briefly, for double-label experiments, dewaxed and rehydrated sections of all animal groups from regions between − 1.5 and − 3.4 mm bregma were stained with primary and secondary anti-sera as described earlier. Immunohistochemical staining was visualized by exposure to 3-amino-9-ethylcarbazole in N,N'-dimethylformamide (Sigma). Sections were then rinsed thoroughly and incubated with labeling mix (TdT buffer containing 100 U/mL TdT and 20 nM/mL biotin-conjugated 16 deoxyuridine) in a humidified chamber for 60 min at 37°C. After three washes in TBS, slides were incubated in Converter alkaline phosphatase for 15 min in a humidified chamber at 37°C. All reagents were purchased from Roche Molecular Biochemicals. The reaction was visualized by treatment for 3 min with 5-bromo-4-chloro-3-indolyl phosphate/nitro blue tetrazolium substrate system (Dako Corpora-tion, Carpinteria, CA, USA). Primary antibody, labeling mix or

secondary antibody were omitted in control sections. Sections were mounted using an aqueous mounting fluid (Dako Corporation) and examined under the light microscope.

Statistical analysis

Semiquantitative evaluation of RT-PCR band density and of immunoreactivity detected by western blotting was performed using computer-assisted two-dimensional densitometric scanning with a MacIntosh computer using the public domain NIH IMAGE program (developed at the US National Institutes of Health and available on the internet at http://rsb.info.nih.gov/nih-image/). Relative band densities on RT-PCR and western blots ($n = 1/$ blot) were expressed as arbitrary densitometric units for each time point. This procedure was performed for the data of four independent experiments for a total of four different animals per time point. Data acquired in arbitrary densitometric units were transformed to percentages of the densitometric levels observed for scans from sham animals on the same agarose gel (for RT-PCR analysis) and same blot. Group differences were determined by ANOVA and Tukey's *post hoc* honestly significant difference (HSD) test. Values given are means ± SD of four independent experiments. Differences were considered significant when $p \leq 0.05$. For quantitative analysis of immunohistochemistry, the numbers of caspase 8 and caspase 3 positive cells of three non-consecutive sections (each separated by at least 50 μm) of four different animals for each time point were counted by an independent observer in the entire anatomic regions of the cortex from the primary injury zone at bregma -3.4 mm ± 0.2 mm (Paxinos and Watson 1997) using light microscopy at a magnification of 100×. The total number of caspase 8- and caspase 3-immunopositive cells was obtained for each section. Further, the numbers of cells labeled with anti-caspase 8 antibody and NeuN, GFAP and CNPase were counted on sections (three sections per animal) processed for double-label immunohistochemistry. Values for each animal (four animals per time point) were averaged to calculate the mean number of immunopositive cells per time point (6–72 h after TBI). Cell counts (caspase 8 vs. caspase 3 and double-labeled neurons vs. double-labeled glia) were analyzed with ANOVA and Bonferroni's *post hoc* analysis for selected pairs of columns. Values given are means ± SD of four different animals. Differences were considered significant when $p \leq 0.05$.

Results

Caspase 8 messenger RNA levels increase after TBI

Caspase 8 messenger RNA was detected by semiquantitative RT-PCR analysis in cortical and hippocampal samples (not shown) of sham and injured animals, respectively (Fig. 1). Cortical impact injury resulted in an increase of caspase 8 messenger RNA levels in the ipsilateral cortex (Fig. 1). Starting at 1 h after injury, a significant increase in caspase 8 messenger RNA levels was observed. Rising rapidly, band intensity reached a maximum level by 6 h after the trauma (386% increase relative to sham animals) and remained thereafter at a steady-state level (332% increase relative to sham animals) at 24 h after TBI. Caspase 8 messenger RNA levels then declined thereafter to a level of approximately
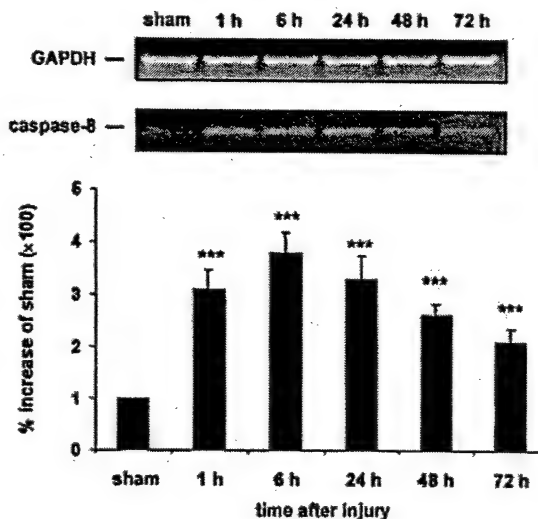

Fig. 1 RT-PCR analysis of caspase 8 mRNA in the ipsilateral cortex following TBI. Cortical samples of single control animals (sham) and single injured animals were prepared for RT-PCR at the indicated times after TBI *in vivo*. Values are presented as percentages of the densitometric levels observed on scans from sham animals visualized on the same agarose gel. Data are mean ± SD values of four independent experiments. Levels of caspase 8 mRNA increased within 1 h after TBI as compared with controls. Levels of caspase 8 mRNA peaked at 6 h after TBI and remained elevated as late as 72 h after the injury. ***$p < 0.001$.

two-fold (220% increase relative to sham animals) above controls at 72 h after the impact. No statistically significant increases in caspase 8 messenger RNA levels were observed in cortical samples contralateral to the injury site and hippocampal samples ipsi- and contralateral to the injury site from 1 h to 72 h after the impact (data not shown).

Proteolytic processing of caspase 8 and caspase 3 occurs after TBI

To determine whether caspase 8 and caspase 3 are activated after TBI, brain extracts from cortex and hippocampus ipsi- and contralateral to the injury site were examined for the expression of the p55 subunit (procaspase 8), the p20 subunit (processed caspase 8) and of the p18 subunit (cleaved caspase 3) by western blotting. Cortical impact injury resulted in an increase of p55 and p20 caspase 8 immunoreactivity in the ipsilateral cortex (Fig. 2a). The p55 and p20 caspase 8 immunoreactivity increased within 6 h after TBI and peaked at 24 h after the impact (376% increase relative to sham animals for p55, and 653% increase as compared with sham animals for p20, respectively), declining thereafter. After 7 and 14 days, no significant increases were evident in the p55 and p20 fragments when compared with levels in sham-injured control animals. Similar to a previous study (Beer *et al.*
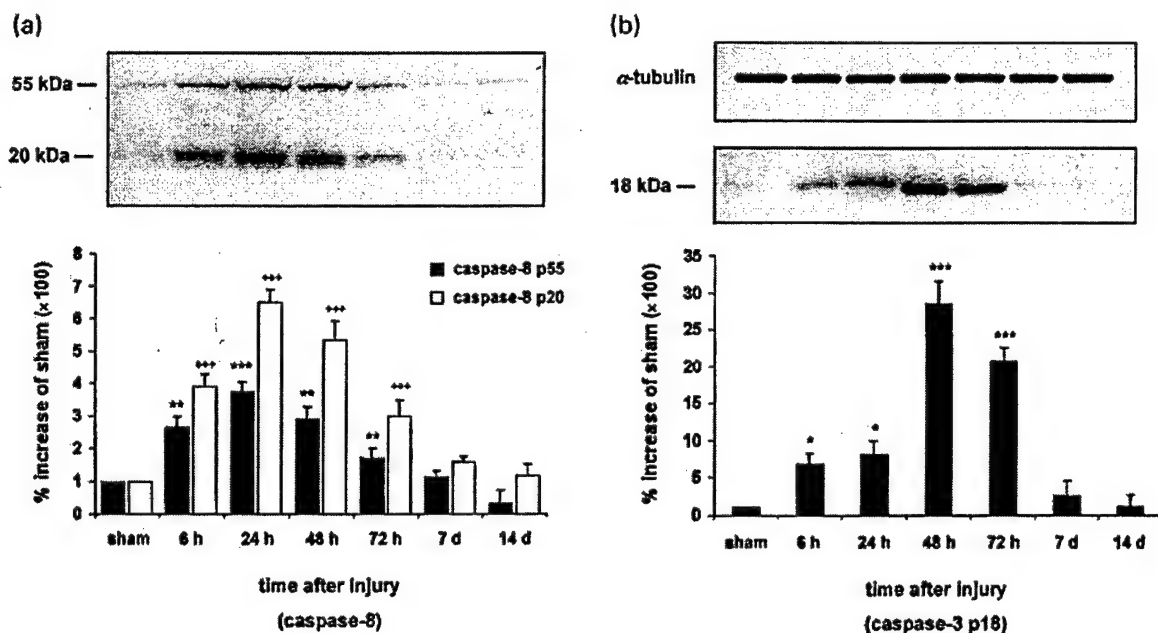
(a)

(b)

Fig. 2 Time-course of caspase 8 (a) and caspase 3 p18 (b) protein expression after TBI. Samples from single control (sham) and single injured animals were prepared for western blotting between 6 h and 14 days after TBI. Levels of protein are expressed as arbitrary densitometric units. Data were transformed to percentages of the densitometric levels observed on scans from sham animals visualized on the same blot. Values given are mean ± SD of four independent experiments. (a) Ipsilateral cortex: immunoblots demonstrated that procaspase 8 (p55) is constitutively expressed in sham-injured brains. Following TBI, immunoreactivity of p55 (filled bars) (**p < 0.01) and

p20 (processed caspase 8; open bars) ($^{+++}$p < 0.001) increased significantly at 6 h after TBI and peaked at 24 h post injury. Immunoreactivity of p55 (*p < 0.05) and p20 ($^{+++}$p < 0.001) was still significantly increased up to 72 h post trauma. (b) Ipsilateral cortex: the proteolytically active p18 fragment of caspase 3 increased significantly within 6 h after TBI (*p < 0.05). p18 immunoreactivity peaked at 48 h after TBI (***p < 0.001) and was still significantly elevated at 72 h after impact injury (***p < 0.001). α-tubulin was used as an internal standard.

2000b), immunoreactivity for activated caspase 3 (p18) increased within 6 h after TBI in the traumatized cortex (Fig. 2b). However, the maximal increase of p18 immunoreactivity was seen at later times (48 h after TBI; 2850% increase relative to sham animals), when compared with caspase 8 p20. Caspase 3 p18 immunoreactivity then declined to a 2060% increase relative to sham at 72 h after TBI. Similar to proteolyzed caspase 8, no statistically significant differences in caspase 3 p18 immunoreactivity were observed between cortical samples ipsilateral to the injury site at 7 and 14 days after TBI and in cortical samples from sham-injured animals. In addition, no significant increases in p55, p20 and p18 immunoreactivity were seen between sham and injured animals in cortical samples contralateral to the injury site and hippocampal samples ipsi- and contralateral to the injury site between 6 h and 14 days after TBI (data not shown).

Caspase 8 is expressed in traumatized cortical neurons, astrocytes and oligodendrocytes

Ipsilateral and contralateral cortical and hippocampal tissues were examined rostrocaudally from + 0.2 to − 3.8 mm

bregma. No caspase 8 immunoreactivity was present in the tissue from sham-injured (Fig. 3a) or naive (data not shown) control rats. Positive immunoreactivity for caspase 8 was found throughout the ipsilateral cortex at the primary injury zone (from − 1.5 to − 3.4 mm bregma) from 6 h to 72 h after the trauma (Figs 3b and c; time point = 24 h after TBI; − 3.4 mm bregma). To further investigate if caspase 8 is expressed in glial and/or neuronal cells, we performed double-labeling experiments for caspase 8 using the neuronal cell specific marker NeuN, the astrocytic marker GFAP, the microglial marker ED-1, and the oligodendroglial marker CNPase. These immunohistochemical analyses of caspase 8-positive cells from 6 to 72 h after TBI (Figs 3i–k; time point = 24 h after trauma; − 3.4 mm bregma) identified labeling with NeuN, GFAP and CNPase, and demonstrated the expression of caspase 8 in cortical neurons (Fig. 3i), astrocytes (Fig. 3j) and oligodendrocytes (Fig. 3k), respectively. Interestingly, immunoreactivity for caspase 8 was observed to be mainly cytosolic in neurons (Figs 3g and i), but appeared rather nuclear in astrocytes (Fig. 3j) and oligodendrocytes (Fig. 3k). No caspase 8 immunoreactivity was detected in microglial cells.
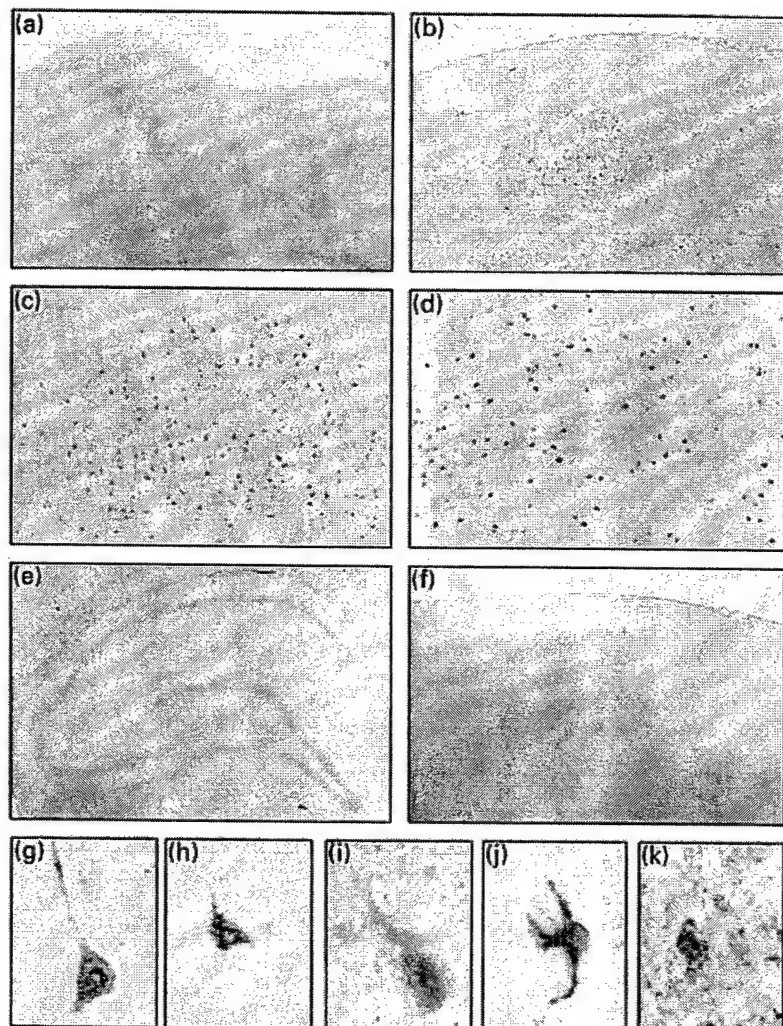
Fig. 3 Cell subtype distribution of caspase 8 in the traumatized cortex (− 3.4 mm bregma) at 24 h after TBI. Sham injured brains showed no specific caspase 8 immunolabeling (a). Low (b), intermediate (c) and high magnification (g) photomicrographs revealed specific caspase 8 expression in the ipsilateral cortex following cortical impact injury. Cells immunopositive for activated caspase 3 are found within similar brain regions (d and h). Double immunostaining experiments with caspase 8 (brown color; i, j and k) and NeuN (blue color; i), GFAP (blue color; j), and CNPase (blue color; k) provided evidence that caspase 8 is expressed in cortical neurons (i), astrocytes (j), and oligodendrocytes (k) after TBI. Magnifications: (a) and (b), 40×; (c) and (d), 100×; (e), 20×; (f), 40×; (g–k), 1000×.
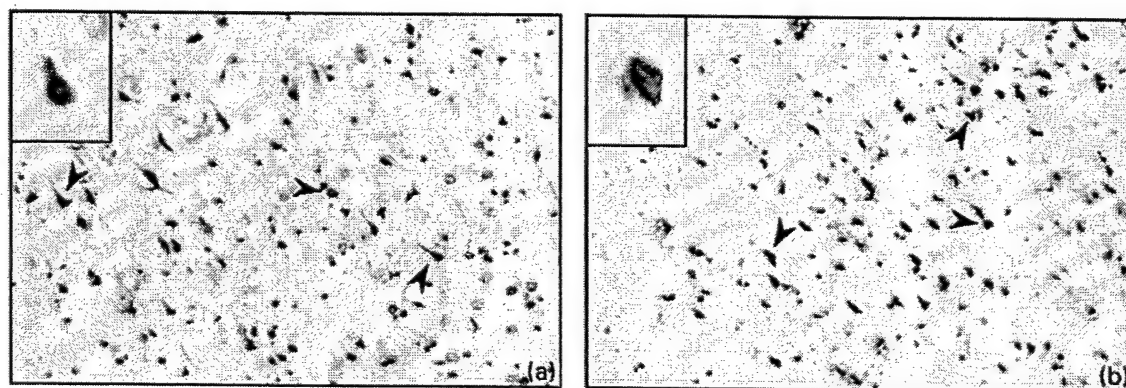

Fig. 4 Appearance of caspase 8 and processed caspase 3 p18 in TUNEL-positive cells. Combined immunohistochemistry for caspase 8 (red color; a) and TUNEL (dark blue color; a) (24 h after TBI) and caspase 3 p18 (red color; b) and TUNEL (dark blue; b) (48 h after TBI) demonstrated caspase 8 (a) and activated caspase 3 (b) in cells with gross nuclear apoptotic-like morphology. TUNEL-positive cells exhibited chromatin condensation and nuclear fragmentation (arrows). Magnifications: (a) and (b), 200×; inserts, 1000×.
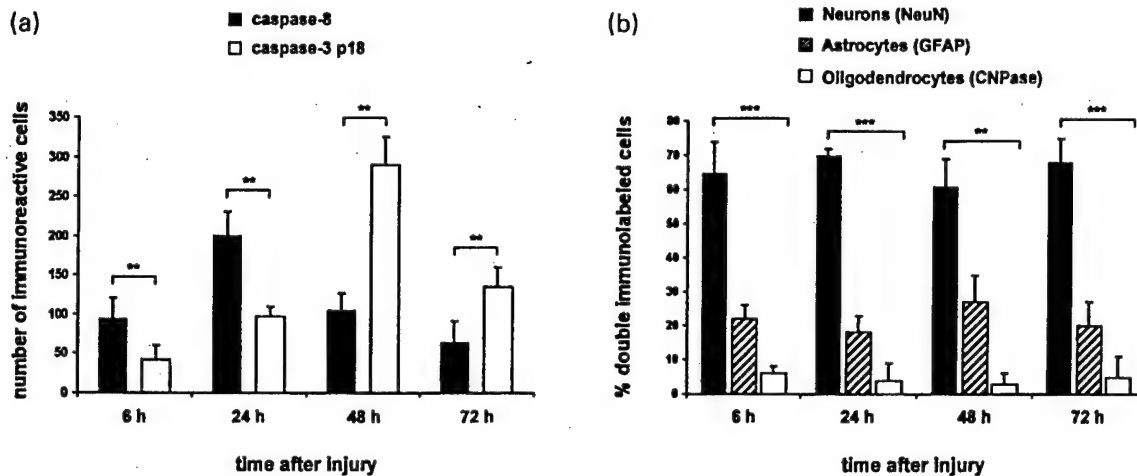
Fig. 5 Quantification of caspase 8 and caspase 3 p18 positive cells in the ipsilateral cortex after TBI (a) and quantification of caspase 8 cell subtype staining (b). Cells were counted in the entire anatomic regions of the cortex at the primary injury zone (bregma − 3.4 mm). (a) The number of caspase 8 positive cells (filled bars) was significantly greater than that of caspase 3 p18 positive cells (open bars) before 48 h after TBI. (b) Quantitative analysis was conducted of caspase 8 and NeuN (filled bars), caspase 8 and GFAP (hatched bars), and caspase 8 and CNPase (open bars) immunopositive cells. Columns indicate double-labeled neurons (filled bars), double-labeled astrocytes (hatched bars), and double-labeled oligodendrocytes (open bars) as percentages of caspase 8-positive cells from 6 to 72 h after TBI. Cell counts of caspase 8-positive neurons were significantly higher as compared with caspase 8-positive glia (i.e. astrocytes and oligodendrocytes at 6, 24, 48 and 72 h after TBI, respectively). Cell counts were evaluated by ANOVA with Bonferroni's *post hoc* analysis (**$p < 0.01$, ***$p < 0.001$). Values given are mean ± SD of four different animals per time point.

Caspase 8 immunoreactivity was absent in ipsilateral hippocampal samples (Fig. 3e) and contralateral samples of cortex (Fig. 3f) and hippocampus (data not shown) at all times investigated.

Caspase 8- and caspase 3-immunopositive cells exhibit nuclear apoptotic-like morphology

To verify further an apoptotic component of post-traumatic cell death and to support the possibility that caspase 8 and caspase 3 are associated with trauma-induced apoptosis, sections immunopositive for caspase 8 and caspase 3 p18 were stained with TUNEL to assess DNA damage. Double-labeling experiments demonstrated that a substantial proportion of TUNEL positive cells with shrunken morphology, condensed nuclei and chromatin margination also expressed caspase 8 (Fig. 4a) and activated caspase 3 (Fig. 4b) in layers 2–5 of the injured parietal cortex after TBI. However, cells with either caspase 8 or activated caspase 3 reactivity or gross apoptotic-like morphology alone were also detected.

Quantification of caspase 8- and caspase 3-positive cells and caspase 8 cell subtype staining after TBI

Activated caspase 3 was detected in the ipsilateral traumatized cortex from 6 to 72 h after impact injury. Similar to our findings for caspase 8, p18 positive cells were seen within cortical layers 2–5 at the primary impact zone (Fig. 3d) (Beer *et al.* 2000b). In contrast to caspase 8, the intracellular localization of activated caspase 3 was pre-dominantly nuclear (Fig. 3h). Quantitative analysis of caspase 8- and p18-positive cells revealed that the number of caspase 8- and p18-labeled cells increased up to 24 and 48 h after trauma, respectively, with the number of caspase 8-positive cells being significantly higher until 24 h after TBI (Fig. 5a).

Quantification of caspase 8 and NeuN, GFAP and CNPase revealed that the number of caspase 8-positive neurons is significantly higher as compared with glia (i.e. astrocytes and mature oligodendrocytes) from 6 to 72 h after injury, respectively (Fig. 5b).

Discussion

Our results provide the first evidence for caspase 8 expression and processing after experimental TBI. Proteolyzed caspase 8 appeared in samples of the traumatized cortex from 6 to 72 h after impact injury. Furthermore, double labeling experiments revealed expression of caspase 8 in neurons, astrocytes and oligodendrocytes after experimental brain injury. Moreover, our data indicate that expression of caspase 8 and cleaved caspase 3 p18 is associated with apoptotic-like cell death phenotypes detected in TUNEL-positive cells. Finally, our results suggest that caspase 8 may at least in part contribute to caspase 3-mediated cell death after experimental TBI in the rat.

Reverse transcription PCR and western blotting data revealed increased expression of caspase 8 messenger RNA and increased immunoreactivity for procaspase 8 and caspase 8 p20 in the ipsilateral cortex from 1 h to 72 h after the impact. Similar to our results, current data also suggest that caspase 8 messenger RNA, procaspase 8 and activated caspase 8 are over-expressed at early time points after experimental spinal cord ischemia (Matsushita *et al.* 2000) and focal cerebral ischemia (Harrison *et al.* 2001) in the mouse. Moreover, increased expression of proteolyzed caspase 8 has also been described after experimental focal ischemia in the rat up to 48 h after the insult (Velier *et al.* 1999). In this regard, it is noteworthy that cortical impact injury may produce focal ischemia in the cortex ipsilateral to the injury site (Bryan *et al.* 1995). Thus, reduced cerebral blood flow may have also contributed to activation of caspase 8 in our experiments. Taken together, these data demonstrate that caspase 8 is up-regulated and activated as an early event after various acute CNS injuries *in vivo*.

Previous reports on the cell subtype distribution have found increased immunoreactivity for caspase 8 in neurons after focal ischemia in the rat (Velier *et al.* 1999). In addition, recent data provided evidence that caspase 8 is also over-expressed in neurons following experimental spinal cord ischemia in the mouse (Matsushita *et al.* 2000) and in oligodendrocytes undergoing staurosporine-induced apoptosis *in vitro* (Gu *et al.* 1999). These findings indicate that whereas caspase 8 has been reported only to be weakly expressed in normal brain parenchyma (Velier *et al.* 1999), the brain readily over-expresses caspase 8 after a variety of pathological stimuli. Our immunohistochemical results, however, are the first to show that caspase 8 is over-expressed in neurons, astrocytes and oligodendrocytes after experimental brain injury *in vivo*. Moreover, our findings suggest that caspase 8 expression is mainly cytosolic in neurons, but has a rather nuclear distribution in astrocytes and oligodendrocytes after TBI *in vivo*. In this regard it is noteworthy that caspase 8 can be expressed in both the nuclear and cytosolic compartment (Xerri *et al.* 2000). Therefore, future studies are needed to further investigate the significance of caspase 8 expression in different subcellular compartments of CNS cells after experimental brain injuries *in vivo*.

The exact mechanisms leading to the activation of caspase 8 after CNS injuries have yet not been determined. Recent data suggest that caspase 8 may be activated by receptor-mediated mechanisms including the tumor necrosis factor receptor type-1 (TNF-R1) (Schulze-Osthoff *et al.* 1998) and Fas signaling pathways (Muzio *et al.* 1996; Medema *et al.* 1997). For example, it has been reported that over-expression of α-TNF and Fas ligand may induce apoptosis after experimental cerebral ischemia and brain trauma *in vivo* (Kokaia *et al.* 1998; Shohami *et al.* 1996; Martin-Villalba *et al.* 1999). Moreover, increased Fas expression has been implicated in glutamate-induced apoptotic cell death of CNS neurons *in vitro* (Li *et al.* 1998). Importantly, excessive excitatory amino acid release with subsequent neurotoxicity also has been described after TBI *in vivo* (for review see Globus *et al.* 1995). Finally, recent data by Beer *et al.* (2000a) indicate that the Fas/Fas ligand system is also up-regulated in similar brain regions and at similar times after TBI as caspase 8 expression seen in our study (cortical layers 2–5, and 15 min to 72 h after impact injury, respectively). Taken together, these results suggest that excitatory amino acids and the Fas/Fas ligand system may indeed participate in activation of caspase 8 after TBI. In this regard, it is noteworthy that coexpression of Fas and caspase 8 has been observed in spinal cord neurons after experimental spinal cord ischemia *in vivo* (Matsushita *et al.* 2000).

Recent data suggest that cell loss induced by traumatic spinal cord injury and TBI may be attributed in part to apoptotic mechanisms (for a review see Beattie *et al.* 2000; Raghupathi *et al.* 2000). Moreover, several *in vivo* and *in vitro* studies have documented the significance of caspases in apoptotic cell degeneration following acute CNS injuries (for reviews see Eldadah and Faden 2000; Mattson *et al.* 2000). In addition, it has also been reported that caspase 3 is activated after experimental cerebral ischemia (Namura *et al.* 1998; Velier *et al.* 1999), fluid percussion (Yakovlev *et al.* 1997), and cortical impact models of TBI (Beer *et al.* 2000b; Clark *et al.* 2000). Our western blotting data also indicate that caspase 3 is activated after TBI, and our double-labeling immunohistochemical studies using TUNEL and p18 antiserum demonstrated caspase 3-positive cells with gross DNA damage in the traumatized cortex, suggesting a mechanistic link between caspase 3 activation and apoptosis.

Recent evidence from *in vitro* studies suggests that caspase 3 can be activated directly by caspase 8 (Stennicke *et al.* 1998). However, coexpression of caspase 8 and activated caspase 3 after various CNS injuries *in vivo* has not been studied extensively. One recent report indicated that caspase 8 and activated caspase 3 are coexpressed within CNS cells after experimental spinal cord ischemia up to 24 h after the insult (Matsushita *et al.* 2000). Our present findings provide further evidence of expression of both, caspase 8 and activated caspase 3 in multiple cortical CNS cell populations after TBI *in vivo*. Importantly, the expression of caspase 8 and activated caspase 3 in similar cortical brain regions suggests that caspase 8 may participate in caspase 3 activation in cortical CNS cells after TBI. Moreover, the greater number of caspase 8 positive cells (compared with caspase 3 immunoreactive cells) at early time points (6 and 24 h post trauma) followed by a greater number of caspase 3 positive cells (compared with caspase 8 positive cells) at later time points (48 h and 72 h post trauma) supports the hypothesis that caspase 8 may indeed be upstream of caspase 3. However, it was of interest that

caspase 8 immunoreactivity is found also in cells with evidence of DNA damage as indicated by TUNEL. In this regard it is noteworthy that caspase 8 may also function as an amplifying executioner caspase in drug-induced apoptosis *in vitro* (Engels *et al.* 2000). Therefore, future studies have to investigate the exact role of caspase 8 in the activation and/or execution phase of the apoptotic cascade after acute CNS injuries *in vivo*. This also implicates the need for further investigations on the significance of caspase 8 independent activation of caspase 3, including the mitochondrial pathway (Eldadah and Faden 2000).

Our study failed to detect increased expression of caspase 8, activated caspase 3 and apoptotic CNS morphology in the hippocampus ipsilateral to the injury site from 6 h to 14 days after the trauma. This is in contrast to previous reports, which clearly describe features of apoptotic neuronal degeneration in the hippocampus following fluid percussion injury (Yakovlev *et al.* 1997; Conti *et al.* 1998) and cortical impact injury (Clark *et al.* 2000; Colicos and Dash 1996). However, previous studies from our laboratory (Franz *et al.* 1999; Beer *et al.* 2000a,b) have shown that cortical impact injury may not necessarily be associated with hippocampal neuronal degeneration. Probable reasons for discrepancies in the appearance of hippocampal damage may be subtle methodological differences in animal models of TBI. For example, differences in angulation and velocity of the impact devices could account for the presence or absence of hippocampal cell degeneration.

In conclusion, our results provide evidence for induction of caspase 8 expression in cortical neurons and glial cells after TBI *in vivo*. Moreover, our data raise the possibility that caspase 8 may contribute to caspase 3 activation after impact injury in the rat. In addition to these *in vivo* findings, we also provided evidence that caspase 8 and activated caspase 3 may participate in mechanisms of apoptotic CNS cell degeneration in the traumatized cortex. However, future studies are needed to further elucidate the precise role of caspase 8 and activated caspase 3 for cellular CNS degeneration after TBI, including the significance of apoptotic cell death on functional outcome after acute brain injuries *in vivo*.

Acknowledgements

References

Beattie M. S., Farooqui A. A. and Bresnahan J. C. (2000) Review of current evidence for apoptosis after spinal cord injury. *J. Neurotrauma* 17, 915–925.

Beer R., Franz G., Schöpf M., Reindl M., Zelger B., Schmutzhard E., Poewe W. and Kampfl A. (2000a) Expression of Fas and Fas ligand after experimental traumatic brain injury in the rat. *J. Cereb. Blood Flow Metab.* 20, 669–677.

Beer R., Franz G., Srinivasan A., Hayes R. L., Pike B. R., Newcomb J. K., Zhao X., Schmutzhard E., Poewe W. and Kampfl A. (2000b) Temporal profile and cell subtype distribution of activated caspase-3 following experimental traumatic brain injury. *J. Neurochem.* 75, 1264–1273.

Bryan R. M., Cherian L. and Robertson C. (1995) Regional cerebral blood flow after controlled cortical impact injury in rats. *Anesth. Analg.* 80, 687–695.

Cerretti D. P., Kozlosky C. J., Mosley B., Nelson N., Van Ness K., Greenstreet T. A., March C. J., Kronheim S. R., Druck T. and Cannizzaro L. A. (1992) Molecular cloning of the interleukin-1 beta converting enzyme. *Science* 256, 97–100.

Charriaut-Marlangue C., Remolleau S., Aggoun-Zouaoui D. and Ben-Ari Y. (1998) Apoptosis and programmed cell death: a role in cerebral ischemia. *Biomed. Pharmacother.* 52, 264–269.

Clark R. S., Kochanek P. M., Watkins S. C., Chen M., Dixon C. E., Seidberg N. A., Melick J., Loeffert J. E., Nathaniel P. D., Jin K. L. and Graham S. H. (2000) Caspase-3 mediated neuronal death after traumatic brain injury in rats. *J. Neurochem.* 74, 740–753.

Cohen G. M. (1997) Caspases: the executioners of apoptosis. *Biochem. J.* 326, 1–16.

Colicos M. A. and Dash P. K. (1996) Apoptotic morphology of dentate gyrus granule cells following experimental cortical impact injury in rats: possible role in spatial memory deficits. *Brain Res.* 739, 120–131.

Conti A. C., Raghupathi R., Trojanowski J. Q. and McIntosh T. K. (1998) Experimental brain injury induces regionally distinct apoptosis during the acute and delayed post-traumatic period. *J. Neurosci.* 18, 5663–5672.

Crowe M. J., Bresnahan J. C., Shuman S. L., Masters J. N. and Beattie M. S. (1997) Apoptosis and delayed degeneration after spinal cord injury in rats and monkeys. *Nat. Med.* 3, 73–76.

Cryns V. and Yuan J. (1998) Proteases to die for. *Genes Dev.* 12, 1551–1570.

Debus E., Weber K. and Osborn M. (1983) Monoclonal antibodies specific for glial fibrillary acidic (GFA) protein and for each of the neurofilament triplet polypeptides. *Differentiation* 25, 193–203.

Dixon C. E., Clifton G. L., Lighthall J. W., Yaghmai A. A. and Hayes R. L. (1991) A controlled cortical impact model of traumatic brain injury in the rat. *J. Neurosci. Meth.* 39, 253–262.

Eldadah B. A. and Faden A. I. (2000) Caspase pathways, neuronal apoptosis, and CNS injury. *J. Neurotrauma* 17, 811–829.

Engels I. H., Stepczynska A., Stroh C., Lauber K., Berg C., Schwenzer R., Wajant H., Jänicke R. U., Porter A. G., Belka C., Gregor M., Schulze-Osthoff K. and Wesselborg S. (2000) Caspase-8/FLICE functions as an executioner caspase in anticancer drug-induced apoptosis. *Oncogene* 19, 4563–4573.

Ertel W., Keel M., Stocker R., Imhof H. G., Leist M., Steckholzer U., Tanaka M., Trentz O. and Nagata S. (1997) Detectable concentrations of Fas ligand in cerebrospinal fluid after severe head injury. *J. Neuroimmunol.* 80, 93–96.

Faden A. I. (1996) Pharmacologic treatment of acute traumatic brain injury. *J. Am. Med. Assoc.* 276, 569–570.

Felderhoff-Mueser U., Taylor D. L., Greenwood K., Kozma M., Stibenz D., Joashi U. C., Edwards A. D. and Mehmet H. (2000) Fas/CD95/APO-1 can function as a death receptor for neuronal cells in vitro

and in vivo and is upregulated following cerebral hypoxic-ischemic injury to the developing rat brain. *Brain Pathol.* **10**, 17–29.

Franz G., Reindl M., Patel S. C., Beer R., Unterrichter I., Berger T., Schmutzhard E., Poewe W. and Kampfl A. (1999) Increased expression of apolipoprotein D following experimental traumatic brain injury. *J. Neurochem.* **73**, 1615–1625.

Gavrieli Y., Sherman Y. and Ben-Sasson S. A. (1992) Identification of programmed cell death in situ via specific labeling of nuclear DNA fragmentation. *J. Cell Biol.* **119**, 493–501.

Globus M. Y., Alonso O., Dietrich W. D., Busto R. and Ginsberg M. D. (1995) Glutamate release and free radical production following brain injury: effects of posttraumatic hypothermia. *J. Neurochem.* **65**, 1704–1711.

Graeber M. B., Streit W. J., Kiefer R., Schoen S. W. and Kreutzberg G. W. (1990) New expression of myelomonocytic antigens by microglia and perivascular cells following lethal motor neuron injury. *J. Neuroimmunol.* **27**, 121–132.

Graham D. I., McIntosh T. K., Maxwell W. L. and Nicoll J. A. (2000) Recent advances in neurotrauma. *J. Neuropathol. Exp. Neurol.* **59**, 641–651.

Gu C., Casaccia-Bonnefil P., Srinivasan A. and Chao M. V. (1999) Oligodendrocyte apoptosis mediated by caspase activation. *J. Neurosci.* **19**, 3043–3049.

Harrison D. C., Davis R. P., Bond B. C., Campbell C. A., James M. F., Parsons A. A. and Philpott K. L. (2001) Caspase mRNA expression in a rat model of focal cerebral ischemia. *Brain Res. Mol. Brain Res.* **89**, 133–146.

Hayashi T., Sakurai M., Abe K., Sadahiro M., Tabayashi K. and Itoyama Y. (1998) Apoptosis of motor neurons with induction of caspases in the spinal cord after ischemia. *Stroke* **29**, 1007–1012.

Hayes R. L., Jenkins L. W. and Lyeth B. G. (1992) Neurotransmitter-mediated mechanisms of traumatic brain injury: acetylcholine and excitatory amino acids. *J. Neurotrauma* **9**, S173–S187.

Kato H., Kanellopoulos G. K., Matsuo S., Wu Y. J., Jacquin M. F., Hsu C. Y., Kouchoukos N. T. and Choi D. W. (1997) Neuronal apoptosis and necrosis following spinal cord ischemia in the rat. *Exp. Neurol.* **148**, 464–474.

Kermer P., Klocker N. and Bähr M. (1999) Neuronal death after brain injury. Models, mechanisms, and therapeutic strategies in vivo. *Cell Tissue Res.* **298**, 383–395.

Khan S. M., Cassarino D. S., Abramova N. N., Keeney P. M., Borland M. K., Trimmer P. A., Krebs C. T., Bennett J. C., Parks J. K., Swerdlow R. H., Parker W. D. and Bennett J. P. (2000) Alzheimer's disease cybrids replicate beta-amyloid abnormalities through cell death pathways. *Ann. Neurol.* **48**, 148–155.

Kokaia Z., Andsberg G., Martinez-Serrano A. and Lindvall O. (1998) Focal cerebral ischemia in rats induces expression of P75 neurotrophin receptor in resistant striatal cholinergic neurons. *Neuroscience* **84**, 1113–1125.

Krajewska M., Wang H. G., Krajewski S., Zapata J. M., Shabaik A., Gascoyne R. and Reed J. C. (1997) Immunohistochemical analysis of in vivo patterns of expression of CPP32 (Caspase-3), a cell death protease. *Cancer Res.* **57**, 1605–1613.

Krinke G. J. (2000) Part 6: Physiology in, *The Laboratory Rat* (Bullock, G., Bunton, T., eds). San Diego, Academic Press.

Li Y., Maher P. and Schubert D. (1998) Phosphatidylcholine-specific phospholipase C regulates glutamate-induced nerve cell death. *Proc. Natl Acad. Sci. USA* **95**, 7748–7753.

Liu X. Z., Xu X. M., Du Hu R. C., Zhang S. X., McDonald J. W., Dong H. X., Wu Y. J., Fan G. S., Jacquin M. F., Hsu C. Y. and Choi D. W. (1997) Neuronal and glial apoptosis after traumatic spinal cord injury. *J. Neurosci.* **17**, 5395–5406.

McIntosh T. K., Saatman K. E., Raghupathi R., Graham D. I., Smith

D. H., Lee V. M. and Trojanowski J. Q. (1998) The Dorothy Russell Memorial Lecture. The molecular and cellular sequelae of experimental traumatic brain injury: pathogenetic mechanisms. *Neuropathol. Appl. Neurobiol.* **24**, 251–267.

Martin-Villalba A., Herr I., Jeremias I., Hahne M., Brandt R., Vogel J., Schenkel J., Herdegen T. and Debatin K. M. (1999) CD95 ligand (Fas-L/APO-1L) and tumor necrosis factor-related apoptosis-inducing ligand mediate ischemia-induced apoptosis in neurons. *J. Neurosci.* **19**, 3809–3817.

Matsushita K., Wu Y., Qiu J., Lang-Lazdunski L., Hirt L., Waeber C., Hyman B. T., Yuan J. and Moskowitz M. A. (2000) Fas receptor and neuronal cell death after spinal cord ischemia. *J. Neurosci.* **20**, 6879–6887.

Mattson M. P., Culmsee C. and Yu Z. F. (2000) Apoptotic and anti-apoptotic mechanisms in stroke. *Cell Tissue Res.* **301**, 173–187.

Medema J. P., Scaffidi C., Kischkel F. C., Shevchenko A., Mann M., Krammer P. H. and Peter M. E. (1997) FLICE is activated by association with the CD95 death-inducing signaling complex (DISC). *EMBO J.* **16**, 2794–2804.

Mogi M., Togari A., Kondo T., Mizuno Y., Komure O., Kuno S., Ichinose H. and Nagatsu T. (2000) Caspase activities and tumor necrosis factor receptor R1 (p55) level are elevated in the substantia nigra from parkinsonian brain. *J. Neural. Transm.* **107**, 335–341.

Muzio M., Chinnaiyan A. M., Kischkel F. C., O'Rourke K., Shevchenko A., Ni J., Scaffidi C., Bretz J. D., Zhang M., Gentz R., Mann M., Krammer P. H., Peter M. E. and Dixit V. M. (1996) FLICE, a novel FADD-homologous ICE/CED-3-like protease, is recruited to the CD95 (Fas/APO-1) death-inducing signaling complex. *Cell* **85**, 817–827.

Namura S., Zhu J., Fink K., Endres M., Srinivasan A., Tomaselli K. J., Yuan J. and Moskowitz M. A. (1998) Activation and cleavage of caspase-3 in apoptosis induced by experimental cerebral ischemia. *J. Neurosci.* **18**, 3659–3668.

Newcomb J. K., Zhao X., Pike B. R. and Hayes R. L. (1999) Temporal profile of apoptotic-like changes in neurons and astrocytes following controlled cortical impact injury in the rat. *Exp. Neurol.* **158**, 76–88.

Nicholson D. W. (1999) Caspase structure, proteolytic substrates, and function during apoptotic cell death. *Cell Death Differ.* **6**, 1028–1042.

Nitatori T., Sato N., Waguri S., Karasawa Y., Araki H., Shibanai K., Kominami E. and Uchiyama Y. (1995) Delayed neuronal death in the CA1 pyramidal cell layer of the gerbil hippocampus following transient ischemia is apoptosis. *J. Neurosci.* **15**, 1001–1011.

Paxinos G. and Watson C. (1997). *The Rat Brain in Stereotaxic Coordinates*, 4th edn. San Diego, CA: Academic Press.

Pike B. R., Zhao X., Newcomb J. K., Glenn C. C., Anderson D. K. and Hayes R. L. (2000) Stretch injury causes calpain and caspase-3 activation and necrotic and apoptotic cell death in septo-hippocampal cell cultures. *J. Neurotrauma* **17**, 283–298.

Qin Z. H., Wang Y., Kikly K. K., Sapp E., Kegel K. B., Aronin N. and DiFiglia M. (2001) Pro-caspase-8 is predominatly localized in mitochondria and released into cytoplasm upon apoptotic stimulation. *J. Biol. Chem.* **276**, 8079–8086.

Raghupathi R., Graham D. I. and McIntosh T. K. (2000) Apoptosis after traumatic brain injury. *J. Neurotrauma* **17**, 927–938.

Rink A., Fung K. M., Trojanowski J. Q., Lee V. M., Neugebauer E. and McIntosh T. K. (1995) Evidence of apoptotic cell death after experimental traumatic brain injury in the rat. *Am. J. Pathol.* **147**, 1575–1583.

Scaffidi C., Fulda S., Srinivasan A., Friesen C., Li F., Tomaselli K. J.,

Debatin K. M., Krammer P. H. and Peter M. E. (1998) Two CD95 (APO-1/Fas) signaling pathways. *EMBO J.* **17**, 1675–1687.

Schulze-Osthoff K., Ferrari D., Los M., Wesselborg S. and Peter M. E. (1998) Apoptosis signaling by death receptors. *Eur. J. Biochem.* **254**, 439–459.

Shah P. T., Yoon K. W., Xu X. M. and Broder L. D. (1997) Apoptosis mediates cell death following traumatic injury in rat hippocampal neurons. *Neuroscience* **79**, 999–1004.

Shikama Y. (2001) Comprehensive studies on subcellular localizations and cell death-inducing activities of eight gfp-tagged apoptosis-related caspases. *Exp. Cell Res.* **264**, 315–325.

Shohami E., Bass R., Wallach D., Yamin A. and Gallily R. (1996) Inhibition of tumor necrosis factor alpha (TNF alpha) activity in rat brain is associated with cerebroprotection after closed head injury. *J. Cereb. Blood Flow Metab.* **16**, 378–384.

Springer J. E., Azbill R. D. and Knapp P. E. (1999) Activation of the caspase-3 apoptotic cascade in traumatic spinal cord injury. *Nat. Med.* **8**, 943–946.

Sprinkle T. J. (1989) 2′,3′-cyclic nucleotide 3′-phosphodiesterase, an oligodendrocyte-Schwann cell and myelin-associated enzyme of the nervous system. *Crit. Rev. Neurobiol.* **4**, 235–301.

Srinivasan A., Roth K. A., Sayers R. O., Shindler K. S., Wong A. M., Fritz L. C. and Tomaselli K. J. (1998) In situ immunodetection of activated caspase-3 in apoptotic neurons in the developing nervous system. *Cell Death Differ.* **5**, 1004–1016.

Stadelmann C., Deckwerth T. L., Srinivasan A., Bancher C., Bruck W., Jellinger K. and Lassmann H. (1999) Activation of caspase-3 in single neurons and autophagic granules of granulovacuolar degeneration in Alzheimer's disease. Evidence for apoptotic cell death. *Am. J. Pathol.* **155**, 1459–1466.

Stennicke H. R., Jurgensmeier J. M., Shin H., Deveraux Q., Wolf B. B., Yang X., Zhou Q., Ellerby H. M., Ellerby L. M., Bredesen D., Green D. R., Reed J. C., Froelich C. J. and Salvesen G. S. (1998)

Pro-caspase-3 is a major physiologic target of caspase-8. *J. Biol. Chem.* **273**, 27084–27090.

Stoka V. V., Turk B., Schendel S. L., Kim T. H., Cirman T., Snipas S. J., Ellerby L. M., Bredesen D., Freeze H., Abrahamson M., Bromme D., Krajewski S., Reed J. C., Yin X. M., Turk V. V. and Salvesen G. S. (2001) Lysosomal protease pathways to apoptosis: cleavage of bid, not pro-caspases, is the most likely route. *J. Biol. Chem.* **276**, 3149–3157.

Thurman D. J., Alverson C., Dunn K. A., Guerrero J. and Sniezek J. E. (1999) Traumatic brain injury in the United States: a public health perspective. *J. Head Trauma Rehabil.* **14**, 602–615.

Velier J. J., Ellison J. A., Kikly K. K., Spera P. A., Barone F. C. and Feuerstein G. Z. (1999) Caspase-8 and caspase-3 are expressed by different populations of cortical neurons undergoing delayed cell death after focal stroke in the rat. *J. Neurosci.* **19**, 5932–5941.

Walker N. P., Talanian R. V., Brady K. D., Dang L. C., Bump N. J., Ferenz C. R., Franklin S., Ghayur T., Hackett M. C. and Hammill L. D. (1994) Crystal structure of the cysteine protease interleukin-1 beta-converting enzyme: a (p20/p10), 2 homodimer. *Cell* **78**, 343–352.

Wolf H. K., Buslei R., Schmidt-Kastner R., Schmidt-Kastner P. K., Pietsch T., Wiestler O. D. and Bluhmke I. (1996) NeuN: a useful neuronal marker for diagnostic histopathology. *J. Histochem. Cytochem.* **44**, 1167–1171.

Xerri L., Palmerini F., Devilard E., Defrance T., Bouabdallah R., Hassoun J. and Birg F. (2000) Frequent nuclear localization of ICAD and cytoplasmic co-expression of caspase-8 and caspase-3 in human lymphomas. *J. Pathol.* **192**, 194–202.

Yakovlev A. G., Knoblach S. M., Fan L., Fox G. B., Goodnight R. and Faden A. I. (1997) Activation of CPP32-like caspases contributes to neuronal apoptosis and neurological dysfunction after traumatic brain injury. *J. Neurosci.* **17**, 7415–7424.

TNF-α Stimulates Caspase-3 Activation and Apoptotic Cell Death in Primary Septo-Hippocampal Cultures

Xiurong Zhao,[1] Brian Bausano,[1] Brian R. Pike,[2] Jennifer K. Newcomb-Fernandez,[1] Kevin K.W. Wang,[3] Esther Shohami,[4] N.C. Ringger,[2] S.M. DeFord,[2] Douglas K. Anderson,[5] and Ronald L. Hayes[2]*

[1]The Vivian L. Smith Center for Neurologic Research, Department of Neurosurgery, The University of Texas Health Science Center, Houston, Texas
[2]Center for Traumatic Brain Injury Studies, Department of Neuroscience, University of Florida, Gainesville, Florida
[3]Pfizer, Ann Arbor, Michigan
[4]Department of Pharmacology, The Hebrew University School of Pharmacy, Jerusalem, Israel
[5]Department of Neuroscience and Malcolm Randall VAMC, University of Florida, Gainesville, Florida

Primary septo-hippocampal cell cultures were incubated in varying concentrations of tumor necrosis factor (TNF-α; 0.3–500 ng/ml) to examine proteolysis of the cytoskeletal protein α-spectrin (240 kDa) to a signature 145 kDa fragment by calpain and to the apoptotic-linked 120-kDa fragment by caspase-3. The effects of TNF-α incubation on morphology and cell viability were assayed by fluorescein diacetate-propidium iodide (FDA-PI) staining, assays of lactate dehydrogenase (LDH) release, nuclear chromatin alterations (Hoechst 33258), and internucleosomal DNA fragmentation. Incubation with varying concentrations of TNF-α produced rapid increases in LDH release and nuclear PI uptake that were sustained over 48 hr. Incubation with 30 ng/ml TNF-α yielded maximal, 3-fold, increase in LDH release and was associated with caspase-specific 120-kDa fragment but not calpain-specific 145-kDa fragment as early as 3.5 hr after injury. Incubation with the pan-caspase inhibitor, carbobenzosy-Asp-CH$_2$-OC (O)-2-6-dichlorobenzene (Z-D-DCB, 50-140 μM) significantly reduced LDH release produced by TNF-α. Apoptotic-associated oligonucleosomal-sized DNA fragmentation on agarose gels was detected from 6 to 72 hr after exposure to TNF-α. Histochemical changes included chromatin condensation, nuclear fragmentation, and formation of apoptotic bodies. Results of this study suggest TNF-α may induce caspase-3 activation but not calpain activation in septo-hippocampal cultures and that this activation of caspase-3 at least partially contributes to TNF-α-induced apoptosis. J. Neurosci. Res. 64:121–131, 2001. © 2001 Wiley-Liss, Inc.

Key words: apoptosis; calpain; caspase; cytokine; neural injury; proteolysis

Tumor necrosis factor-α (TNF-α) is a 17-kDa pleiotrophic cytokine with both secreted and transmembrane forms, which that is known to mediate immune and inflammatory responses. TNF-α can be synthesized and released by astrocytes, microglia, and some neurons (Lieberman et al., 1989; Chung and Benveniste, 1990; Morganti-Kossmann et al., 1992). Although TNF-α was originally named for its degeneration-inducing action in some types of tumor cells, data now suggest that TNF-α has a variety of effects on different types of cells (Cheng et al., 1994). A substantial body of evidence indicates that TNF-α has a pro-inflammatory role that is acutely up-regulated in ischemic and traumatic brain injury (TBI) (Taupin et al., 1993; Shohami et al., 1994; Fan et al., 1996; Saito et al., 1996; Liu et al., 1994; Wang et al., 1994; Uno et al., 1997; Gong et al., 1999; Buttini et al., 1996). Immunocytochemical studies confirm the presence of TNF-α antigen in the brain as early as 30 min after occlusion of the middle cerebral artery in the same regions where TNF-α mRNA-positive cells were detected (Buttini et al., 1996). Increased levels of TNF-α in brain tissue, cerebral spinal fluid, and plasma have been found in several central nervous system (CNS) disorders including Alzheimer's disease (Fillet et al., 1991), Guillain-Barre Syndrome (Sharief et al., 1993), Parkinson's disease (Mogi

et al, 1994, 1996), and spinal cord injury (Xu et al., 1998). Other studies have shown that TNF-α can mediate apoptotic cell death (Gelbard et al., 1993; Aggarwal et al., 1999) and can modulate Bax/BcL-2 protein levels (Pulliam et al., 1998). A variety of TNF-α antagonists or antibodies decreased TNF-α levels, improved behavioral outcome, and reduced brain damage following experimental ischemia and TBI in rats and mice (Shohami et al., 1996, 1997; Meirstrell et al., 1997; Barone et al., 1997; Dawson et al., 1996; Nawashiro et al., 1997; Leker et al., 1999; Knoblach et al., 1999).

Although the inflammatory responses evoked by TNF-α are well known, a number of investigations have posited a protective role of TNF-α against neuronal cell death. For example, it has been shown that TNF-α mediates damage to myelin and oligodendrocytes (Selmaj and Raine, 1988) but is not toxic to CNS neurons in vitro (Garcia et al., 1992). TNF-α under in vitro conditions may protect neurons against metabolic, excitotoxic, or oxidative insults by promoting maintenance of intracellular calcium homeostasis, suppression of reactive oxygen species (Cheng et al., 1994), and by activation of transcription factor NF-κB (necrosis-factor-κB; Barger et al., 1995). Mice genetically deficient in TNF-α receptor R1 or both R1 and R2, also show exacerbated neuronal damage compared to wild type controls following middle cerebral artery occlusion (Bruce et al., 1996; Gary et al., 1998) or TBI (Scherbel et al., 1999; Sullivan et al., 1999). In addition, Stahel et al. (2000) reported that in mice lacking both genes for TNF-α and lymphotoxin-α, mortality at 7 days after closed head injury was significantly higher, as compared to their matched wild type controls. Based on the literature, the concept that emerges suggests that TNF-α can have a detrimental role, in the acute postinjury phase, whereas it is protective in the delayed posinjury phase, probably by activating cellular repair mechanisms (Shohami et al., 1999). Therefore, the present study was designed to further investigate the acute mechanism(s) of TNF-α-induced cell death within 3 days of exposure of septo-hippocampal neurons to exogenous TNF-α.

In order to examine the role of TNF-α on cell viability, we investigated the effects of TNF-α stimulation on calpain and caspase-3 protease activation and on necrotic and apoptotic cell death phenotypes. Calpains are calcium-activated cysteine proteases that have been implicated in a variety of neuropathological conditions (Kampfl et al., 1997; Wang et al., 1994; Wang, 2000). Caspase-3 is a cysteine protease and a known effector of apoptosis in various cell lines (Nath et al., 1995; Pike et al., 1998; Eldadah et al., 1997; Fraser and Evan, 1996; Miura et al., 1993; Zhivotovsky et al., 1997). Caspase-3 is activated only during apoptosis and not during necrosis (Nath et al., 1998; Armstrong et al., 1996; Wang et al., 1996). In contrast, calpain activation can contribute to apoptotic as well as necrotic cell death (Pike et al., 1998; Zhao et al., 1999). The cytoskeletal protein α-spectrin is a preferred substrate of calpain and caspase-3 cysteine protease. Acti-

vated calpain and caspase-3 process α-spectrin into a signature 145-kDa fragment by calpain and to an apoptotic-linked 120-kDa fragments by caspase-3 (Pike et al., 1998; Zhao et al., 1999; Nath et al., 1995). Thus, the investigation examined calpain and caspase-3 activation, inferred by proteolysis of the cytoskeletal protein α-spectrin, in mixed rat glial-neuronal septo-hippocampal cell cultures following exposure to TNF-α. Experiments also employed morphopathological assessments and measures of DNA fragmentation to characterize necrotic and apoptotic cell death profiles in neurons and glia (Pike et al., 1998; Zhao et al., 1999). This study provides the first evidence that TNF-α produces caspase-3 but not calpain activation in mixed septo-hippocampal cell cultures. In addition, cell death in this model following TNF-α challenge manifested exclusively apoptotic-like characteristics.

MATERIALS AND METHODS

Materials

Septi and hippocampi neuronal cells were obtained from rat fetuses. Cell culture reagents were from Life Technologies, Rockville, MD, and Sigma Chemical, Inc. (St. Louis, MO). The TNF-α and actinomycin D (Act D) in which the cells were incubated were obtained from R&D Systems (Minneapolis, MN) and Sigma, respectively. Z-D-DCB was a generous gift from Pfizer, while CalpInh-II was obtained from Boehringer Mannheim (Indianapolis, IN). All other reagents used in these experiments were analytical grade quality of higher.

Septo-Hippocampal Cultures

Eighteen-day-old rat fetuses were removed from deeply anesthetized dams. Septi and hippocampi were dissected in a dissect buffer (HBSS, with 4.2 mM bicarbonate, 1 mM pyruvate, 20 mM HEPES, 3 mg/ml bovine serum albumin [BSA], pH 7.25). After rinsing in Dulbeccos'Modified Eagle Medium (DMEM)-DM, tissue was dissociated by trituration through the narrow pore of flame-constricted Pasteur pipette. Dissociated cells were resuspended in DMEM with 10% fetal calf serum (DMEM-10S) and plated onto 24-well poly-L-lysine- coated plastic culture plates or 12 mm of German glass (Erie Scientific Co., Portsmith, NH) at a density of 4.36×10^5 cells/mL. Cultures were maintained in a humidified incubator in an atmosphere of 5% CO_2 at 37°C. After 5 days of culture, the media was changed to DMEM-DM with 5% horse serum. Subsequent media changes were carried out three times a week. By day 10 in vitro, astrocytes formed a confluent monolayer beneath morphologically mature neurons.

In addition, we confirmed the presence of TNF-α receptors 1 and 2 (TNF-R1, TNF-R2) in this system by immunohistochemistry (TNFR1, sc-1070; TNFR2, sc-1074: Santa Cruz Biotechnology, Santa Cruz, CA). We found both receptor types to be condensed on the neurons as well as most glial cells (data not shown).

Pharmacological Treatment of Septo-Hippocampal Cells

TNF-α. Ten-day-old septo-hippocampal cultures were challenged with 0.3–500 ng/mL of TNF-α and 3 ng/ml of Act

D in DMEM-DM and cell viability was monitored at various postinjury time points. Cultures were exposed to TNF-α and Act D for the entire duration of each experiment. Coadministration of Act D (3 ng/ml) has been reported to enhance TNF-α induced cell death (Ruff anf Gifford, 1981), we therefore have treated parallel cultures with Act D, alone for the entire period of the experiment. Act D (3 ng/ml) alone had no effect on LDH release in septo-hippocampal cultures (data not shown). Following TNF-α challenge, cells were fixed for staining or protein was isolated and DNA extraction performed.

Calpain, caspase and protein synthesis inhibitors. Sister cultures were pretreated with either 25–50 μM calpain inhibitor-II (CalpInh-II), 30–140 μM of the pan-caspase inhibitor (Z-D-DCB), or 1 μg/mL of the protein synthesis inhibitor, cycloheximide (Sigma) 1 hr prior to TNF-α challenge. The inhibitor concentrations used have been previously shown to provide optimal inhibition of calpains (Pike et al., 1998; Kampfl et al., 1996), caspase-3 (Nath et al., 1996; Pike et al., 1998), and protein synthesis (Pike et al., 1998; Koh et al., 1995; Martin et al., 1988). In addition, other experiments in our laboratory have independently confirmed that these doses of CalpInh-II and Z-D-DCB antagonize calpain and caspase-3 activation accompanying staurosporine-induced apoptosis in septo-hippocampal cultures (Pike et al., 1998).

Morphological and Enzymatic Assessments of Cell Damage and Cell Death

Morphological assessments of cell injury and necrotic and apoptotic cell death phenotypes are controversial (Zhao et al., 1999). We have used multiple morphological criteria to examine cell injury and cell death phenotype.

Fluorescein diacetate and propidium iodide assay of cell viability. Fluorescein diacetate (FDA) and propidium iodide (PI) dyes were used to assess cell viability after TNF-α incubation. FDA enters normal cells and emits a green fluorescence when it is cleaved by esterases. Once cleaved, FDA can no longer permeate cell membranes. Propidium iodide is an intravital dye that is normally excluded from cells. After injury, PI penetrates cells and binds to DNA in the nucleus and emits a red fluorescence. This technique is commonly used to quantitate cell injury (Jones and Senft, 1985). As per Jones and Senft (1985), a stock solution of FDA (20 mg/mL) was dissolved in acetone. A PI stock solution was prepared by dissolving 5 mg/mL in phosphate-buffered saline (PBS). The FDA and PI working solutions were freshly prepared by adding 10 μL of the FDA and 3 μL of PI stock to 10 mL of PBS. Two hundred microliters per well of FDA-PI working solution were added directly to the cells, the cells were stained for 3 min at room temperature. Stained cells were observed and photographed with a fluorescence microscope equipped with epi-illumination, band pass 450–490 nm exciter filter, 510 nm chromatic beam splitter, and a long pass 520 nm barrier filter. This filter combination permitted both green and red fluorescing cells to be seen simultaneously.

Hoechst staining of apoptotic nuclei. The A-T base-pair-specific dye, Hoechst 33258 (bis-benzimide; Sigma) was used to stain cell nuclei for characterization of cell death phenotype. Following overnight fixation in 4% paraformaldyhide at 4°C, cells grown on German glass were washed three times with PBS and labeled with 1 μg/mL of the DNA dye Hoechst 33258 in PBS for 5–10 min at room temperature, using enough solution to cover the cells completely. The cells were rinsed twice with PBS and then mounted with Crystal-mount medium (Biomeda, Foster City, CA). Cells were observed and photographed on a phase contrast and fluorescence microscope with a UV2A filter.

LDH assay. This colorimetric assay quantifies cell death based on the measurement of lactate dehydrogenase (LDH) activity released from the cytosol of damaged cells into the supernatant. After TNF-α challenge, 300 μL of culture medium was collected from each well and centrifuged at 1,000 rpm for 5 min. 100 μL of supernatant was collected from each sample, and transferred to a 96-well flat bottom plate. One hundred μL of LDH (Boehringer Cat. 1 664 793) was mixed with the sample and incubated for 30 min at room temperature. A plate reader (Bio-Rad Model 450 Microplate Reader, Richmond, CA) measured the absorbance of each sample at 490 nm with a reference wavelength of 650 nm. Absorbency values were analyzed by analysis of variance (ANOVA) with Post-hoc comparisons and values were expressed as percent of control.

DNA fragmentation assay. DNA gel electrophoresis was performed as described in Gong et al. (1994). Briefly, cells were collected in the same manner as for immunoblotting. Cells in each treatment condition were collected by centrifugation and fixed in suspension in 70% cold ethanol and stored in fixative at 20°C (24–72 hrs). Cells were then centrifuged at 800 g for 5 min and ethanol was thoroughly removed. Cell pellets were resuspended in 40 μL of phosphate-citrate (PC) buffer consisting of 192 parts of 0.2 M Na_2HOP_4 and 8 parts of 0.1 M citric acid (pH 7.8) at room temperature for 1 hr. After centrifugation at 1,000 g for 5 min, the supernatant was transferred to new tubes and concentrated by vacuum in a SpeedVac concentrator for 15–30 min. Three μL of 0.25% Nonidet NP-40 in distilled water was added followed by 3 μL of DNase-free RNase (1 mg/mL). After 30 min incubation at 37°C, 3 μL of proteinase K (1 mg/mL) was added and the extract was incubated for additional 30 min at 37°C. After the incubation, 1 μL of 6× loading buffer (0.25% bromophenol blue, 0.25% xylene cyanol FF, 30% glycerol in water) was added and the entire content of the tube was transferred to a 1.5% agarose gel and electrophoresis was performed in 1× TBE (0.1 M Tris, 0.09 M boric acid, 1 mM EDTA, pH 8.4) at 40 V for 2 hr. The DNA in the gels was visualized and photographed under UV light after staining with 5 μg/mL of ethidium bromide.

Assessment of α-Spectrin Degradation by Calpains and Caspase-3

Sodium dodecylsulfate-polyacrylamide gel electrophoresis (SDS-PAGE) and immunoblotting. Because α-spectrin contains sequence motifs preferred by both calpains and caspase-3 proteases, activation of these two families of cysteine proteases can be assessed concurrently by immunoblot identification of calpain and/or caspase-3 signature cleavage products (Nath et al., 1996; Wang et al., 1998). N-terminal sequencing of the major α-spectrin fragments has confirmed specific calpain and caspase-3 target sites for the 145-kDa and 120-kDa fragments, respectively (Wang et al., 1998). Calpain has a high affinity for two sites on the native 280-kDa α-spectrin

protein. Following calpain activation, intact α–spectrin (280 kDa) is proteolyzed into distinct 150-kDa and 145-kDa fragments detected on immunoblots. The first site is rapidly attacked following calpain activation resulting in a 150-kDa spectrin breakdown product (BDP). Further calpain processing of 150-kDa BDPs at the N-terminal yields a calpain-specific 145-kDa BDP (Nath et al., 1995, 1996; Wang et al., 1998). Caspase-3 cleaves intactα-spectrin to produce 150-kDa BDPs with a different N-terminal from the calpain-generated fragments. Further processing of the caspase-3-generated 150-kDa fragment results in a unique caspase-3-specific 120-kDa BDP (Wang et al., 1998). Moreover, the 120-kDa fragment has been shown to be associated with caspase-3 activation in various in vitro systems of apoptosis (Nath al., 1995, 1996; Pike at al., 1998; Wang et al., 1998).

Cells were lysed in ice-cold homogenization buffer (20 mM PIPES, pH 7.6, 1 mM EDTA, 2 mM EGTA, 1 mM DTT, 0.5 mM PMSF, 50 μg/mL Leupeptin, and 10 μg/mL of AEBSF, apotinin, pepstatin, TLCK, and TPCK) for 30 min, then sheared through a 1.0-mL syringe with a 25-gauge needle 15 times. Protein content in the samples was assayed by the Micro BCA method (Pierce, Rockford, IL). For protein electrophoresis, equal amounts of total protein (30 μg) were prepared in two fold loading buffer containing 0.25 M Tris (pH 6.8), 0.2 M DTT, 8% SDS, 0.02% Bromophenol Blue, and 20% glycerol, and heated at 95°C for 10 min. Samples were resolved in a vertical electrophoresis chamber using a 4% stacking gel over a 7% acrylamide resolving gel for 1 hr at 200 V. For immunoblotting, separated proteins were laterally transferred to nitrocellulose membranes (0.45 μM) using a transfer buffer consisting of 0.192 M glycine and 0.025 M Tris (pH 8.3) with 10% methanol at a constant voltage (100 V) for 1 hr at 4°C Coomassie Blue and Panceau Red (Sigma) were used to stain gels and nitrocellulose membranes, respectively, to confirm that equal amounts of protein were loaded in each lane.

Immunoblots were probed with an anti-α-spectrin monoclonal antibody (Afiniti Research Products, U.K.; Cat. FG 6090, clone AA6) that detects intact α-spectrin (280 kDa) and 150-, 145-, and 120-kDa SBDPs. Following incubation with the primary antibody (1:4,000) for 2 hr at room temperature, the blots were incubated in peroxidase-conjugated sheep anti-mouse 1gG (Cappel) for 1 hr (1:10,000). Enhanced chemiluminescence reagents (ECL, Amersham, Arlington Heights, IL) were used to visualize the immunolabeling on Hyperfilm (Hyperfilm ECL, Amersham).

Statistical analyses.   Each experiment was performed three times and data was evaluated by ANOVA with a post-hoc Tukey test. Values are given as mean ± S.E.M. Differences were considered significant if $P < 0.05$.

RESULTS

Effects of TNF-α on Septo-Hippocampal Glial-Neuronal Cocultures

Dose- and time-dependent cell death.   An initial dose-response assay was performed to determine the best concentration of TNF-α for all subsequent experiments. LDH release was used to quantify cell death, based on the measurement of LDH activity released from the cytosol of damaged cells into the supernatant. Exposure of septo-hippocampal cultures to 0.3–500 ng/mL TNF-α alone produced minimal toxicity (data not shown); however, with the addition of Act D, toxicity was significant. TNF-α with 3 ng/ml of Act D induced dose-dependent cell death (Fig. 1A). Three ng/ml of Act D did not significantly produce cell death compared with media control at any exposure duration (data not shown). Concentrations of TNF-α between 30 and 500 ng/ml produced approximately equivalent levels of cell death. Thus, the dose of 30 ng/mL was used for all subsequent experiments. The percent of LDH release following exposure to 30 ng/mL of TNF-α compared to control was 167%, 261%, 319%, 383%, and 573% at 3.5 hr, 7 hr, 48 hr, and 72 hr, respectively (Fig. 1B).

Morphological response to TNF-α challenge. TNF-α-treated septo-hippocampal cultures underwent morphological alterations in cell structure that were characteristic of apoptosis. Within 3.5 hr after incubation with 30 ng/mL of TNF-α, PI Molecular Probes, Eugene, OR) was taken up by cells and became even more apparent at 7 hr, 24 hr, and 72 hr after injury (Fig. 2B vs. C–E). In addition, nuclei stained with PI appeared shrunken and irregularly shaped. FDA indicated appearance of membrane blebbing by 3.5 hr that became more evident at 7 hr. By 24–72 hr, the plasma membrane integrity was lost and FDA staining was lost, giving way to nuclear PI staining (Fig. 2A vs. B– E).

To further characterize cell death characteristics of TNF-α toxicity in septo-hippocampal cultures, Hoechst 33258 was used to stain nuclear chromatin (Fig. 3). Treatment with TNF-α (30 ng/ml) and Act D produced irregularly shaped nuclei (Fig. 3B,G) as early as 3.5 hr. Chromatin of TNF-α-treated cells appeared condensed with smaller and brighter Hoechst staining. Formation of apoptotic nuclei changes are evident by 7 hr (Fig. 3C,H) and became more clear by 24 hr (Fig. 3D,I). Apoptotic bodies were scattered throughout every field of view by 72 hr (Fig. 3E, J).

DNA fragmentation.   Condensation and aggregation of chromatin at the nuclear membrane may occur independently of endonuclease activation (Oberhammer et al., 1993). Thus, a DNA fragmentation assay was used to determine whether DNA alterations in septo-hippocampal cultures assessed by Hoechst 33258 were associated with endonuclease activity. Figure 4 shows that TNF-α (30 ng/mL) with 3 ng/ml of Act D induced detectable DNA laddering on agarose gels, most apparent at 24 hr following treatment. However, gels showed substantial smearing even at 24 hr, indicating random DNA fragmentation characteristic of necrosis.

Caspase-3 but not Calpain Proteolysis of α-Spectrin

Exposure to 30 ng/ml of TNF-α caused a time dependent proteolysis of by caspase-3 but not calpain proteases (Fig. 5). There was a significant increase in caspase-3-specific 120- kDa breakdown products to α-spectrin as early as 3.5 hr following TNF-α administra-

A.

Dose Curve (24h)

B.

Time Course (30ng/ml)

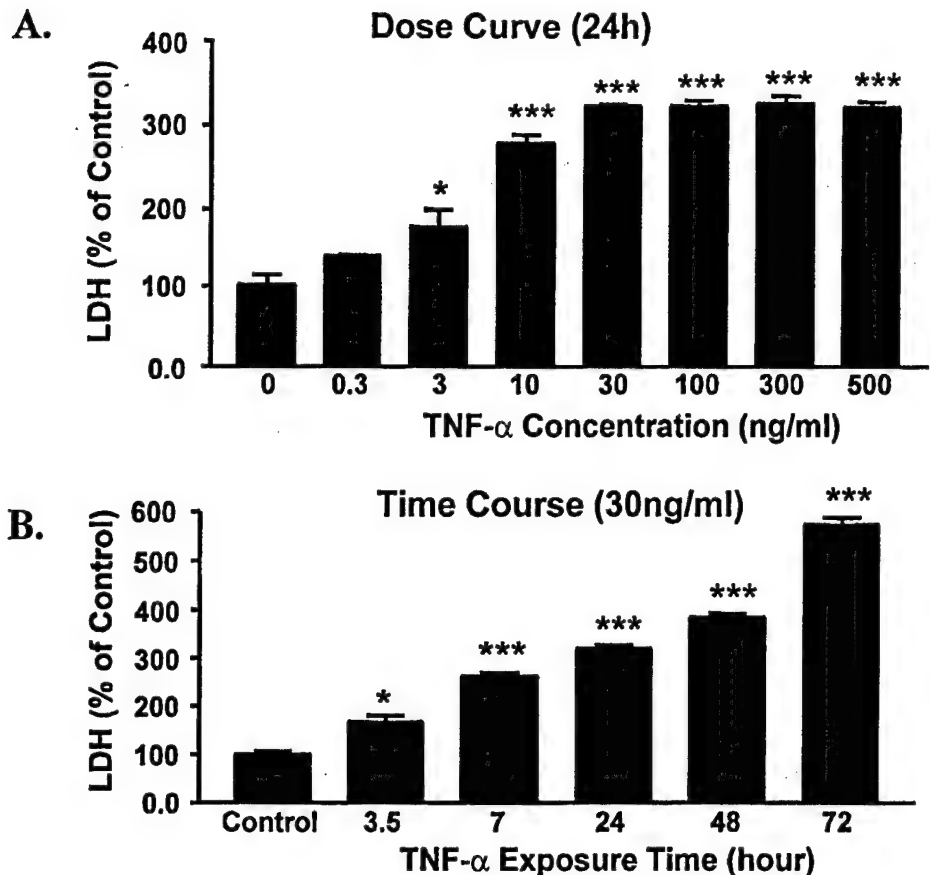
Fig. 1. Concentration and time course assays of tumor necrosis factor (TNF-α)-induced lactate dehydrogenase (LDH) release. **A:** Primary septo-hippocampal cultures were exposed to various doses of exogenous TNF-α (0.3–500 ng/ml) for 48 hr. Release of LDH was measured for each treatment condition and was expressed as mean percentages, ±S.E.M., of control. **B:** Percentage of control of LDH release to the media following addition of 30 ng/ml of TNF-α for 1 hr to 48 hr. Data are expressed as mean percentages, ± S.E.M., of control. *P < 0.005, ***P < 0.001.

tion. Over the next 72 hr, a further increase in the accumulation of caspase-3-specific 120-kDa breakdown product of α-spectrin was more evident. In contrast, there was no evidence of accumulation of calpain-specific 145-kDa SBDP at any time point after TNF-α treatment.

Effects of CalpInh-II, Z-D-DCB, or Cycloheximide on TNF-α-Induced Cell Death and α-Spectrin Proteolysis

To investigate the relative contribution of calpain and/or caspase-like proteases to TNF-α-induced cell death and α-spectrin proteolysis, the effect of a calpain inhibitor (CalpInh-II) and a pan caspase inhibitor (Z-D-DCB) were examined. Since de novo protein synthesis is required for at least some forms of apoptosis and specifically for staurosporine-induced apoptosis in septo-hippocampal cultures, the effects of a nonselective inhibitor of protein synthesis (cycloheximide) were also examined.

Cell viability measurements. LDH assay was used to assess cell viability at 7 hr following TNF-α and/or administration of CalpInh-II, Z-D-DCB, or cycloheximide (Fig. 6B). Seven hrs after administration of 30 ng/ml of TNF-α with 3 ng/ml of Act D, LDH release increased to 261.4% over control. Administration of Z-D-DCB (30, 100, 140 μM) significantly reduced the percentage of

LDH release to 183.1%, 175.0%, and 156.0%, respectively. CalpInh-II (37.5, 50 μM) had no protection against LDH release (268.3%, 278.3%, respectively; Fig. 6B). Cycloheximide (1 μg/ml) had the greatest effect against LDH release (137.0%) following 7 ht of TNF-α treatment.

α-spectrin proteolysis. Administration of Z-D-DCB or cycloheximide with TNF-α stimulation significantly decreased the accumulation of the 120-kDa caspase specific breakdown product of α-spectrin (Fig. 6A). In contrast, CalpInh-II did not provide any protection against proteolysis of α-spectrin. The results of these experiments confirm that caspase-3 but not calpain was activated after TNF-α stimulation in primary septo-hippocampal cultures.

DISCUSSION

Although caspases 8 and 3 were shown to mediate TNF-α-induced apoptosis in neutrophils (Yamashita et al., 1999), this study is the first demonstration that TNF-α induces activation of caspase-3 in a mixed neuro-glial culture system. Importantly, these results indicate that TNF-α may play an important role as an effector of receptor-mediated apoptotic cell death in the CNS. Characterization of apoptotic cell death responses to TNF-α in primary septo-hippocampal cultures is an important feature of this study since TNF-α protein is expressed in the
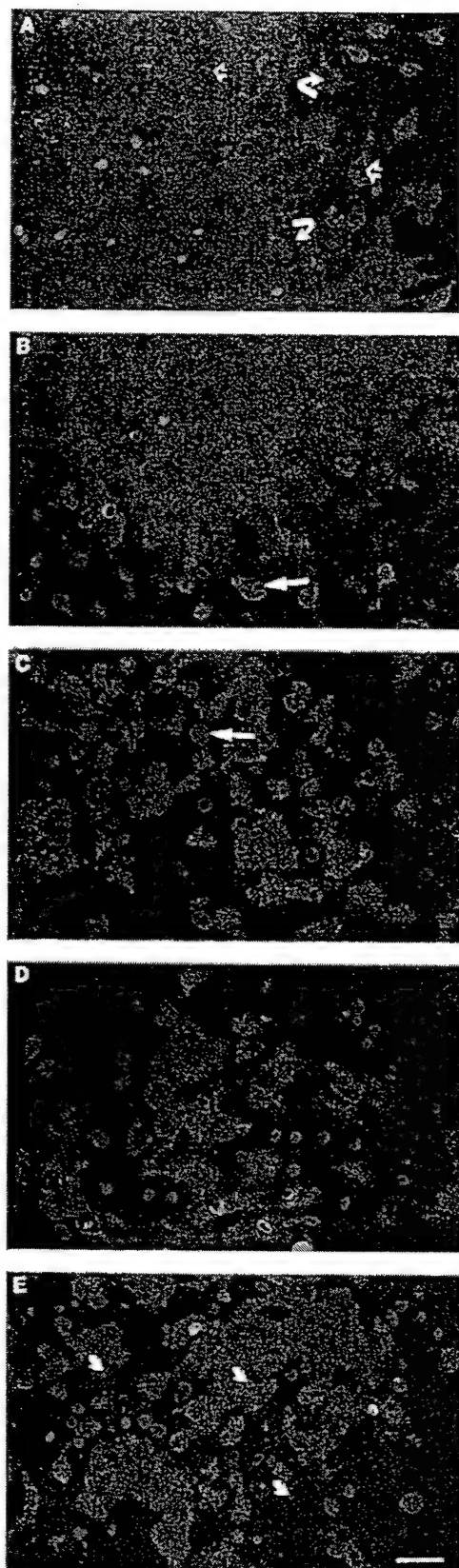
Figure 2.

hippocampus during various CNS injuries in vivo, including cerebral ischemia (Gong et al., 1998), traumatic brain injury (Shohami et al., 1997), and epilepsy (de Bock et al., 1996). Thus, primary septo-hippocampal cell cultures can provide an efficient in vitro tool for investigation of cellular and molecular mechanisms underlying apoptotic cell death relevant to in vivo CNS neuropathologies. Since Act D alone did not affect the viability of septo-hippocampal cell cultures, as assessed by LDH release, it is unlikely that Act D significantly contributed to the cell death profile observed in these studies.

Characterization of TNF-α-Induced Apoptotic Cell Death

In mixed primary septo-hippocampal cultures, TNF-α (0.3–500 ng/ml) produced apoptotic cell death characterized by the appearance of membrane blebbing, shrunken condensed nuclei, uneven distribution of DNA staining, formation of apoptotic bodies, and DNA fragmentation. These are typical phenotypic characteristics of apoptosis (Wyllie et al., 1980). Additionally, cell death was significantly prevented by the broad range protein synthesis inhibitor, cycloheximide. We have previously shown that protein synthesis is a requirement for caspase-3 activation and apoptotic cell death in this same culture system during staurosporine induced apoptosis (Pike et al., 1998). Cycloheximide is thought to protect cells from apoptosis through inhibition of de novo protein synthesis of pro-apoptotic proteins that are up-regulated during apoptosis (Koh et al., 1995; Pike et al., 1998). However, neuroprotective concentrations of cycloheximide can induce expression of the anti-apoptotic gene product Bcl-2 in hippocampal cell cultures (Furukawa et al., 1997). Further research is required to elucidate the role of transcriptional and translational regulators on apoptotic cascades. Although calpain activation can contribute to staurosporine-induced apoptotic cell death in septo-hippocampal cell cultures (Pike et al., 1998), calpain inhibition had no effect on TNF-α-induced cell death in the present model. TNF-α induced caspase-3 but not calpain proteolysis of α-spectrin during apoptotic cell death in septo-hippocampal culture.

The cytoskeletal protein α-spectrin is a preferred substrate of calpain and caspase-3 cysteine proteases. Ter-

Fig. 2. Fluorescein diacetate (FDA) and propidium iodide (PI) staining of septo-hippocampal cultures treated with TNF-α and actinomycin D. A: Control cultures demonstrate normal somal integrity and lack of nuclear PI uptake. Note confluent astroglial cell layer (curved arrows) beneath mature neuronal cell phenotypes (open arrows). Cells were treated with TNF-α for 3.5 (B), 7 (C), 24 (D), or 72 (E) hr. By 3.5 hr, some cells have lost retention of FDA and bind PI to their nucleus, thus indicating cell death. Membrane blebbing is observed (B, arrow), indicating a preserved integrity of the plasma membrane characteristic of apoptosis. After 7 hr of TNF-α treatment, an increase in the number of PI-stained nuclei is observed. In addition, membrane blebbing is more evident. After 24 (D) and 72 (E) hr of TNF-α treatment, the majority of cell nuclei are stained with PI and appear shrunken (curved arrows in E) compared to those observed at 3.5 hr (B). Scale bar = 10 μM.
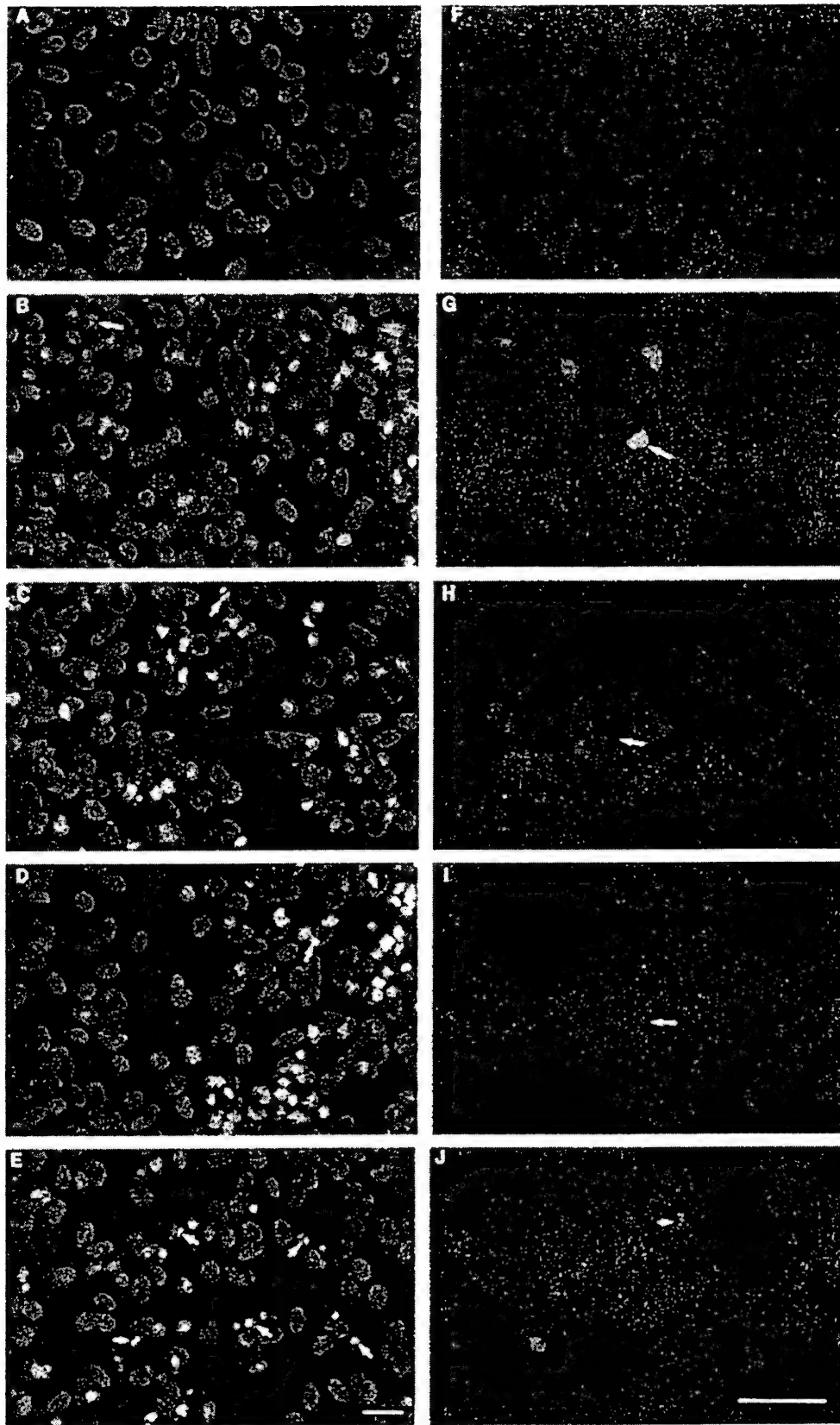
Fig. 3. Course of nuclear morphologic alterations during exogenous TNF-α–induced apoptosis detected by Hoechst 33258 staining. **A,F:** Control cultures. Cells were treated with 30 ng/ml of TNF-α and Actinomycin D for 3.5 (**B,G**), 7 (**C,H**), 24 (**D,I**), or 72 (**E,J**) hr. TNF-α-treated cells possess irregularly shaped nuclei with condensed chromatin, which are brightly stained with Hoechst (B,G–I, arrows). While some characteristic apoptotic nuclear changes such as nuclear membrane breakdown and formation of apoptotic bodies was evident as early as 7 hr (C, arrow), widespread apoptotic bodies (E, J, arrows) were not evident until 72 hr following TNF-α treatment. Scale bars = 10 μM.
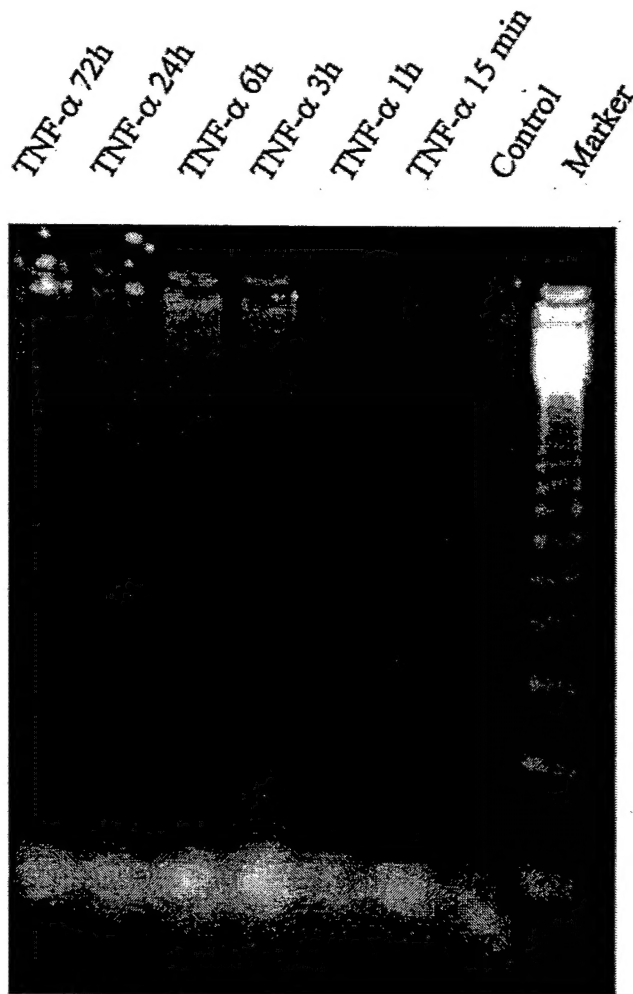
Fig. 4. Oligonucleosomal size fragmentation of DNA produced by TNF-α on septo-hippocampal cultures. TNF-α (30 ng/mL) induced readily apparent DNA laddering on agarose gels at 24 hr, and faint DNA laddering at 6 hr and 72 hr, but none at 15 min, 1 hr, or 3 hr following treatment.

minal sequencing of the major α-spectrin fragments has confirmed specific calpain and caspase-3 target sites for the 145-kDa and 120-kDa fragments, respectively (Wang et al., 1998). The distribution of calpain and caspases acting on α-spectrin to produce a calpain-specific 145-kDa fragment and an apoptotic-linked caspase-specific 120-kDa fragment during neuronal apoptosis and necrosis has been well characterized (Pike et al., 1998; Zhao et al., 1999; Nath et al., 1995). Our data did not show any 150-kDa and 145-kDa SBDPs, only the 120-kDa SBDP which appeared as early as 3.5 hr after the treatments and lasted over the 72 hr. These data supports the activation of caspase-3 and not calpain.

Effects of Calpain and Caspase Inhibitors on TNF-α-Induced Apoptosis

The pan-caspase inhibitor Z-D-DCB but not calpain inhibitor CalpInh-II attenuated cell death. Importantly, we confirmed that the dose of Z-D-DCB used in this study inhibited caspase-3 activation inferred by decreased proteolysis of α-spectrin. Reduced cell death produced by Z-D-DCB suggests that TNF-α-induced apoptosis in septo-hippocampal cultures is at least partially attributable to caspase-3 activation. In models of ischemia and status epilepticus, caspase-3 inhibitors have decreased apoptosis, loss of neurons, and ameliorated neurologic deficits (Kondratyev and Gale, 2000; Weissner et al., 2000; Endress et al., 1998; Gillardon et al., 1999). However, caspase-3 inhibition only partially reduced cell death, indicating that non-caspase-3-dependent pathways could also be activated, or that caspase-3 activation may be associated with other cellular pathways. For example, Miossec et al. (1997) demonstrated that caspase-3 (CPP32) processing could be a physiological step during T lymphocyte activation, independent of apoptosis.

A receptor-mediated pathway can trigger caspase-3 activation (for review, see Goeddel, 1999; Ksontini et al., 1998). Most cell types, including neural cells, express TNF-α receptor 1 (TNFR1; 55 kDa) which is activated by soluble TNF-α. Apoptosis through TNF-R2 appears
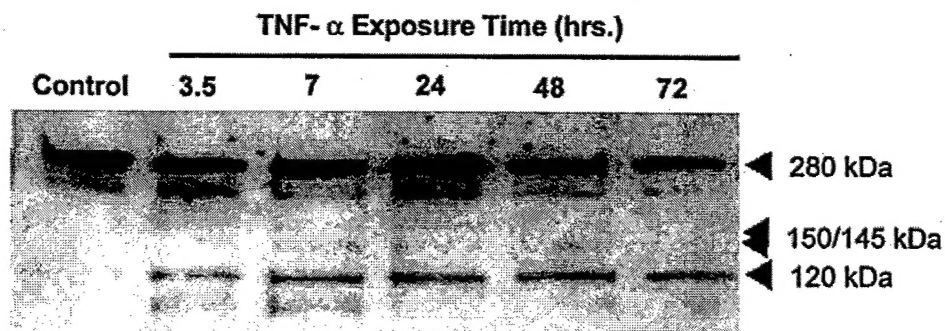
TNF-α Exposure Time (hrs.)

Fig. 5. TNF-α produced caspase-3-specific but not calpain-specific α-spectrin breakdown products (BDPs). Western blots examining proteolysis of α-spectrin into 150-kDa, calpain-specific 145-kDa, and caspase 3-specific 120-kDa BDPs detected after 3 hr, 7 hr, 24 hr, and 72 hr following TNF-α (30 ng/ml) with 3 ng/ml of Actinomycin D treatment. TNF-α treatment produced no increases in calpain-specific 145-kDa BDPs, but caused a marked increase in the caspase-3-specific 120-kDa BDP.

Fig. 6. TNF-α produced caspase-3 but not calpain protease activation associated with LDH release. **A:** Western blots examine proteolysis of α-spectrin into 150-kDa, calpain-specific 145-kDa, and caspase-3-specific 120-kDa breakdown products. Accumulation of 120-kDa breakdown products to α-spectrin was seen 7 hr following TNF-α treatment (30 mg/ml), as compared to untreated controls. TNF-α treatment produced no increases in 150-kDa and 145-kDa BDPs. Administration of carbobenzosy-Asp-CH₂-OC (O)-2-6-dichlorobenzene (Z-D-DCB) or cycloheximide (CHX) markedly decreased accumulation of 120-kDa breakdown products to α-spectrin. Calpain inhibitor II had no effect on α-spectrin processing. **B:** LDH release (percentage of untreated controls) was calculated 7 hr after administration of TNF-α (30 mg/ml) or coadministration of caspase inhibitor, Z-D-DCB (50 μM, 100 μM), the protein synthesis inhibitor cycloheximide (1 μg/ml), or the calpain inhibitor, calpain inhibitor II (25 μM, 37.5 μM). Z-D-DCB and cycloheximide, but not calpain inhibitor II, significantly decreased LDH release induced by TNF-α (**P < 0.01, ***P < 0.001).
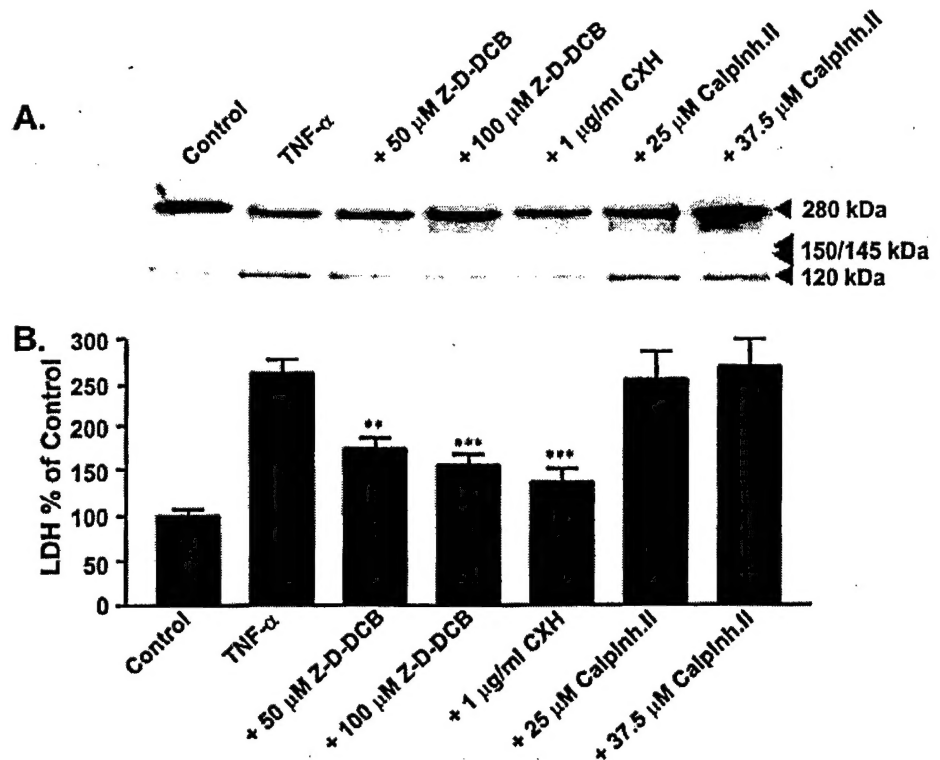
to signal through a different pathway involving induction of sphingomyelinases (Grell et al., 1994). TNF-R1, when activated, recruits TRADD (TNF-associated Death Domain protein) and RIP (Receptor Interacting Protein). TRADD can interact with TRAF2 (TNF-associated factor 2) or with another adapter protein, FADD (Fas associating protein with Death Domain; Ashkenazi and Dixit, 1998; Goeddel, 1999). A TRADD-FADD-caspase-8/10 interaction has been reported to produce the autolytic activation of caspase-8/10, which in turn processes and activates the common apoptosis mediator, caspase-3 (Villa et al., 1997). In the present study, we report on the cytotoxic effect of TNF-α on septo-hippocampal cell culture, which contained both astrocytes and neurons. Taken from a brain area which is vulnerable to ischemic and traumatic injury, this mixed culture is a highly relevant model to investigate the role of TNF-α in the pathophysiology of brain injury. The question of whether this cytokine is toxic or protective in the injured brain has been raised in numerous publications in the past decade. Contradiction appears in the literature between reports on protective effects of anti- TNF-α agents, and the deleterious effects of TNF-α receptor knockouts in models of cerebral ischemia and trauma (for review, see Shohami et al., 1999). The present study sheds light on the toxic role TNF-α might play, within the first days after exposure to higher than normal physiologic levels of TNF-α, by activating apoptotic response. In contrast, Barger et al. (1995) demonstrated that TNF-α is protective against iron

and amyloid-β peptide in cultured hippocampal and neocortical astrocytes 1995, and Mattson et al. (1995) showed protective effects of TNF-α under conditions of glucose deprivation and glutamate toxicity. These authors have demonstrated up-regulation of calbindin and of MnSOD in response to exposure to TNF-α. The difference between the various experimental paradigms, namely, different cell types, different insults and time of exposure, may explain the difference between the role TNF-α plays under these conditions. In conclusion, we propose that under the experimental conditions employed in the present study, TNF-α is pro-apoptotic and therefore, its inhibition in the acute postinjury phase may be beneficial.

REFERENCES

Aggarwal S, Gollapudi S, Gupta S. 1999. Increased TNF-alpha-induced apoptosis in lymphocytes from aged humans: changes in TNF-alpha receptor expression and activation of caspases. J Immunol 162:2154–2161.

Armstrong RC, Aja T, Xiang J, Gaur S, Krebs JF, Hoang K, Bai X, Korsmeyer SJ, Karanewsky DS, Fritz LC, Tomaselli KJ. 1996. Fas-induced activation of the cell death-related protease CPP32 is inhibited by Bcl-2 and by ICE family protease inhibitors. J Biol Chem 271:16850–16855.

Ashkenazi A, Dixit VM. 1998. Death receptors: signaling and modulation. Science 281:1305–1308.

Barger SW, Hoster D, Furukawa K, Goodman Y, Krieglstein J, Mattson MP 1995. Tumor necrosis factors alpha and beta protect neurons against amyloid beta-peptide toxicity: evidence for involvement of a kappa B-binding factor and attenuation of peroxide and Ca²⁺ accumulation. Proc Natl Acad Sci USA 92:9328–9332.

Barone FC, Arvin B, White RF, Miller A, Webb CL, Willette RN, Lysko PG, Feuerstein GZ. 1997. Tumor necrosis factor-alpha: a mediator of focal ischemic brain injury. Stroke 28:1233–1244.

Bruce AJ, Boling W, Kindy MS, Peschon J, Kraemer PJ, Carpenter MK, Holtsberg FW, Mattson MP. 1996. Altered neuronal and microglial responses to excitotoxic and ischemic brain injury in mice lacking TNF-α receptors. Nature Med 2:788–795.

Buttini M, Appel K, Sauter A, Gebicke-Haerter PJ, Boddeke HM. 1996. Expression of tumor necrosis factor alpha after focal cerebral ischemia in the rat. Neuroscience 71:1–16.

Cheng B, Christakos S, Mattson MP. 1994. Tumor necrosis factors protect neurons against metabolic-excitotoxic insults and promote maintenance of calcium homeostasis. Neuron 12:139–153.

Chung IY, Benveniste EN. 1990. Tumor necrosis factor alpha production by astrocytes. Induction by lipopolysaccharide, interferon gamma and interleukin-1-beta. J Immunol 144:2999–3007.

Dawson D, Martin D, Hallenbeck JM. 1996. Inhibition of tumor necrosis factor-alpha reduces focal cerebral ischemic injury in the spontaneously hypertensive rat. Neurosci Lett 218:41–44.

de Bock F, Dornand J, Rondouin G. 1996. Release of TNF-alpha in the rat hippocampus following epileptic seizures and excitotoxic neuronal damage. Neuroreport 7:1125–1129.

Eldadah BA, Yakovlev AG, Faden AI. 1997. The role of CED-3-related cysteine proteases in apoptosis of cerebellar granule. J Neurosci 17:6105–6113.

Endres M, Namura S, Shiimizu-Sasamata M, Waeber C, Zhang L, Gomez-Isla T, Hyman BT, Moskowitz MA. 1998. Attenuation of delayed neuronal death after mild focal ischemia in mice by inhibition of the caspase family. J Cereb Blood Flow Metab 18:238–247.

Fan L, Young PR, Barone FC, Feuerstein GZ, Smith DH, McIntosh TK. 1996. Experimental brain injury induces differential expression of tumor necrosis factor-α mRNA in the CNS. Mol Brain Res 36:287–291.

Fillit H, Ding W, Buee L, Kalman J, Altstiel L, Lawlor B, Wolf-Klein G. 1991. Elevated circulating tumor necrosis factor levels in Alzheimer's disease. Neurosci Lett 131:318–320.

Fraser A, Evan G. 1996. A license to kill. Cell 85:781–784.

Furukawa K, Estus S, Fu W, Mattson MP. 1997. Neuroprotective action of cyclohexamide involves induction of Bcl-2 and anti-oxidant pathways. J Cell Biol 136:1137–1150.

Garcia JE, Nonner D, Ross D, Barrett JN. 1992. Neurotoxic components in normal serum. Exp Neurol 118:309–316.

Gary DS, Bruce-Keller AJ, Kindy MS, Mattson MP. 1998. Ischemic and excitotoxic brain injury is enhanced in mice lacking the p55 tumor necrosis factor receptor. J Cereb Blood Flow Metab 18:1283–1287.

Gelbard HA, Dzenko KA, DiLoreto D, del Cerro C, del Cerro M, Epstein LG. 1993. Neurotoxic effects of tumor necrosis factor alpha in primary human neuronal cultures are mediated by activation of the glutamate AMPA receptor subtype: implications for AIDS neuropathogenesis. Dev Neurosci 15:417–422.

Gillardon F, Kiprianova I, Sandkuhler J, Hossman KA, Spranger M. 1999. Inhibition of caspases prevents cell death of hippocampal CA1 neurons, but not impairment of hippocampal long-term potentiation following ischemia. Neuroscience 93:1219–1222.

Goeddel DV. 1999. Signal transduction by tumor necrosis factor. Chest 116:69S–73S.

Gong C, Qin, Z, Bet AL, Liu X, Yang G. 1998. Cellular localization of tumor necrosis factor-alpha following focal cerebral ischemia in mice. Brain Res 801:1–8.

Gong J, Traganos F, Dzrzynkiewicz Z. 1994. A selective procedure for DNA extraction from apoptotic cells applicable for gel electrophoresis and flow cytometry. Analyt Biochem 218:314–319.

Grell M, Zimmermann G, Husler D, Pfizenmaier K, Scheurich P. 1994. TNF receptors TR60 and TR80 can mediate apoptsis via induction of distinct signal pathways. J Immunol 153:1963–1972.

Jones KH, Senft AJ. 1985. An improved method to determine cell viability by simultaneous staining with fluorescein diacetate-propidium iodide. J Histochem Cytochem 33:77–79.

Kampfl A, Zhao X, Whitson JS, Posmantur R, Dixon CE, Yang K, Clifton GL, Hayes RL. 1996. Calpain inhibitors protect against depolarization induced neurofilament protein loss of septo-hippocampal neurons in culture. Eur J Neurosci 8:344–352.

Kampfl A, Posmantur RM, Zhao X, Schmutzhard E, Clifton GL, Hayes RL. 1997. Mechanisms of calpain proteolysis following traumatic brain injury: implications for pathology and therapy: a review and update. J Neurotrauma 14:121–134.

Knoblach SM, Fan L, Faden AI. 1999. Early neuronal expression of tumor necrosis factor-alpha after experimental brain injury contributes to neurological impairment. J Neuroimmunol 95:115–125.

Koh J, Wie MB, Gwag BJ, Sensi SL, Canzoniero MT, Demaro J, Csernansky C, Choi DW. 1995. Staurosporine-induced neuronal apoptosis. Exp Neurol 135:153–159.

Kondratyev A, Gale K. 2000. Intracerebral injection of caspase-3 inhibitor prevents neuronal apoptosis after kainic acid-evoked status epilepticus. Brain Res Mol Brain Res 75:216–224.

Ksontini R, MacKay SLD, Moldawer LL. 1998 Revisting the role of tumor necrosis factor alpha and the response to surgical injury and inflammation. Arch Surg 133:558–567.

Leker R, Shohami E, Abramsky O, Ovadia H. 1999. Dexanabinol: a novel neuroprotective drug in experimental focal cerebral ischemia. J Neurol Sci 162:114–119.

Lieberman AP, Pitha PM, Shin HS, Shin MN. 1989. Production of tumor necrosis factor and other cytokines by astrocytes stimulated with lipopolysaccharide or neurotropic virus. Proc Nat Acad Sci USA 86:6348–6352.

Liu T, Clark RK, McDonnell PC, Young PR, White RF, Brone FC, Feuerstein GZ. 1994. Tumor necrosis factor alpha expression in ischemic neurons. Stroke 25:1481–1488.

Martin DP, Schmidt RE, DiStefano PS, Lowry OH, Carter JG, Johnson EM. 1988. Inhibitors of protein synthesis and RNA synthesis prevent neuronal death caused by nerve growth factor deprivation. J Cell Biol 106:829–844.

Mattson MP, Lovell MA, Furukawa K, Markesbery WR. 1995. Neurotrophic factors attenuate glutamate-induced accumulation of peroxides, elevation of Ca^{2+} and neurotoxicity, and increase antioxidant enzyme activities in hippocampal neurons. J Neurochem 65:1740–1751.

Meirstrell ME 3rd, Botchkina GI, Wang H, Di Snato E, Cockroft KM, Bloom O, Vishnubhakat JM, Ghezzi P, Tracey KJ. 1997. Tumor necrosis factor is a brain damaging cytokine in cerebral ischemia. Shock 8:341–348.

Miossec C, Dutilleul V, Rassy F, Diu-Hercend A. 1997. Evidence for CPP32 activation in the absence of apoptosis during T lymphocyte stimulation. J Biol Chem 272:13489–62.

Miura M, Zhu H, Rotello R, Hartwieg EA, Yuan J. 1993. Induction of apoptosis in fibroblasts by IL-1 beta-converting enzyme, a mammalian homolog of the C. elegans cell death gene ced-3. Cell 75:653–660.

Mogi M, Harada M, Kondo T, Reiderer P, Nagatsu T. 1994. Tumor necrosis factor-alpha increases both in the brain and in the cerebrospinal fluid from parkinsonian patients. Neurosci Lett 165:208–210.

Mogi M, Harada M, Narabayashi H, Inagaki H, Minami M, Nagatsu T. 1996. Interleukin-1 beta, interleukin-6, epidermal growth factor and transforming growth factor-alpha are elevated in ventricular cerebrospinal fluid in juvenile parkinsonian and Parkinson's disease. Neurosci Lett 211:13–16.

Morganti-Kossman MC, Kossman T, Wahl SM 1992. Cytokines and neuropathology. Trends Pharmacol 13:286–290.

Nath R, Raser KJ, Stafford D, Hajimohammadreza I, Posner A, Allen H, Talanian RV, Nitatori T, Sato N, Waguri S, Karasawa Y, Araki H, Shibanai K, Kominami E, Uchiyama Y. 1995. Delayed neuronal death in the CA1 pyramidal cell layer of the gerbil hippocampus following transient ischemia is apoptosis. J Neurosci 15:1001–1011.

Nath R, McGinnis KJ, Nadimpalli R, Stafford D, Wang KKW. 1996. Effects of ICE-like proteases and calpain inhibitors on neuronal apoptosis. Neuroreport 8:249–255.

Nath R, Robert A, McGinnis KM, Wang KKW. 1998. Evidence for activation of caspase-3-like protease in excitotoxins and hypoxia/hypoglycemia-injured cerebrocortical neurons. J Neurochem 71:186–195.

Nawashiro H, Martin D, Hallenbeck JM. 1997. Inhibition of tumor necrosis factor ameliorated brain infarction in mice. J Cereb Blood Flow Metab 17:229–232.

Oberhammer F, Fritsch G, Schmied M, Pavelka M, Printz D, Purchio T, Lassmann H, Schulte-Hermann R. 1993. Condensation of the chromatin at the membrane of an apoptotic nucleus is not associated with activation of an endonuclease. J Cell Sci 104:317–326.

Pike BR, Zhao X, Newcomb JK, Wang KKW, Posmantur RM, Hayes RL. 1998. Temporal relationships between de novo protein synthesis, calpain and caspase 3-like protease activation, and DNA fragmentation during apoptosis in septo-hippocampal cultures. J Neurosci Res 52:505–520.

Pulliam L, Zhou M, Stubbelbine M, Bitler CM 1998. Differential modulation of cell death proteins in human brain cells by tumor necrosis factor alpha and platelet activating factor. J Neurosci Res 54:530–538.

Ruff MR, Gifford GE. 1981. Rabbit tumor necrosis factor: mechanisms of action. Infect Immun 31:380–385.

Saito K, Suyama K, Nishida K, Sei Y Basile AS. 1996. Early increases in TNF-alpha, IL-6 and IL-1 beta levels following transient cerebral ischemia in gerbil brain. Neurosci Lett 206:149–152.

Scherbel U, Raghupathi R, Nakamura M, Saatman KE, Trojanowski JQ, Neugebauer E, Marino MW, McIntosh TK. 1999. Differential acute and chronic responses of tumor necrosis factor-deficient mice to experimental brain injury. Proc Natl Acad Sci USA 96:8721–8726.

Selmaj KW, Raine CS. 1998. Tumor necrosis factor mediates myelin and oligodendrocyte damage in vitro. Ann Neurol 23:339–346.

Sharief MK, McLean B, Thompson EJ. 1993. Elevated serum levels of tumor necrosis factor-alpha in Guillain-Barre syndrome. Ann Neurol 33:591–596.

Shohami E, Novikov M, Bass R, Yamin A, Galily R. 1994. Closed head injury triggers early production of TNF-alpha and IL-6 by brain tissue. J Cereb Blood Flow Metab 14:615–619.

Shohami E, Bass R, Wallach D, Yamin A, Galily R. 1996. Inhibition of tumor necrosis factor alpha (TNF-α) activity in rat brain is associated with cerebroprotection after closed head injury. J Cereb Blood Flow Metab 3:378–384.

Shohami E, Galilly R, Mechoulam R, Bass R, Ben-Hur T. 1997. Cytokine production in the brain following closed head injury: dexanabinol (HU-211) is a novel TNF-alpha inhibitor and an effective neuroprotectant J Neuroimmunol 72:169–177.

Shohami E, Ginis I, Hallenbeck JM. 1999. Dual role of tumor necrosis factor alpha in brain injury. Cytokines Growth Factors Rev 10:119–130.

Stahel PF, Shohami E, Younis FM, Kariya K, Otto VI, Lenzlinger PM, Eugster HP, Trentz O, Kossmann T, Morganti-Kossmann MC. 1999. Experimental closed head injury: analysis of neurological outcome, blood brain barrier dysfunction and intracranial polymorphnuclear leukocyte in mice deficient in genes for pro-inflammatory cytokines. J Cereb Blood Flow Metab 20:369–380.

Sullivan PG, Bruce-Keller AJ, Rabchevsky AG, Christakos S, Clair DK, Mattson MP, Scheff SW. 1999. Exacerbation of damage and altered NF-kappaB activation in mice lacking tumor necrosis factor receptors after traumatic brain injury. J Neurosci 19:6248–6256.

Taupin V, Toulmond S, Serrano A, Benavides J, Zavala F. 1993. Increase in IL-6, IL-1 and TNF-α levels in rat brain following traumatic lesion: Influence of pre- and post-traumatic treatment with Ro5 4864, a peripheral-type (p-site) benzodiazepine ligand. J Neuroimmunol 42:177–185.

Uno H, Matsuyama T, Akita H, Nishimura H, Sugita M. 1997. Induction of tumor necrosis factor-alpha in the mouse hippocampus following transient forebrain ischemia. J Cereb Blood Flow Metab 17:491–499.

Villa P, Kaufman SH, Earnshaw WD. 1997. Caspases and caspase inhibitors. Trends Biochem Sci 22:388–393.

Wang KK. 2000. Calpain and caspase: can you tell the difference? Trends Neurosci 23:59.

Wang KKW, Yuen P. 1994. Calpain inhibition: an overview of its therapeutic potential. Trends Pharmacol Sci 15:412–419.

Wang KKW, Nath R, Raser KJ, Hajimohammadreza I. 1996. Maitotoxin induces calpain activation in SH-SY5Y neuroblastoma cells and cerebrocortical cultures. Arch Biochem Biophys 331:208–214.

Wang KKW, Posmantur RM, Nath R, McGinnis K, Whitton M, Talanian RV, Glartz SB, Morrow JS. 1998. Simultaneous degradation of alpha II- and beta-II- spectrin by caspase 3 (CPP32) in apoptotic cells. J Biol Chem 273:22490–22497.

Wang XK, Yue TL, Barone FC, White RF, Gagnon RC, Feuerstein GZ. 1994. Concomitant cortical expression of TNF-α and IL-1 mRNAs follows early response gene expression in transient focal ischemia. Mol Chem Neuropathol 23:103–114.

Weissner C, Sauer D, Alaimo D, Allegrini PR. 2000. Protective effect of a caspase inhibitor in models for cerebral ischemia in vitro and in vivo. Cell Mol Biol 46:53–62.

Wyllie AH, Kerr SF, Currie AR. 1980. Cell death: the significance of apoptosis. Rev Cytol 68:251–306.

Xu IS, Grass S, Xu XJ, Wiesenfeld-Hallin Z. 1998. On the role of galanin in mediating spinal flexor reflex excitability in inflammation. Neuroscience 85:827–835.

Yamashita K, Takahashi A, Kobayashi S, Hirata H, Mesner PW, Kaufmann SH, Yonehara S, Yamamoto K, Uchiyama T, Sasada M. 1999. Caspases mediate tumor necrosis-alpha-induced neutrophil apoptosis and down-regulation of reactive oxygen production. Blood 93:674–685.

Yuen P, Gilbertsen RB, Wang KKW. 1996. Non-erythroid α-spectrin breakdown by calpain and interleukin 1-converting-enzyme-like protease(s) in apoptotic cells: contributory roles of both protease families in neuronal apoptosis. Biochem J 319:683–690.

Zhao X, Pike BR, Newcomb JK, Wang KKW, Posmantur RM, Hayes RL. 1999. Maitotoxin induces calpain but not caspase-3 activation and necrotic cell death in primary septo-hippocampal cultures. Neurochem Res 24:371–382.

Zhivotovsky B, Burgess DH, Vanags DM, Orrenius S. 1997. Involvement of cellular proteolytic machinery in apoptosis. Biochem Biophys Res Comm 230:481–488.